Finite Group Lattice Gauge Theories for Quantum Simulation

Presentata da
Sunny Pradhan

Coordinatore Dottorato

Prof. Michele Cicoli

Supervisore

Prof. Elisa Ercolessi

Contents

Introduction

Introduction to Lattice Gauge Theories

1.1 Review of Yang-Mills theory

A Yang-Mills theory is a gauge field theory on Minkowski space $\mathbb{R}^{1,d}$, where the gauge group $U(1)$ or $SU(N)$, with matter fields, which are defined by a representation of the gauge group. For example, *Quantum Chromodynamics* (QCD) is an $SU(3)$ gauge theory with Dirac spinors in the fundamental representation. Keeping in mind the example of QCD, the Lagrangian of the theory is

$$\mathcal{L} = -\frac{1}{2g^2}\mathrm{tr}(F_{\mu\nu}F^{\mu\nu}) + \overline{\psi}(i\gamma^\mu D_\mu - m)\psi, \tag{1.1}$$

where the fermions ψ are taken in the fundamental representation of $SU(N)$ and the covariant derivative is $D_\mu = \partial_\mu - iA_\mu$. We choose the convention where the Lie algebra generators T^a are Hermitian and $[T^a, T^b] = if^{abc}T^c$, with real structure constants f^{abc}. Furthermore, the generators are such that $\mathrm{tr}(T^a T^b) = \frac{1}{2}\delta^{ab}$. The strength-field tensor $F_{\mu\nu}$ is given by

$$F_{\mu\nu} = \partial_\mu A_\nu - \partial_\nu A_\mu - i[A_\mu, A_\nu] \tag{1.2}$$

and transforms in the adjoint representation of $SU(N)$. Both the gauge field A_μ and the curvature tensor $F_{\mu\nu}$ live in the Lie algebra $\mathfrak{su}(N)$.

Under a gauge transformation given by a group-valued function $g(x) \in SU(N)$, such that $\psi \mapsto g(x)\psi(x)$, then

$$A_\mu(x) \mapsto g(x)A_\mu(x)g(x)^{-1} + ig(x)\partial_\mu g(x)^{-1}, \tag{1.3}$$

so that $D_\mu\psi(x) \mapsto g(x)D_\mu\psi(x)$, while

$$F_{\mu\nu} \mapsto g(x)F_{\mu\nu}g(x)^{-1}, \tag{1.4}$$

leaving the action invariant.

The action of the theory in $d + 1$ dimensions is the given by

$$S[A, \psi, \overline{\psi}] = \int \mathrm{d}^{d+1}\mathcal{L} \tag{1.5}$$

and the path integral

$$Z = \int \mathcal{D}A\mathcal{D}\overline{\psi}\mathcal{D}\psi \, e^{iS[A,\psi,\overline{\psi}]}. \tag{1.6}$$

1.1.1 Euclidean field theory

In order to work in a Euclidean space-time, we need first to perform a *Wick rotation*, where the time coordinate x_0 is mapped a forth space coordinate x_4, through $x_0 = -ix_4$. The has the effect of changing the path-integral integrand from e^{iS}, which is oscillatory, to e^{-S}, which is positive and can be interpreted as a probability distribution of the configurations of the fields.

The Euclidean path integral is

$$Z_E = \int \mathcal{D}A\mathcal{D}\overline{\psi}\mathcal{D}\psi e^{-S}, \tag{1.7}$$

so that the Minkowski action and the Euclidean action satisfy $iS_M = -S_E$. The respective actions are given by

$$S_M = \int \mathrm{d}^{d+1}x_M \mathcal{L}_M, \qquad S_E = \int \mathrm{d}^{d+1}x_E \mathcal{L}_E. \tag{1.8}$$

The rotation $x_0 = -ix_4$ leads to $\mathcal{L}_E = -\mathcal{L}_M$.

The Wick rotation does not change the form of the gauge kinetic term, i.e.,

$$-\frac{1}{2g^2}\mathrm{tr}(F_{\mu\nu}F^{\mu\nu}). \tag{1.9}$$

The sum is a simple Euclidean sum, where there are no minus signs when raising or lowering indices and $\mu = 1, \ldots, d + 1$.

Considering now the fermionic part of the Yang-Mills Lagrangian, we need to perform the Wick rotation on the Dirac operator. In Minkowski space-time

$$\overline{\psi}(i\gamma_M^\mu D_\mu - m)\psi = \overline{\psi}(i\gamma_M^\mu \partial_\mu + \gamma_M^\mu A_\mu - m)\psi, \tag{1.10}$$

where γ_M^μ are the gamma matrices of the Clifford algebra, and they satisfy $\{\gamma_M^\mu, \gamma_M^\nu\} = 2\eta^{\mu\nu}$. In the Euclidean Clifford algebra instead the gamma matrices γ_E^μ satisfy $\{\gamma_E^\mu, \gamma_E^\nu\} = 2\delta^{\mu\nu}$. Given the fact that we have $\partial_0 = i\partial_4$ and $A_0 = iA_4$, in order to obtain the correct form we have to put $\gamma_M^0 = \gamma_E^4$. This procedure yields

$$\overline{\psi}(i\gamma_M^\mu \partial_\mu + \gamma_M^\mu A_\mu - m)\psi = -\overline{\psi}(\gamma_E^\mu \partial_\mu + i\gamma_E^\mu A_\mu + m)\psi. \tag{1.11}$$

Since $\mathcal{L}_E = -\mathcal{L}_M$, we finally arrive at

$$\mathcal{L}_E = \frac{1}{2g^2}\mathrm{tr}(F_{\mu\nu}F^{\mu\nu}) + \overline{\psi}(\gamma^\mu D_\mu)\psi, \qquad (1.12)$$

where the indices are all Euclidean and $D_\mu = \partial_\mu + iA_\mu$.

1.1.2 Hamiltonian formulation

The Hamiltonian formulation of a Yang-Mills theory can be tricky, especially the part about the gauge field. Usually, one has to procede by computing the conjugate momenta and performing a Legendre transform. The main issue here is that the gauge field component A_0, does not have a conjugate momentum:

$$\frac{\partial \mathcal{L}}{\partial \dot{A}_0} = 0. \qquad (1.13)$$

Hence, the transformation is not invertible. The easiest way to remedy to the situation is to impose the gauge condition $A_0 = 0$, which is called *canonical gauge* or *temporal gauge*. With this condition, the kinetic term for the gauge fields can be written as

$$\mathcal{L} = -\frac{1}{2g^2}\mathrm{tr}(F_{\mu\nu}F^{\mu\nu}) = \frac{1}{g^2}\left(\mathrm{E}^2 - \mathrm{B}^2\right) = \frac{1}{g^2}(E_i^a E_i^a - B_i^a B_i^a), \qquad (1.14) \quad \text{\{eq:YM\_lagrang\_temporal\_ga}}$$

where E and B are, respectively, the "chromoelectric" and the "chromomagnetic" fields. In the temporal gauge $\mathrm{E} = \dot{\mathrm{A}}$, the time derivative of the spatial components A of the gauge field A_μ, while B corresponds to the spatial components of the strength-field tensor $F^{\mu\nu}$ and does not involve any time derivative. From the Legendre transformation of (1.14) we obtain the Hamiltonian density:

$$\mathcal{H} = \frac{1}{g^2}E_i^a \dot{A}_i^a - \frac{1}{2g^2}(E_i^a E_i^a - B_i^a B_i^a) = \frac{1}{2g^2}\mathrm{tr}(\mathrm{E}^2 + \mathrm{B}^2), \qquad (1.15)$$

hence the Hamiltonian in d spatial dimensions is

$$H = \int \mathrm{d}^d x \frac{1}{2g^2}\mathrm{tr}(\mathrm{E}^2 + \mathrm{B}^2). \qquad (1.16)$$

In the Hamiltonian formulation, the fields A and E are now operators, satisfying the commutation relations

$$\left[A_i^a(x), E_j^b(y)\right] = ig^2\delta_{ij}\delta_{ab}\delta(x-y)$$
$$\left[E_i^a(x), E_j^b(y)\right] = \left[A_i^a(x), A_j^b(y)\right] = 0. \qquad (1.17) \quad \text{\{eq:comm\_rel\_E\_A\_continuu}}$$

The B operator is defined from A.

In order to impose the canonical gauge $A_0 = 0$, the equation of motion for A_0 has to be satisfied. This leads [citation?] to the fact that one must have

$$D_i E_i = 0, \qquad (1.18)$$

where D_i are the spatial components of the covariant derivative and E_i the spatial components of the chromoelectric field. Unfortunately, the equation above is inconsistent with the commutation relation (1.17) and so it cannot be implemented as an operator equation. The easiest solution is to impose it on states that are considered *physical*:

$$D_i E_i \left| \psi_{\text{phys}} \right\rangle = 0, \qquad (1.19)$$

for each component of $D_i E_i$. The constraints select a subspace of the overall Hilbert space, which will be labeled as the *physical Hilbert space*. The condition above for a $U(1)$ theory reduces to the well known *Gauss law* $\nabla \cdot \mathrm{E} = 0$.

1.1.3 The Sign Problem

Even though interesting phases have been predicted for QCD in the $\mu - T$ plane[citation?], such as quark-gluon plasma[citation?]o superconductivity[citation?], detailed quantitative analysis has been limited to the $\mu = 0$ region only. This is due mainly to the difficulty of studying QCD in the low energy regime, where the perturbative approach fails[citation?]. Moreover, even *lattice gauge theories*, a non-perturbative approach to Yang-Mills theory (and gauge theories in general), is not applicable for $\mu \neq 0$ due to the *sign problem.*

In the Hamiltonian formulation, the chemical potential in the same manner as statistical mechanics. If $\hat{H}$ is the Hamiltonian operator and $\hat{N}$ a number operator, then one can simply replace $\hat{H}$ with $\hat{H} - \mu \hat{N}$. In the case of a Yang-Mills theory, the number operator corresponds to fermion number, i.e., $\hat{N} = \psi^\dagger \psi$.

In the path integral formalism, fermions are Grassmann variables, which we can integrate over:

$$\int \mathcal{D}\psi \mathcal{D}\overline{\psi} \exp(-\int d^{d+1}\overline{\psi} K \psi) = \det K, \qquad (1.20)$$

where K is the kinetic operator for the fermions. If the fermions are coupled to gauge field, as one would expect from a Yang-Mills theory, then K has some complicated dependence on the fields A_μ. If one includes the chemical potential term $\mu \overline{\psi}^\dagger \psi$ in the Lagrangian, then the fermion determinant $\det K$ turns out to be complex[citation?], with a non-trivial phase factor.

As a result, the integrand of the path-integral is no longer positive, and it canot be interpreted as a probability distribution. This is the infamous *sign*

problem and poses severe limitation to Monte Carlo simulations in the finite μ region.

1.2 Wilson approach to gauge theories

Starting from the path integral formulation, the first step in the formulation of a *lattice field theory* (LFT) is the discretization of space-time, where a discrete $d + 1$-dimensional lattice substitutes the continuum space-time. The simplest choice in this regard is a hypercubic lattice with lattice spacing a, but in theory an LFT can be defined on any type of lattice. An immediate advantage of using a lattice instead of a continuum is the natural ultraviolet cutoff given by the inverse of the lattice spacing.

Formally a lattice Λ is defined as

$$\Gamma = \left\{ x \in \mathbb{R}^4 : x = \sum_{\mu=1}^{d+1} a n_\mu \hat{\mu} \quad n_\mu \in \mathbb{Z} \right\}, \tag{1.21}$$

where $\mu = 1, \ldots, d + 1$ and $\hat{\mu}$ is the unit vector in the direction μ. The edges will be labeled by a pair $(x, \hat{\mu})$, meaning that we are referring to the edge in the $\hat{\mu}$ direction from the vertex x. It is important to fix an orientation for each direction in the lattice. The most natural choice is to choose $+\hat{\mu}$ for each $\hat{\mu}$. So, even though $(x, \hat{\mu})$ and $(x + \hat{\mu}, -\hat{\mu})$ refers to the same link, the former is traversed in the positive direction while the latter in the negative direction.

In an LFT, both the vertices and edges (also called links) host degrees of freedom (d.o.f). In particular, the matter fields lives on the vertices while the gauge fields live on the links between vertices. However, the definition of these d.o.f. will need some care, because we have two main requirements, especially if we are interested in Yang-Mills theory:

- The lattice action should reduce to the continuum action in the continuum limit, i.e., $a \to 0$;

- The lattice action should respect the gauge symmetry.

Lorentz invariance is naturally broken on a lattice but we expect to recover it in the continuum limit.

1.2.1 Gauge fields on a lattice

[spiegazione perché usiamo il gruppo di Lie e non l'algebra di Lie] Considering a general group G, we associate an element $U_\mu(x) \in G$ to each link (x, μ). If one traverse the link in the opposite direction, one should obtain the

inverse element U^{-1}. In the case of $SU(N)$, we take $U_\mu(x)$ to be the matrices in the fundamental representation. We can obtain a vector potential in the continuum limit by writing

$$U_\mu(x) = e^{iaA_\mu(x)}, \tag{1.22}$$

where a is the lattice spacing.

It is necessary to discuss about gauge invariance before moving to the dynamics of these gauge fields. A gauge transformation is described by a group-valued function $g(x)$ (in the appropriate representation), which acts on the vertices x. The variable $U_\mu(x)$ sits in the middle of the site x and $x + \hat{\mu}$, then it is reasonable to think its transformation is

$$U_\mu(x) \mapsto g(x)U_\mu(x)g(x + a\hat{\mu})^\dagger. \tag{1.23}$$

{eq:gauge_transf_field_lattice}

In order to introduce a dynamics for the gauge fields $U_\mu(x)$, we need to define their action which need two satisfy two requirements: it has to be gauge-invariant and reduce to the pure gauge Yang-Mills action in the continuum limit. From (1.23), we can immediately deduce that taking the product of $U_\mu(x)$ along a closed curve will yield a gauge-invariant quantity. The simplest close curve we can consider is a *plaquette*, i.e., the smallest square face. Hence, on a plaquette $\square$ we introduce $W_\square$ to put in the action, defined as

$$W_\square = U_\mu(x)U_\nu(x + a\hat{\mu})U_\mu(x + a\hat{\nu})^\dagger U_\nu(x)^\dagger. \tag{1.24}$$

{eq:single_plaquette_Wilson_

Notice that we do not have any sum in the indices μ and ν because they are not Lorentz indices. The quantity in (1.24) is called a single plaquette *Wilson loop*.

We can only have scalar quantities in the action, so we need to take the trace of $W_\square$. Then, our lattice action will be defined as the sum over the plaquettes of $\mathrm{tr}W_\square$ (and its Hermitian conjugate):

$$\mathcal{S} = -\frac{1}{g^2} \sum_\square \left(\mathrm{tr}W_\square + \mathrm{tr}W_\square^\dagger\right). \tag{1.25}$$

{eq:wilson_action}

This is known as the *Wilson action* [citation?]. The quantity $\mathrm{tr}W_\square$ behaves as expected in the continuum limit, where we have to work with the strength field $F^{\mu\nu}$:

$$\mathrm{tr}W_\square \approx N - \frac{a^4}{2}\mathrm{tr}F_{\mu\nu}F^{\mu\nu} + \mathcal{O}(a^6), \tag{1.26}$$

The lattice action is not unique. The Wilson action in (1.25) is the simplest choice that one can make that satisfy our requirement. Some other

modification, for example, can include other types of closed loops and these modification can have their place. However, they will not be considered here.

Obviously, in a path-integral formulation of lattice gauge theories we need to define the path integral, which is immediate. The partition function is given by

$$Z = \int \prod_{(x,\hat{\mu})} \mathrm{d}U_\mu(x) e^{-\mathcal{S}}, \qquad (1.27)$$

where the integration measure $\mathrm{d}U_\mu(x)$ is understood to be the Haar measure. In case of a compact group, like $SU(N)$, it is well defined and yields a finite value. Now that the path integral measure has been defined, the average of an observable $\mathcal{O}$ can be computed as

$$\langle \mathcal{O} \rangle = \frac{1}{Z} \int \prod_{(x,\hat{\mu})} \mathrm{d}U_\mu(x) \mathcal{O} e^{-\mathcal{S}} \qquad (1.28)$$

1.2.2 Order parameters and gauge invariance

The Wilson formulation of lattice gauge theories can resemble spin models studied in statistical mechanics. The link variables $U_\mu(x)$ can be thought as some sort of generalization of the spin degrees of freedom. They are distributed in a crystal-like structure and interact with their nearest neighbours, in this case through a four-body interaction (the plaquette action), instead of two-body interaction (like the Ising model). If one wants to pursue this analogy, then it is reasonable to look at order parameters that behaves like the spontaneous magnetization, where a non-vanishing expectation value signals a phase transition. The analogue of such an order parameter in lattice gauge theory would be something like

$$\langle U_\mu(x) \rangle \neq 0, \qquad (1.29)$$

{eq:non_zero_link_var_expt_v

rut it has been shown[citation?][teorema di Elitzur] that this is impossible in Wilson theory.

In standard spin models, a non-zero magnetization represents a spontaneous breaking of the global symmetry of the system. Consider the simplest case of the classical Ising model, where the degrees of freedom are binary variables $\sigma = \pm 1$. Without an external field, the energy is given by the interaction of nearest neighbouring spins, i.e., $\sigma_i \sigma_j$. This system has an obvious global $\mathbb{Z}_2$ symmetry, that corresponds to the inversion $\sigma_i \mapsto -\sigma_i$ off all the spins. A ferromagnetic phase is, by definition, signaled by $\langle \sigma \rangle \neq 0$, which necessarily breaks the global $\mathbb{Z}_2$ symmetry of the model. Once a direction is selected by $\langle \sigma \rangle \neq 0$, it remains stable under thermal fluctuations because they cannot

coherently shift of the magnetization of an infinite (or rather large) number of spins.

In a lattice gauge theory, an expectation value like (1.29) would *breaks* gauge invariance, which is a *local symmetry*, not a global one. As explained previously, gauge invariance means that the action is unchanged under local arbitrary "rotations" of the link variables $U_\mu(x)$, see (1.23). Hence, thermal fluctuations will induce such rotations and in the long rung it will average on all the possible gauges. This leads to

$$\langle U_\mu \rangle = \int \mathrm{d}U_\mu U_\mu = 0 \tag{1.30}$$

if U_μ contains only non-trivial irreducible representations of the group. This means that "magnetization" is always vanishing in a lattice gauge theory and gauge invariance cannot be spontaneously broken, which is the contents of the Elitzur theorem[citation?].

The conclusion of this brief discussion may seem rather grim, as magnetization in spin models is the most convenient and used order parameter. But this does not mean that there are no other order parameters in a lattice gauge theory. We have just showed that the problem when considering something like $\langle U_\mu \rangle$ is gauge invariance. So, the most reasonable step forward is to consider *gauge-invariant quantities*. We have already seen that tracing over a product of U_μ variables along a closed curve is a gauge-invariant quantity, called *Wilson loop*.

In so far, we have considered only single plaquette loops but nothing restraints us from considering arbitrary large loops, indeed it serves as a *confinement test* for pure gauge theories. It has been shown [citation?] that confinement is equivalent to the *area law* behaviour of Wilson loops, i.e.,

$$\langle W(\mathcal{C}) \rangle \sim \exp(-\sigma A(\mathcal{C})), \tag{1.31}$$

{eq:wilson_area_law}

where $A(\mathcal{C})$ is the minimal area inside the closed path $\mathcal{C}$ and σ the *string tension* (the coefficient of the linear potential between two quarks). On the other hand, in the absence of confinement one finds instead the *perimeter law*

$$\langle W(\mathcal{C}) \rangle \sim \exp(-kP(\mathcal{C})), \tag{1.32}$$

{eq:wilson_perimeter_law}

where $P(\mathcal{C})$ is the perimeter of the curve $\mathcal{C}$ and k just some constant.

The reason behind this behaviour can be seen with a simple qualitative picture. A closed timelike Wilson loop basically represents a process in which a quark-antiquark pair is produced, moved along the sides of the loop and annihilated. If we are confining phase we can then expect a liner potential between the quark and antiquark. We can imagine a flux tube *binding* the two

charges, which swoops the whole inside the loop. Then, it is easy to image that the energy of this whole process will necessarily depend on the area of the loop. On the other hand, if we are in a deconfined phase then there is no potential binding the two quarks. In this case the energy of the whole process depends only on the self-energy of quarks, which move along the sides of the loop. Therefore, the leading energy contribution of this process depends on the perimeter, instead of the area. Obviously, this picture is no longer valid when dynamical matter is involved. In a confining phase, pair production is always preferred when separating two quarks at large distances. [inserire immagine]

From (1.31) and (1.32), we can deduce that the string tension σ can be used as an order parameter. It is non-zero for a confining phase, while it vanishes for a deconfined phase. But it is *non-local* in nature, as it involves the asymptotic behaviour of potential, and therefore of the correlation functions of the theory.

1.2.3 Fermions on a lattice

Defining fermions is not an easy task due to the known *doubling problem*. In simple terms, when introducing fermions on a lattice, instead of a continuous space, it leads to a extra spurious fermions, which are just lattice artifacts.

In order to briefly see this, consider the correlation function for a single fermionic species. If K is the kinetic matrix for the fermions, then $G = K^{-1}$ gives their correlation matrix. One finds [citation?] that the correlation function between two sites x and y has the form

$$(G)_{x,y} = \frac{1}{a^d L^d} \sum_k \tilde{G}_k e^{2\pi i k \cdot (x-y)/L}, \qquad (1.33) \quad \text{\{eq:fermionic\_corr\_func\_real\}}$$

where a is the lattice spacing, L^d the total volume and $\tilde{G}_k$ the correlation function in momentum space:

$$\tilde{G}_k^{-1} = m + \frac{i}{a} \sum_\mu \gamma_\mu \sin(2\pi k_\mu/L). \qquad (1.34) \quad \text{\{eq:fermionic\_corr\_func\_latt\}}$$

It involves a trigonometric function because the derivative term involves nearest neighbouring sites. One can then take the model to a large lattice, which justifies in substituting the discrete sums with integrals:

$$\frac{2\pi k_\mu}{La} \to q_\mu \qquad \text{and} \qquad \frac{1}{a^d L^d} \sum_k \to \int \frac{\mathrm{d}q^d}{(2\pi)^d}, \qquad (1.35) \quad \text{\{eq:limit\_large\_lattice\}}$$

where the q_μ's are continuous momentum variables. This substitution maps (1.34) into

$$\tilde{G}_k^{-1} = m + \frac{i}{a} \sum_\mu \gamma_\mu \sin(aq_\mu). \tag{1.36}$$

{eq:fermionic_corr_func_large}

One can naively think of taking the limit $a \to 0$ and expand $\sin(aq_\mu)$ around the zero and obtain something that look like the correct continuum limit:

$$\tilde{G}_\mu^{-1} = m + i\slashed{q} + \mathcal{O}(a^2). \tag{1.37}$$

But one should not be fooled by this sloppy procedure just because it appears to give the wanted result. Each component q_μ takes values in the region $[-\pi/a, +\pi/a]$, hence we have to integrate on the whole volume $[-\pi/a, +\pi/a]^d$. Looking at (1.36), it is clear that the major contributions to G in (1.33) comes from the zeros of $\tilde{G}_k^{-1}$. This, not only vanishes in the region $q_\mu \sim 0$ but also for large momentum $q_\mu \sim \pi/a$. The propagator has no suppression of momentum values near π/a. We can isolate the large momenta region by considering

$$\tilde{q}_\mu = q_\mu - \pi/a \tag{1.38}$$

for each direction in space. In this way, we de facto half the integration region,

$$\int_{-\pi/a}^{\pi/a} \mathrm{d}q_\mu \; \to \; \int_{-\pi/2a}^{\pi/2a} (\mathrm{d}q_\mu + \mathrm{d}\tilde{q}_\mu) \tag{1.39}$$

and now the limit $a \to 0$ can be taken safely, but it comes with a price to pay. For each direction in space, we have two independent regions that gives a free fermion contribution to the propagator in the continuum limit. We have effectively *doubled* the number of fermions for each direction. In a d-dimensional lattice we end up with 2^d independent fermions, even though we initially started with just one. [qualcosa a che fare con la chiralità]

There are many solutions to this fermion doubling problem[citation?], but we will focus only on one in this manuscript: *the staggered fermions*[citation?]. We have seen that these fictitious fermions come from the large momenta regions, where $q_\mu \sim \pi/a$. Brutally cutting out this large momenta regions spoils the completeness of the Fourier transform, so it is not a solution, but a smarter solution can give out the same effect. The idea is to spread the fermionic degrees of freedom over multiple lattice sites, reducing effectively the momenta space. For example, in two dimensions it would correspond to placing the *particles* on *even* sites and the *antiparticles* on *odd* sites. A site is considered even or odd when $(-1)^x = (-1)^{x_1 + \cdots + x_d} = +1$ or -1.

To obtain a staggered fermion, we define a new fermionic species $\chi(x)$ such that

$$\psi(x) = \prod_\mu (\gamma^\mu)^{n_\mu} \chi(x), \tag{1.40}$$

where $x_\mu = a n_\mu$. Now, if we want to express the discredited covariant derivative, the term $\gamma^\mu \psi(x + a n_\mu)$ have two extra powers of γ^μ compared to $\overline{\psi}$. Since $(\gamma^\mu)^2 = \pm 1$, we have therefore

$$\overline{\psi}(x) \gamma^\mu \psi(x) = (-1)^{\eta_\mu(x)} \chi(x)^\dagger \chi(x + a n_\mu), \qquad (1.41)$$

where $\eta_\mu(x)$ is some sign function depending on the site x. This function can be obtained from the commutation relations of the gamma matrices. In particular, in two dimensions we have

$$\eta_1(x) = 1 \quad \text{and} \quad \eta_2(x) = (-1)^{n_1}, \qquad (1.42)$$

while in four (Euclidean) dimension we have instead [Citare Tong, gauge theories]

$$\eta_1(x) = 1, \quad \eta_2(x) = (-1)^{n_1}, \quad \eta_3(x) = (-1)^{n_1 + n_2}, \quad \eta_4(x) = (-1)^{n_1 + n_2 + n_3}. \qquad (1.43)$$

A similar reasoning can be applied to the mass term $m \overline{\psi}(x) \psi(c)$, where it becomes

$$m \overline{\psi}(x) \psi(x) = (-1)^{\eta(x)} \chi(x)^\dagger \chi(x), \qquad (1.44)$$

for some sign function $\eta(x)$ that can be obtained from the commutation relations of the gamma functions.

Quantum Simulation of Lattice Gauge Theories

2.1   Quantum simulation

Simulating quantum mechanics is a very challenging task, in particular if one is interested in many-body systems. The description of the state requires a large number of parameters, for keeping track of all the quantum amplitudes, that grows exponentially with the system size. Hence, one would have an *exponential explosion* in terms of *classical* resources (i.e., computer memory). If simulating a quantum system is not a task for classical computers, then it should be a task for *quantum computers*. This kind of devices, first envisioned from Feynman[citation?], promises much more than simulating quantum mechanics. Indeed, quantum computation and quantum information theory are, still today, very active research fields.

A quantum computer can encodes the large amount of information of a quantum system in its large number of amplitudes. So, the size of a quantum computer would only be proportional to the size of the quantum system it intends to simulate, *without* an exponential explosion in *quantum* resources. In fact, a quantum computer can indeed act as a *universal quantum simulator* (Lloyd 1996[citation?]). This is basically the idea behind *digital quantum simulations*.

However, another approach is possible. One can mimic the evolution of a given quantum system by means of another *analogous* and *controllable* quantum system. Hence, we will only need a specific quantum machine for a specific class of problems. This is, instead, the idea behind *analog quantum simulations*. In this case, for a specific set of problems the full implementation of a quantum computer may not be necessary.

In general, *quantum simulation* can be (loosely) defined as simulating a quantum system by quantum mechanical means, There are three paths that can be taken in this regard:

- digital quantum simulation

- analog quantum simulation

- quantum-information inspired algorithms for classical simulation

We will discuss briefly each one of them. By *quantum simulator* we mean a *controllable* quantum system used to simulate or emulate other quantum systems. We see that only digital and analog quantum simulations employ a quantum simulator. The last option employs techniques, inspired by quantum information theory, that make it possible to truncate and approximates quantum states in order to have efficient classical simulations.

[Inserire figura schematica di un quantum simulator]

2.1.1 Digital quantum simulations

This approach employs the circuit model for quantum computation. Generally, the quantum simulator is a collection of *qubits* (i.e., two-level quantum systems). This constitutes the *quantum register*. A wave function of the simulated system using the computation basis, in other words a superposition of binary bit string. Each bit of a string refers to the state of a qubit in the registry, which can be either $|0\rangle$ or $|1\rangle$ in the computational basis. On this register, any many-qubit unitary transformation U is implemented through the application of a sequence of single- and two-qubit unitary operations, called *quantum gates*. An immediate example of relevant unitary transformation is the time-evolution operator, that solves the time-independent Schrödinger equation.

Even though it has been proven (Lloyd 1996[citation?]) that "anything" can be simulated on a quantum computer, not all unitary operations can be simulated *efficiently*. Therefore, there are *mathematically possible* Hamiltonians that cannot be efficiently simulated with a circuit-based model. Luckily, it is believed that *physically relevant* Hamiltonians can indeed be simulated efficiently. Furthermore, it should be stressed that the implemented unitary operations are often just approximations of the desired unitary operation. With greater precision comes a greater number of gates.

The typical setup for a digital simulation is made of three steps:

- *Initial-state preparation* — where the quantum register has to prepared in the state $|\psi(0)\rangle$. This step can be by itself difficult, and it is not always guaranteed that an efficient algorithm may exist.

- *Unitary evolution* — where the circuit has to reproduce or simulate the action of a unitary operator U. In case of a unitary time evolution

16

and local Hamiltonian this can be achieved approximately with some "trotterization" scheme.

- *Final measurement* — after obtained the wanted state $|\psi(t)\rangle = U |\psi(0)\rangle$, a *measurement* is needed in order to extract the relevant physical information. Instead of capturing the whole wave function $|\psi(t)\rangle$, with for example quantum tomography, one may proceed with the direct estimation of certain physical quantities, such as correlation functions or spectra of operators.

2.1.2 Analog quantum simulations

Analog quantum simulation (AQS) in another possible approach to quantum simulation, where a one quantum system mimics or emulate another. The Hamiltonian of the system to be simulated H_{sys} is directly mapped onto the Hamiltonian of the simulator H_{sim}. Obviously, this can be done if there is a mapping between the system and the simulator. Note that the simulator may only partly reproduce the dynamics of the system, or simulate some effective description of the system.

An important advantage of AQS is that it does not require a full quantum computer, even more the simulator does not even need to be a computer at all. Finding the mapping in an AQS might look, at first, simpler than finding the most efficient gate decomposition of a Hamiltonian, but it is not always guaranteed and there are no recipes ready for such mappings. The obvious drawback of AQS is that the quantum simulators are problem specific.

[Aggiungere altro]

2.1.3 Quantum-inspired algorithms

Classical numerical algorithms for the simulation of quantum many-body systems came out of research on quantum information theory in these later years. The most important examples of quantum-inspired algorithms are *tensor networks* methods. Tensor networks make it possible to compress the information about a many-body wave function by expressing it as a contraction of a network of tensors (as suggested by the name). For a large class of physically relevant models, the ground state is gapped and has, in a certain sense, a finite amount of entanglement. This fact is expressed by the so-called *area law*, where the entanglement between two partitions of the system grows with size of the boundary, the area between the two partitions, and not with the size of the partition itself. The main advantage of tensor networks is their ability to capture this area law.

[Aggiungere altro]

2.2 Quantum simulation for gauge theories

The problem of lattice gauge theories is arguably one of the most computationally intensive quantum many-body problem of all, due to the large numbers of degrees of freedom per site and the necessity of simulation in three spatial dimensions. We have already show a formulation of LGT in the path integral formalism. It can be used for simulations with Monte Carlo methods and indeed it already quite some results [inserire quali][citation?]. However, Monte Carlo methods suffers some problem. Simulation in Euclidean space time cannot approach several problems. For example, we already shown that the presence of fermionic matter leads to the so-called sign problem, which makes it very difficult to simulate situations with finite chemical potential. Another desirable feature it the real time evolution in Minkowski space time, which is absent when time is imaginary.

Recently, different approaches have been proposed for the quantum simulation of LGTs, from different communities, one for each possible path in quantum simulation (showed previously). For quantum-inspired classical simulation, different methods have been proposed for the simulation of LGTs using *tensor networks states*, to study the ground state, time evolution, and phase structure with both numerical and analytical models. The second type of approach relies on *analog simulation* with different kind of controllable experimental devices. The options ranges from ultracold atoms in optical lattices[citation?], trapped ions[citation?], or superconducting qubits[citation?]. The proposals have addressed LGTs of different levels of complexity, Abelian or non-Abelian, with or without dynamical matter, etc.... The last but not the least type of approach is digital quantum simulation, where the task of simulating the theory is done by a quantum computer. We will mainly focus on this last approach.

In order to be able to simulate a LGT on a quantum computer, some kind of *digitization* of the fields is necessary. By digitization, we mean the task of formulation, representing, and encoding QFT (choosing the basis) in ways useful for computational calculations. The lattice field theory, presented in Sec. 1.2, is the most conventional digitization scheme of non-perturbative field theory but it is only feasible for classical computers. It relies on resources far beyond near-term quantum computers. In conventional LGT, fermionic fields are integrated out, leaving a non-local action. A direct application of this procedure to quantum computers would require a high connectivity between qubits. Furthermore, for bosons, LGT works with bosons (i.e., the

18

gauge fields) which have a infinite-dimensional local Hilbert space. This is prohibited on a real quantum computer, where we have only finite quantum registers. We will show the different tactics for solving this issue later in the chapter

The starting point for a digital simulation of a LGT is its Hamiltonian formulation. This has been worked by Kogut and Susskind in their seminal paper[citation?], the starting point for any endeavour in quantum simulation of LGTs, which we will review in the following section

Dualities in Abelian Models

3.1 Toric Code and its features

The Toric code is two-dimensional model of spin-$\frac{1}{2}$ degrees of freedom (d.o.f), which can be regarded as an example of a pure $\mathbb{Z}_2$ lattice gauge theory. In particular, we focus on a $L \times L$ square lattice with periodic boundary conditions. The d.o.f. are defined on the links the lattice, where the local Hilbert space is $\mathbb{C}^2$. The main operators we are going to use are the Pauli matrices

$$X = \begin{pmatrix} 0 & 1 \\ 1 & 0 \end{pmatrix} \quad \text{and} \quad Z = \begin{pmatrix} 1 & 0 \\ 0 & -1 \end{pmatrix}, \tag{3.1}$$ {eq:matrices_X_Z}

which we have written in the computational basis $\{|0\rangle, |1\rangle\}$, where the Z-matrix is diagonal. It is important to remember that the matrices X and Z *anticommutes*.

$$[X, Z] = 0. \tag{3.2}$$

The main *local* operators that enters the Hamiltonian are defined on the *stars* and *plaquettes* of the lattice. The term *star* refers to the links attached to a common vertex v, while by *plaquette p* we mean the links around a face of the lattice. A *star operator* and a *plaquette operator* are respectively defined as

$$A_v = \prod_{\ell \in s} Z_\ell, \qquad B_p = \prod_{\ell \in p} X_\ell. \tag{3.3}$$ {eq:star_plaq_op_def}

where v is a vertex and p a plaquette (see Fig. 3.1). One can easily see that

$$[A_v, A_{v'}] = 0 \quad \text{and} \quad [B_p, B_{p'}] = 0 \tag{3.4}$$ {eq:star_plaq_op_comm_1}

for all vertices v and v', and all plaquettes p and p'. But it is also true that

$$[A_v, B_p] = 0 \tag{3.5}$$ {eq:star_plaq_op_comm_2}

for all v and p. This is because a star and a plaquette share zero or two links, so the signs factors from the anticommutation of X and Z cancel out. The
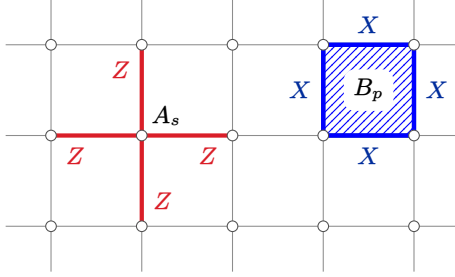
Figure 3.1. Graphical representation of the vertex operator A_v and plaquette operator B_p, defined in (3.3).

eigenvalues of the Pauli matrices are just ± 1, so the same holds true for A_s and B_p. Moreover, like the Pauli matrices, also $A_s^2 = \mathbb{1}$ and $B_p^2 = \mathbb{1}$.

Now, given the operators in (3.3), we can write down the Hamiltonian of the Toric Code:

$$H = -\sum_v A_v - \sum_p B_p \tag{3.6}$$

{eq:toric_code_hamiltonian}

which is *exactly solvable*, due to (3.4) and (3.5).

3.1.1 Topological Ground states

Given the commutation relations of the A_v and B_p operators in (3.4) and (3.5), one can find the ground state $|\Omega\rangle$ by simply imposing the constraints

$$A_v |\Omega\rangle = |\Omega\rangle \quad \text{and} \quad B_p |\Omega\rangle = |\Omega\rangle , \qquad \forall v, p. \tag{3.7}$$

{eq:ground_state_constraints}

From these constraints one can explicitly construct a ground state for the Toric Code in the following way. Working in the Z-basis, we can start from

$$|0\rangle_{\mathrm{TC}} = \bigotimes_{\ell \in \mathbb{L}} |0\rangle_\ell , \tag{3.8}$$

which is the state where every link is in the $|0\rangle$, where $Z|0\rangle = |0\rangle$. This state obviously satisfy the first condition in (3.7).

Now, regarding the B_p's operators, consider a single plaquette in the state $|0\rangle_p$ where every link is in the $|0\rangle$ state. The action of B_p flips the state of every link, from $|0\rangle$ to $|1\rangle$, obtaining $|1\rangle_p$. Therefore, a plaquette is in an eigenstate of B_p if is in an equal superposition of $|0\rangle_p$ and $|1\rangle_p$. Knowing this, it is straightforward to see that the operator $(\mathbb{1} + B_p)/\sqrt{2}$ generates an eigenstate of B_p from $|0\rangle_p$. In fact, a simple calculation

$$B_p \frac{\mathbb{1} + B_p}{\sqrt{2}} |0\rangle_p = \frac{B_p + \mathbb{1}}{\sqrt{2}} |0\rangle_p \tag{3.9}$$

shows that we obtain an eigenstate of B_p with eigenvalue $+1$, due to $B_p^2 = \mathbb{1}$.

Therefore, we can obtain a ground state for the Toric code as

$$|\Omega\rangle = \prod_p \frac{\mathbb{1} + B_p}{\sqrt{2}} |0\rangle_{\text{TC}}. \tag{3.10}$$

More generally, we can define the space of ground states

$$\mathcal{G} = \{|\Omega\rangle : A_s |\Omega\rangle = |\Omega\rangle, \quad B_p |\Omega\rangle = |\Omega\rangle \quad \forall s, p\}, \tag{3.11}$$

{eq:TC_protected_subspace}

which contents *depends on the topology of the lattice*. For example, later we will show that with *periodic boundary conditions* then there are *four degenerate ground states*.

Consider a lattice $\mathbb{L}$ of size $L \times L$ with periodic boundary conditions in both directions, i.e. a torus. From (3.7), we have $2L^2$ constraints. These are not all independent because if we multiply them all, we obtain

$$\prod_v A_v = \mathbb{1} \quad \text{and} \quad \prod_p B_p = \mathbb{1}, \tag{3.12}$$

which actually means that there are $2L^2 - 2$ independent conditions. The total Hilbert space has dimension 2^{2L^2}. Combined with $2L^2 - 2$ independent conditions we obtain $2^{2L^2 - 2L^2 + 2} = 4$ independent states. Therefore, $\dim \mathcal{G} = 4$ because we have four degenerate distinct ground states. These are eigenstates of all A_v and B_p, with all the same eigenvalues. Any other that commutes with the Hamiltonian is given by a product of A_v and B_p, so it cannot distinguish the different ground states.

The only way to distinguish these ground states is through *non-local operators* that commute with the Hamiltonian in (3.6). Non-local in this instance means not expressible as a product or sum of vertex and plaquette operators. But first let look more closely at *local operators*.

Consider any region $\mathcal{R}$ on the lattice $\mathbb{L}$. Without loss of generality, let $\mathcal{R}$ be a connected region, which means it is just a set of jointed plaquettes. On this region $\mathcal{R}$ we can define a local operator W as a product of B_p operators:

$$W = \prod_{p \in \mathcal{R}} B_p. \tag{3.13}$$

This operator commutes will the terms of the Hamiltonian (3.6). Due to $X^2 = \mathbb{1}$, the previous equation can be rewritten as

$$W = \prod_{\ell \in \partial \mathcal{R}} X_\ell. \tag{3.14}$$

In other words, W is equivalent to the product of X's along the closed curve given by the boundary $\partial \mathcal{R}$ of $\mathcal{R}$. In fact, the B_p themselves are defined as
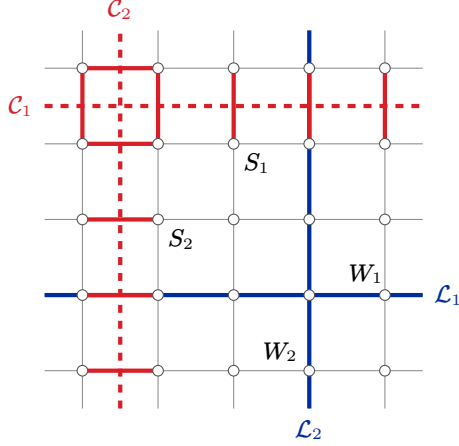
Figure 3.2. Graphical representation of the different types of non-local operators. On the non-contractible loops $\mathcal{L}_1$ and $\mathcal{L}_2$ (in the direct lattice) we have defined $\overline{W}_1$ and $\overline{W}_2$ (see (3.17)). While on the non-contractible cuts $\mathcal{C}_1$ and $\mathcal{C}_2$ (in the dual lattice) we have the operators $\overline{S}_1$ and $\overline{S}_2$.

product of Xs along a closed curve, the plaquette. In a sense, they are all *string operators* on closed curves.

The same argument can be repeated for A_v with the minor caveat that the dual lattice have to considered. In the dual lattice $\mathbb{L}^*$, to each plaquette p of the lattice $\mathbb{L}$ corresponds a vertex v on the dual lattice. Then, to each link ℓ in $\mathbb{L}$ corresponds a link ℓ^* in $\mathbb{L}^*$ in the perpendicular direction. In this way, a star becomes a plaquette in the dual lattice. From here, we can repeat the same argument. Consider a region $\mathcal{R}^*$ a local operator W^* such that

$$W^* = \prod_{v \in \mathcal{R}^*} A_v, \tag{3.15}$$

and, due to $Z^2 = \mathbb{1}$, this is equal to

$$W^* = \prod_{\ell \in \partial \mathcal{R}^*} Z_\ell. \tag{3.16}$$

The local operator W^* is a string of Z's operators along the closed curve given by the boundary $\partial \mathcal{R}$ in $\mathbb{L}^*$. The same can be said for A_v, it is a string operator around the smallest possible curve in $\mathbb{L}^*$. We can conclude that all the local operators that commutes with Hamiltonian are just string operators over closed curve in either $\mathbb{L}$ or $\mathbb{L}^*$. But, these operators have alla a common feature, they are defined on *contractible* curves. Meaning that they can be "continuously" deformed to a single point.

String operators on non-contractible curves, either on the direct or dual lattice, are the non-local operators we have been looking for distinguish the states in $\mathcal{G}$. Consider two non-contractible loops $\mathcal{L}_1$ and $\mathcal{L}_2$ on $\mathbb{L}$ along the $\hat{1}$ and $\hat{2}$ direction respectively, like in Fig. 3.2. On these paths we can define the string operators $\overline{W}_1$ and $\overline{W}_2$ as

$$\overline{W}_1 = \prod_{\ell \in \mathcal{L}_1} X_\ell, \qquad \overline{W}_2 = \prod_{\ell \in \mathcal{L}_2} X_\ell. \tag{3.17} \quad \text{\{eq:nonlocal\_W\_toric\}}$$

It can be proved that they commute with all the terms of the Hamiltonian, even though they cannot be expressed as a product of them. The same can be repeated on the dual lattice $\mathbb{L}^*$, by considering two non-contractible cuts $\mathcal{C}_1$ and $\mathcal{C}_2$ and defining $\overline{S}_1$ and $\overline{S}_2$ as

$$\overline{S}_1 = \prod_{\ell \in \mathcal{C}_1} Z_\ell, \qquad \overline{S}_2 = \prod_{\ell \in \mathcal{C}_2} Z_\ell. \tag{3.18}$$

{eq:nonlocal_S_toric}

Likewise, the operators in (3.18) commutes with all the vertex and plaquettes operators but they do not commute with the operators in (3.17).

In fact, (3.17) and (3.18) anticommutes,

$$\{\overline{W}_1, \overline{S}_2\} = 0 \quad \text{and} \quad \{\overline{W}_2, \overline{S}_1\} = 0, \tag{3.19}$$

{eq:anticommutation_W_S_t…

while

$$\left[\overline{W}_1, \overline{W}_2\right] = 0 \quad \text{and} \quad \left[\overline{S}_1, \overline{S}_2\right] = 0. \tag{3.20}$$

These relations can be thought as the same commutation relations of the X and Z gates of two qubits.

Therefore, the Toric Code (on a torus) has a protected subspace $\mathcal{G}$, see (3.11), that behaves like the Hilbert space of two qubits and the operators (3.17) and (3.18) acts like unitary gates on this space. Unfortunately, we cannot do quantum computation with these topological qubits because there is no entangling gates. Nonetheless they can be used for storing information in a fault-tolerant way, because in order to flip a topological qubit you would need to act with a non-local operator that involves a large amount of links.

3.1.2 Toric Code as a $\mathbb{Z}_2$ Lattice Gauge Theory

The Toric Code was formulated as a type of error-correcting code for quantum computing, but it can be reinterpreted as a pure $\mathbb{Z}_2$ lattice gauge theory. This is a type of lattice gauge theory where we allow only two possible states for the gauge field.

On a single link, we consider the X_ℓ as the gauge field operator, while Z_ℓ the electric field operator. In this way, we can automatically see that the term B_p is the magnetic energy because it has the same form of single-plaquette Wilson loop. Furthermore, the vertex operator A_v can be read as a gauge transformation on the vertex v, because the Z's operators flips the states in the X-basis, which would corresponds to gauge field configurations.

Now that we know the form of gauge transformations, we call a state *physical* or *gauge-invariant* if

$$A_v |\phi\rangle = |\phi\rangle \quad \forall v \in \mathbb{L}, \tag{3.21}$$

{eq:toric_code_physical_stat…
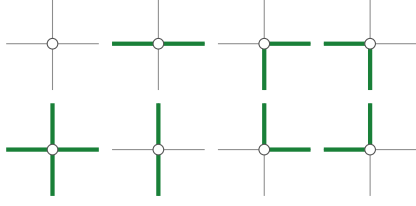
Figure 3.3. Gauge invariant vertex states for the $\mathbb{Z}_2$ lattice gauge theory. Green lines represent the $|1\rangle$ link state.

which leads to the definition of the *physical Hilbert space*:

$$\mathcal{H}_{\text{phys}} = \{|\phi\rangle \text{ s.t. } A_v |\phi\rangle = |\phi\rangle \quad \forall v \in \mathbb{L}\}. \tag{3.22}$$

{eq:phys_Hilbert_space_tori}

For greater clarity, lets work in the *electric basis*, which is just the Z-basis where the electric field is diagonal. The electric field operator Z has eigenvalue $+1$ and -1, corresponding respectively to the states $|0\rangle$ and $|1\rangle$. In order to meet the condition in (3.21), a vertex configuration must have an even number of links in the $|1\rangle$ state (examples can be seen in Fig. 3.3).

We have already argued that the B_p's give the magnetic energy, and obviously the Z's give the electric energy. Hence, the pure gauge theory Hamiltonian is just

$$H_{\mathbb{Z}_2} = -\sum_p B_p - \lambda \sum_\ell Z_\ell, \tag{3.23}$$

{eq:z2_lgt_hamiltonian}

where λ is a generic coupling that tunes the strength of the electric field with respect to the magnetic field. Notice that we no longer have a dynamical vertex term in (3.23) because we have imposed the condition (3.21) on the physical states.

In order to better explain the different phases we can have by varying the coupling λ in (3.23), we want to have a closer look at the physical states. We have already seen that the condition (3.21) constraints the types of vertex configurations. From the allowed configuration, we can see that the only possible lattice states (in the electric basis) are states made of *closed electric loops*. An example of such state can be seen in Fig. 3.4.

For $\lambda = 0$ we recover the Toric Code and its ground state can be reinterpreted as an equal superposition of all the possible configuration of closed electric loops. This kind of phase is also called a *loop condensate*. For large λ the electric term dominates over the magnetic term, hence all the links will favor the state $|0\rangle$. So in the regime of strong coupling we expect to be in a *polarized phase*, where the presence of electric loops is suppressed. Therefore, there is a critical coupling λ_c for which we have a *phase transition*. In the language of gauge theories, the loop condensate corresponds to a *deconfined phase* while the polarized one is a *confined phase*. Hence, for λ_c we have a deconfined-confined phase transition. [inserire diagramma di fase]
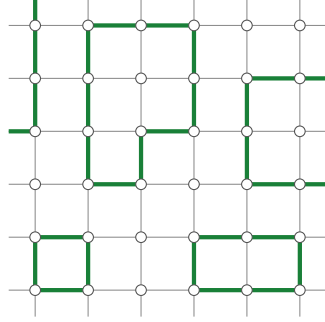
Figure 3.4. Physical states in the $\mathbb{Z}_2$ LGT are made of closed electric loops.

3.1.3 Super-selection sectors

We have already seen in Sec. 3.1.1 the non-local operators $\overline{W}_{1,2}$ and $\overline{S}_{1,2}$ that can classify the topological ground states. They can be treated on equal footing in the pure Toric Code, because they both commutes with all the terms of the Hamiltonian (3.6). This is no longer true in (3.23), when the electric term is present. Both kind of operators are gauge-invariant, in the sense that they commute with the gauge transformations A_v, i.e.

$$\left[\overline{W}_{1,2}, A_v\right] = 0 \quad \text{and} \quad \left[\overline{S}_{1,2}, A_v\right] = 0, \quad \text{for all } v \in \mathbb{L} \qquad (3.24)$$

but only the $\overline{S}_{1,2}$ string operator commute with the electric field Z_ℓ.

This means, that we can classify all the state of $\mathcal{H}_{\text{phys}}$ (see (3.22)) through their $\overline{S}_1$ and $\overline{S}_2$ eigenvalues, because they commute with the Hamiltonian. Therefore, we obtain a decomposition of the physical Hilbert space in super-selection sectors

$$\mathcal{H}_{\text{phys}} = \mathcal{H}_{\text{phys}}^{(0,0)} \oplus \mathcal{H}_{\text{phys}}^{(0,1)} \oplus \mathcal{H}_{\text{phys}}^{(1,0)} \oplus \mathcal{H}_{\text{phys}}^{(1,1)}, \qquad (3.25)$$ {eq:Hilbert_space_decompos

where for each $|\phi\rangle \in \mathcal{H}_{\text{phys}}^{(n,m)}$ we have

$$S_1 |\phi\rangle = (-1)^m |\phi\rangle \quad \text{and} \quad S_2 |\phi\rangle = (-1)^n |\phi\rangle, \qquad (3.26)$$

where $n, m = 0, 1$.

The string operators $\overline{W}_{1,2}$ do not commute with the Hamiltonian (3.23), hence they cannot be used to classify the states in $\mathcal{H}_{\text{phys}}$. On the other hand, given the algebraic relations (3.19), they are able to modify the effect of $\overline{S}_{1,2}$. In fact, $\overline{W}_{1,2}$ can change the super-selection sectors:

$$W_1 : \mathcal{H}_{\text{phys}}^{(n,m)} \mapsto \mathcal{H}_{\text{phys}}^{(n+1,m)} \quad \text{and} \quad W_2 : \mathcal{H}_{\text{phys}}^{(n,m)} \mapsto \mathcal{H}_{\text{phys}}^{(n,m+1)}, \qquad (3.27)$$ {eq:action_W_on_sectors}

where the $n, m = 0, 1$ and the addition is taken modulus 2.

From a more physical point of view, the operator $\overline{S}_i$ (with $i = 1, 2$) measures the presence non-contractible electric loops in the state in the direction
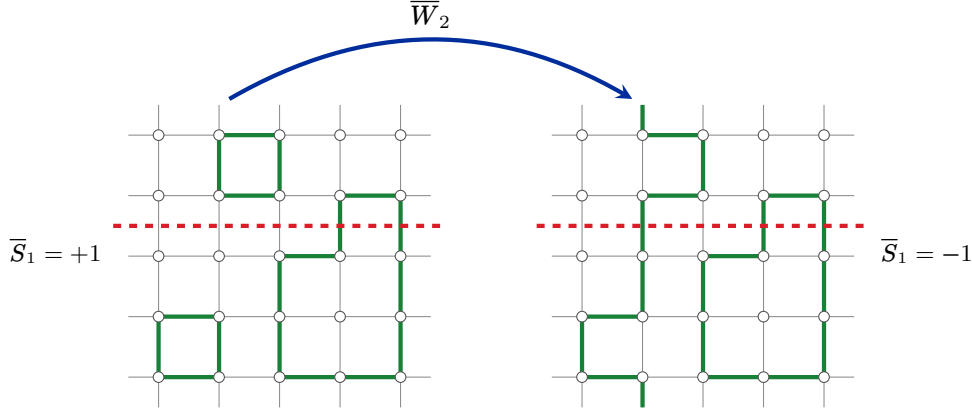
Figure 3.5. Pictorial representation of states of different super-selection sector and the action of the string operator W_2. Notice that the action $\overline{W}_2$ introduces a non-contractible electric loop in the state, which modifies the value of $\overline{S}_1$, which, in a sense, measure the presence of non-contractible electric loops in the orthogonal direction $\hat{2}$.

orthogonal to $\hat{i}$. Therefore, the decomposition in (3.25) divides the physical Hilbert space by the number of non-contractible electric loops in each direction. On the other hand, the operators $\overline{W}_i$ introduces a non-contractible electric loop in the $\hat{i}$ direction, which explains (3.27) . This can be seen in Fig. 3.5. Notice that in the case of $\mathbb{Z}_2$ LGT we can have at most one non-trivial electric loops. For examples, two parallels electric loops can be obtained by a strip of B_p operators, without requiring the $\overline{W}$ string operators.

3.2 Generalization to $\mathbb{Z}_N$

In this section we are going to generalize the $\mathbb{Z}_2$ LGT to a class of Abelian LGT with discrete symmetry $\mathbb{Z}_N$. This class is of particular interest because they approximate a $U(1)$ gauge theory in the limit $N to \infty$.

3.2.1 Schwinger-Weyl algebra

According to Wilson's Hamiltonian approach to lattice gauge theories [1], $U(1)$ gauge fields are defined on the links of a lattice $\mathbb{L}$ either in a pair of conjugate variables, the electric field E_ℓ and either the vector potential A_ℓ, satisfying

$$[E_\ell, A_{\ell'}] = i\delta_{\ell,\ell'}, \tag{3.28}$$

or equivalently the *magnetic operator*, also called *comparator*, $U_\ell = e^{-iA_\ell}$, such that

$$[E_\ell, U_{\ell'}] = \delta_{\ell,\ell'} \, U_\ell, \tag{3.29}$$
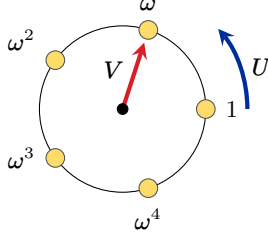
Figure 3.6. The operators U and V of a single link, in the $\mathbb{Z}_5$ case. The V plays the role of a position operator, while U that of a shift operator.

all acting on an infinite dimensional Hilbert space defined on each link $\ell \in \mathbb{L}$. This form of the canonical commutation relations represents the infinitesimal version of the relations:

$$e^{i\xi E}e^{-i\eta A}e^{-i\xi E} = e^{i\xi\eta}e^{-i\eta A}, \tag{3.30}$$

for any $\xi, \eta \in \mathbb{R}$, that define the Schwinger-Weyl group [2–4].

For a discrete group like $\mathbb{Z}_N$, the notion of infinitesimal generators loses any meaning and we are led to directly consider, for each link $\ell \in \mathbb{L}$, two unitary operators V_ℓ, U_ℓ, such that [4, 5]

$$V_\ell U_\ell V_\ell^\dagger = e^{2\pi i/N}U_\ell, \qquad U_\ell^N = \mathbb{1}_N, \qquad V_\ell^N = \mathbb{1}_N. \tag{3.31}$$ {eq:schwinger_weyl_algebra}

while they commute on different links. Thus, by representing $\mathbb{Z}_N$ with the set of the N roots of unity $e^{i2\pi k/N}$ $(k = 1, \cdots, N)$, commonly referred to as the discretized circle, we see that V plays the role of a "position operator" on the discretized circle, while U that of a "momentum operator".

These algebraic relations admit a faithful finite-dimensional representation of dimension N [6], for any integer N, which is obtained as follows. To each link ℓ, we can associate an N-dimensional Hilbert space $\mathcal{H}_\ell \simeq \mathbb{C}^N$. As an orthonormal basis for $\mathcal{H}_\ell$ we choose the *electric basis* $\{|v_{k,\ell}\rangle, k = 1, \ldots, N\}$, that diagonalizes the operator V_ℓ. With this choice, we can promptly write the actions of U_ℓ and V_ℓ:

$$\begin{aligned} U_\ell |v_{k,\ell}\rangle &= |v_{k+1,\ell}\rangle, && (\text{mod } N) \\ V_\ell |v_{k,\ell}\rangle &= \omega^k |v_{k,\ell}\rangle, \end{aligned} \tag{3.32}$$ {eq:elect_basis_op_action}

where $\omega = e^{2\pi i/N}$ and $k = 0, \ldots, N-1$. It is immediate to find the action for the Hermitian conjugates $U_\ell^\dagger$ and $V_\ell^\dagger$:

$$\begin{aligned} U_\ell^\dagger |v_{k,\ell}\rangle &= |v_{k-1,\ell}\rangle, && (\text{mod } N) \\ V_\ell^\dagger |v_{k,\ell}\rangle &= \omega^{-k} |v_{k,\ell}\rangle. \end{aligned} \tag{3.33}$$ {eq:elect_basis_op_action_h
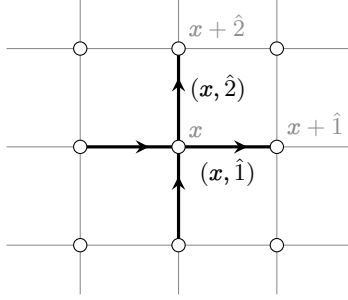
Figure 3.7. Labelling of the sites and the links in the two dimensional lattice. A site is labeled simply with $x = (x_1, x_2)$, while $\hat{1} = (1,0)$ and $\hat{2} = (0,1)$ stand for the unit vectors of the lattice. A link ℓ is denoted with a pair $(x, \pm \hat{i})$, with $\hat{i} = \hat{1}, \hat{2}$.

With this choice, U_ℓ and V_ℓ in matrix form are written as

$$
U_\ell = \begin{pmatrix} 0 & 0 & \cdots & \cdots & 1 \\ 1 & 0 & \cdots & \cdots & 0 \\ 0 & 1 & \ddots & & \vdots \\ \vdots & \vdots & \ddots & \ddots & \vdots \\ 0 & 0 & \cdots & 1 & 0 \end{pmatrix} \quad \text{and} \quad V_\ell = \begin{pmatrix} 1 & & & & \\ & \omega & & & \\ & & \omega^2 & & \\ & & & \ddots & \\ & & & & \omega^{N-1} \end{pmatrix}. \quad (3.34)
$$

We choose to work in this particular basis and the various k can be interpreted as the quantized values of the electric field on the links.

In the $\mathbb{Z}_N$ case it is important to fix the orientation of the lattice $\mathbb{L}$, because for $N \geq 3$ we have $U^\dagger \neq U$ and $V^\dagger \neq V$. We choose the orientation shown in Fig. 3.7. On a two-dimensional square lattice of size $L \times L$, the links ℓ of the lattice can also be labeled with $(x, \pm \hat{i})$, where $x \in \mathbb{L}$ is a site and $\hat{i} = \hat{1}, \hat{2}$ the two independent unit vectors. In this way, $(x, \pm \hat{i})$ will refer to the link that start in x and goes in the positive (negative) direction $\hat{i}$. As we will see later, the choice of the orientation affects the definition of any string operator. The general rule for when defining a string operator as a product of $\mathcal{O}$ operators, where $\mathcal{O}$ is either U or V for example, is to use $\mathcal{O}$ when going in the positive direction or $\mathcal{O}^\dagger$ otherwise.

3.2.2 Gauge invariance and Hamiltonian

Gauge transformations transforms the vector potential while preserving the electric field. For a $U(1)$ gauge theory, a local phase transformation is induced by a real function α_x defined on the vertices $x \in \mathbb{L}$, such that $A_\ell \mapsto A_\ell + (\alpha_{x_2} - \alpha_{x_1})$ or equivalently

$$
U_\ell \mapsto e^{i(\alpha_{x_2} - \alpha_{x_1})E_\ell} U_\ell e^{-i(\alpha_{x_2} - \alpha_{x_1})E_\ell}, \quad (3.35)
$$

where x_1, x_2 are the initial and final vertices of the (directed) link ℓ. In the case of a discrete symmetry, a gauge transformation at a site $x \in \mathbb{L}$ is a product of V's (and $V^\dagger$'s) defined on the links which comes out (and enters)
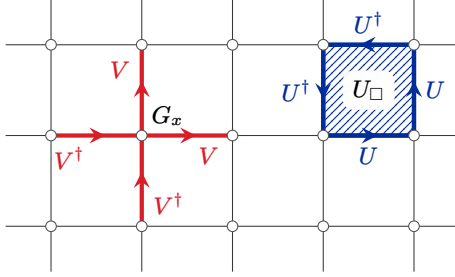
Figure 3.8. Pictorial representation of the Gauss operators G_x in (3.36) (*left*) and plaquette operator $U_\square$ in (3.37) (*right*).

the vertex. More specifically, for a two dimensional lattice, if the link ℓ at site x is oriented in the positive direction, i.e. either $(x, +\hat{1})$ or $(x, +\hat{2})$, then V is used, otherwise $V^\dagger$. Thus, the single local gauge transformation at the site x is enforced by the operator:

$$G_x = V_{(x,\hat{1})} V_{(x,\hat{2})} V^\dagger_{(x,-\hat{1})} V^\dagger_{(x,-\hat{2})}, \qquad (3.36)$$

as shown in the left part of in Fig. 3.8.

The operators that enters the Hamiltonian have to be gauge invariant, i.e. commute with all the operators G_x. Using (3.36) and recalling (3.31), it is possible to see that the V_ℓ's commute with G_x (as expected), while the U_ℓ's do not. In spite of that, we can build gauge-invariant operators out of the comparators U_ℓ. Generalizing directly from Toric Code case, one another gauge-invariant operator is the *plaquette operator*, which we will denote with $U_\square$, that will play the role of the magnetic operator. A plaquette now has an orientation. Given a plaquette $\square$ with vertices $\{x, x + \hat{1}, x + \hat{1} + \hat{2}, x + \hat{2}\}$, we consider the path that start from x and goes in the counterclockwise direction. On this plaquette, the operator $U_\square$ is defined as follows:

$$U_\square = U_{(x,\hat{1})} U_{(x+\hat{1},\hat{2})} U^\dagger_{(x+\hat{1}+\hat{2},-\hat{1})} U^\dagger_{(x+\hat{2},-\hat{2})}, \qquad (3.37)$$

which can be seen on the right in Fig. 3.8.

The whole operator algebra $\mathcal{A}$ of the theory is generated by the set of all U_ℓ and V_ℓ (and their Hermitian conjugates) of all the links of the lattice $\mathbb{L}$, while the *gauge-invariant subalgebra* $\mathcal{A}_{\mathrm{gi}}$ consists of operators that commutes with all the G_x:

$$\mathcal{A}_{\mathrm{gi}} = \{O_{\mathrm{gi}} \in \mathcal{A} \; : \; [O_{\mathrm{gi}}, G_x] = 0 \quad \forall x \in \mathbb{L}\}. \qquad (3.38)$$

Guided by the Toric Code, we already know that the set $\{U_\square, V_\ell\}$ (for all plaquettes $\square$ and all links ℓ) does not generate the whole algebra $\mathcal{A}_{\mathrm{gi}}$, in the case of periodic boundary conditions. Indeed, we have yet to add string operators on non-contractible loops.

In Sec. 3.1.1 we have already introduced the non-local operators $\overline{W}_i$ and $\overline{S}_i$, with $i = 1, 2$. These can readily be generalized to the $\mathbb{Z}_N$ case, by replacing X_ℓ and Z_ℓ with U_ℓ and V_ℓ respectively. More precisely, consider direct non-contractible loops $\mathcal{L}_i$ and cuts $\mathcal{C}_i$ (in the i-th direction). Then $\overline{W}_i$ and $\overline{S}_i$ operators are defined as

$$\overline{W}_i = \prod_{\ell \in \mathcal{L}_i} U_\ell \quad \text{and} \quad \overline{S}_i = \prod_{\ell \in \mathcal{C}_i} V_\ell, \tag{3.39}$$

with the caveat that when going in the negative direction, $U^\dagger$ and $V^\dagger$ have to be used. Operators $\overline{W}_i$ will also be called *Wilson loops*, while the $\overline{S}_i$ will be called *'t Hooft strings*. These operators are pictured in Fig. 3.9.

Both sets of operators, $\overline{W}_i$ and $\overline{S}$, are gauge invariant but only the Wilson loops cannot be expressed as product of neither $U_\square$ and V_ℓ. Therefore, they have to be added explicitly to the set of generators of $\mathcal{A}_{\text{gi}}$ in order to obtain the whole algebra. Similar to the Toric Code, these non-local operators will play a fundamental role in defining the super-selection sectors of the theory.

The class of models we consider are described by the Hamiltonian [7–9]:

$$H_{\mathbb{Z}_N}(\lambda) = -\sum_\square U_\square - \lambda \sum_\ell V_\ell + \text{h.c.}, \tag{3.40}$$

where the first sum is over the plaquettes $\square$ of the lattice while the second sum is over the links ℓ. As stated before, the operators $U_\square$ plays the role of a *magnetic* term, to be more precise it is the magnetic flux inside the plaquette $\square$, while V is the *electric* term. The coupling λ tunes the relative strength of the electric and magnetic energy contribution.

3.2.3 Physical Hilbert space and super-selection sectors

The total Hilbert space $\mathcal{H}_{\text{tot}}$ is given by

$$\mathcal{H}_{\text{tot}} = \bigotimes_{\ell \in \mathbb{L}} \mathcal{H}_\ell, \tag{3.41}$$

where $\mathcal{H}_\ell \simeq \mathbb{C}^N$ in the case of $\mathbb{Z}_N$ theory. A state of the whole lattice $|\phi_{\text{phys}}\rangle \in \mathcal{H}_{\text{tot}}$ is said to be *physical* if it is a *gauge-invariant state*:

$$G_x |\phi_{\text{phys}}\rangle = |\phi_{\text{phys}}\rangle, \qquad \forall\, x \in \mathbb{L}. \tag{3.42}$$

This condition can be translated into a constraint on the eigenvalues v_ℓ of the electric operators V_ℓ. Given that a link ℓ can be referred to as $(x, \hat{i})$, then the constraint (3.42) can be translated to

$$v_{(x,\hat{1})} v_{(x,\hat{2})} v^*_{(x,-\hat{1})} v^*_{(x,-\hat{2})} = 1. \tag{3.43}$$
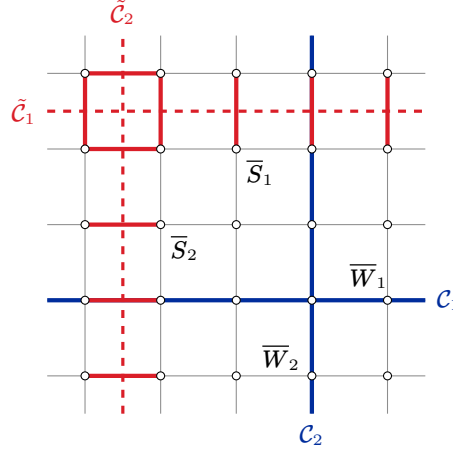
Figure 3.9. Graphical representation of the non-local order parameters $\overline{W}_{1,2}$ (in blue) and $\overline{S}_{1,2}$ (in red) and their respective paths $\mathcal{C}_{1,2}$ and $\tilde{\mathcal{C}}_{1,2}$.

For a $\mathbb{Z}_N$ theory we have $v_\ell = \omega^{k_\ell}$, where $\omega = e^{i2\pi/N}$, which leads to

$$\sum_{i=1,2} \left(k_{(x,\hat{i})} - k_{(x,-\hat{i})} \right) = 0 \mod N. \qquad (3.44)$$

{eq:gauss_law_elec_eigvals}

for (3.42). Given the fact that the k in (3.31) represent the values of the electric field, one can see that (3.44) can be interpreted as a discretized version of the Gauss law $\nabla \cdot \vec{E} = 0$ in two dimensions, for a pure gauge theory.

Consider now the *physical Hilbert space* for a $\mathbb{Z}_N$ theory:

$$\mathcal{H}_{\text{phys}} = \{|\phi_{\text{phys}}\rangle : G_x |\phi_{\text{phys}}\rangle = |\phi_{\text{phys}}\rangle \quad \forall x \in \mathbb{L}\}. \qquad (3.45)$$

{eq:decomposizione_Hphys}

This space can be decomposed into super-selection sectors, like it has been done for the $\mathbb{Z}_2$ theory in Sec. 3.1.3. In fact, it can be generalized in a straightforward way, using the string operators in (3.39) (showed in Fig. 3.9). The physical Hilbert space $\mathcal{H}_{\text{phys}}$ decomposes as

$$\mathcal{H}_{\text{phys}} = \bigoplus_{n,m=0}^{N-1} \mathcal{H}_{\text{phys}}^{(n,m)}, \qquad (3.46)$$

where each sector (n,m) satisfy

$$S_1 |\phi\rangle = \omega^m |\phi\rangle \quad \text{and} \quad S_2 |\phi\rangle = \omega^n |\phi\rangle \qquad (3.47)$$

for $|\phi\rangle \in \mathcal{H}_{\text{phys}}^{(n,m)}$. This is possible because the 't Hooft strings $\overline{S}$ commutes with all the terms of the Hamiltonian.

On the other hand, the Wilson loops $\overline{W}_i$ do not commute with all the Hamiltonian (3.40), in particular with the electric operators V_ℓ, but are still

gauge-invariant. Nonetheless, we are interested in the commutation relation between the Wilson loops $\overline{W}_i$ and 't Hoof string $\overline{S}_i$:

$$W_1 S_2 = \omega S_2 W_1 \quad \text{and} \quad W_2 S_1 = \omega S_1 W_2. \tag{3.48}$$

It is a direct generalization of the relations (3.19) of the Toric Code, where the phase -1 is substituted with a characteristic phase ω. Given (3.48), it is easy to see that the Wilson loops have the ability to change the super-selection sectors:

$$W_1 : \mathcal{H}_{\text{phys}}^{(n,m)} \to \mathcal{H}_{\text{phys}}^{(n+1,m)} \quad \text{and} \quad W_2 : \mathcal{H}_{\text{phys}}^{(n,m)} \to \mathcal{H}_{\text{phys}}^{(n,m+1)}, \tag{3.49}$$

where the addition is taken modulus N.

From a physical point of view, the Wilson loops operators $\overline{W}_1$ and $\overline{W}_2$ create non-contractible electric loops around the lattice, while the 't Hooft strings $\overline{S}_2$ and $\overline{S}_1$ detect the presence and the strength of these electric loops. Exactly like in the case of the $\mathbb{Z}_2$ LGT, but the the difference that now the non-contractible electric strings can have different "strengths", given by the different eigenvalues of $\overline{S}_i$. Therefore, it is clear that the Hilbert subspace $\mathcal{H}_{\text{phys}}^{(n,m)}$ is the subspace of all the states that contains an electric loop of strength ω^n and ω^m along the $\hat{1}$ and $\hat{2}$ direction, respectively.

Furthermore, the evolution of a state in $\mathcal{H}_{\text{phys}}^{(n,m)}$ with the Hamiltonian in (3.40) is confined in $\mathcal{H}_{\text{phys}}^{(n,m)}$. This is because none of the local terms in the Hamiltonian can change the super-selection sector, only the non-local Wilson loops. In this chapter we will see how this fact can have major consequences when considering $\mathbb{Z}_N$ models on particular lattice geometries, in particular on the *ladder*.

3.3 Abelian models on the ladder

In this short chapter we will introduce $\mathbb{Z}_N$ LGT on a *ladder geometry*. This type of lattice can be considered as a strip of a two-dimensional square lattice. The peculiarity of this geometry is that it allows the existence of magnetic terms in a quasi one-dimensional lattice, which usually are not possible in a pure one-dimensional systems. Moreover, since the Hilbert space is highly constrained, it allows the possibility to study systems of moderate size through exact diagonalization. The latter will be analyzed in the last section.

A *ladder* is a lattice $\mathbb{L}$ made of two parallels chains, the *legs*, coupled to each other by the *rungs* to form square plaquettes. On the ladder, each rung is identified by a coordinate $i = 1, \ldots, L$, where L is the length of the ladder, and the two vertices on the rung are denoted with $i^\uparrow$ and $i^\downarrow$ in the upper and
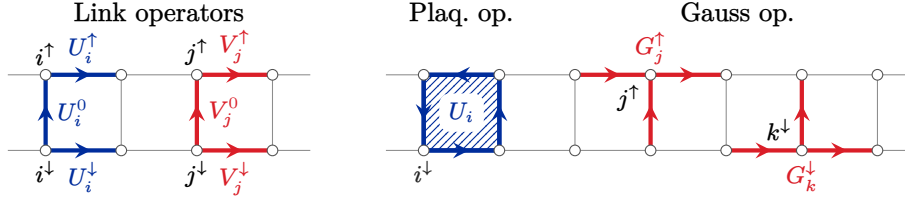
Figure 3.10. Picture of the different ladder operators. *Left*: the magnetic and electric link operators. *Right*: plaquette operator U_i and the Gauss operators $G_j^\uparrow$ and $G_k^\downarrow$. Notice that operators and sites on the upper leg are indicated with an up arrow, on the lower leg with a down arrow and on the rungs with a superscript 0.

lower leg, respectively. Links, as usual, will be denoted by ℓ. On the legs they are labelled as $\ell_i^\uparrow$ (upper leg) or $\ell_i^\downarrow$ (lower leg), while on the rungs they are labelled ℓ_i^0.

We preserve the same formulation of $\mathbb{Z}_N$ LGT but in order to lighten our notation, we use the symbols V_i^0, U_i^0 for the operators defined on the rung i, and V_i^ρ, U_i^ρ with $\rho = \uparrow, \downarrow$ for the operators on the horizontal links of the upper and lower leg, respectively, to the right of the rung. In synthesis:

$$
\begin{aligned}
U_{\ell_i^0} \equiv U_i^0, \quad U_{\ell_i^\downarrow} \equiv U_i^\downarrow, \quad U_{\ell_i^\uparrow} \equiv U_i^\uparrow \\
V_{\ell_i^0} \equiv V_i^0, \quad V_{\ell_i^\downarrow} \equiv V_i^\downarrow, \quad V_{\ell_i^\uparrow} \equiv V_i^\uparrow,
\end{aligned}
\tag{3.50}
$$

and see Fig. 3.10. The plaquette operator on the right of the rung i will be labeled as U_i:

$$
U_i = U_i^\downarrow U_{i+1}^0 (U_i^\uparrow)^\dagger (U_i^0)^\dagger.
\tag{3.51}
$$
{eq:plaq_op_ladder}

Moreover, on a ladder the vertices are three-legged, so the Gauss operators are slightly modified:

$$
G_i^\uparrow = V_i^\uparrow (V_{i-1}^\uparrow)^\dagger (V_i^0)^\dagger \text{ and } G_i^\downarrow = V_i^\downarrow V_i^0 (V_{i-1}^\downarrow)^\dagger,
\tag{3.52}
$$
{eq:gauss_law_ladder}

where $G_i^\uparrow$ and $G_i^\downarrow$ refers, respectively, to the Gauss operators on the vertices $i^\uparrow$ and $i^\downarrow$. As a reference see Fig. 3.10.

Finally, we write explicitly the Hamiltonian for a $\mathbb{Z}_N$ LGT on a ladder:

$$
H^{\text{lad}}(\lambda) = -\sum_i \left[U_i + \lambda \left(V_i^\uparrow + V_i^\downarrow + V_i^0 \right) + \text{h.c.} \right].
\tag{3.53}
$$
{eq:ladder_hamiltonian}

For what concerns the super-selection sectors of the theory, non-contractible loops are possible now only in the $\hat{2}$ direction. Therefore, out of the Wilson loop operators in (3.39) only $\overline{W}_1$ is well defined, meaning that we can create non-contractible electric loops along the $\hat{1}$. Hence, only $\overline{S}_2$ in (3.39) (the 't
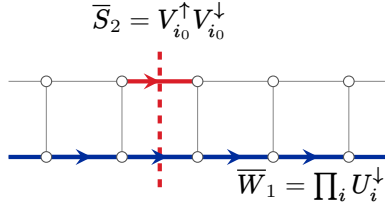
Figure 3.11. Picture of the non-local string operators $\overline{W}_1$ and $\overline{S}_2$ on the ladder.

Hooft string conjugate to W_1) can be used as a mean for distinguishing these different sectors. Explicitly, the Wilson loop $\overline{W}_1$ and $\overline{S}_2$ can be written as

$$\overline{W}_1 = \prod_i U_i^{\downarrow} \quad \text{and} \quad \overline{S}_2 = V_{i_0}^{\uparrow} V_{i_0}^{\downarrow}, \tag{3.54}$$

where i_0 is any chosen rung (see Fig. 3.11). Furthermore, it does not make sense to consider the 't Hooft string S_1 because it is equal to the product of all the Gauss operators on either one of the legs,

$$\overline{S}_1 = \prod_i G_i^{\downarrow} = \prod_i G_i^{\uparrow}, \tag{3.55}$$

so it always equal to the identity on physical states, signaling the obvious fact that we do not have non-contractible electric loops around the $\hat{2}$ direction. We can conclude that the physical Hilbert space can be decomposed in only N sectors as

$$\mathcal{H}_{\text{phys}} = \mathcal{H}_{\text{phys}}^{(0)} \oplus \mathcal{H}_{\text{phys}}^{(1)} \oplus \cdots \oplus \mathcal{H}_{\text{phys}}^{(N-1)}, \tag{3.56}$$

and in each sector we have that

$$S \left| \phi \right\rangle = \omega^n \left| \phi \right\rangle \quad \text{if} \quad \left| \phi \right\rangle \in \mathcal{H}_{\text{phys}}^{(n)}. \tag{3.57}$$

Due to the fact that the ladder is quasi one-dimensional, the presence of non-contractible electric loops can highly affects the physical states. Take the case of a $\mathbb{Z}_2$ theory, which is pictured in Fig. 3.12. It has just two sectors: $n = 0$ and $n = 1$. In the former all the physical configuration are made of closed loop, distributed along the $\hat{1}$ direction. While in the latter, the physical configurations are just deformations of of one single electric loop that goes around the ladder. This can make us reasonably believe that the two sectors might have completely different physical content.

Like in the two-dimensional case, the Hamiltonian can be reduced to a single super-selection sector. One of the main features of this is that once the sector is fixed, it is possible to write a duality transformation of the Hamiltonian to a pure one-dimensional *quantum clock model*, resolving entirely the *gauge symmetries*. Thanks to this duality map, we will see how that the different sectors have very different behaviour and each can have its own unique

$\mathbb{Z}_2$ sector $n = 0$

$\mathbb{Z}_2$ sector $n = 1$
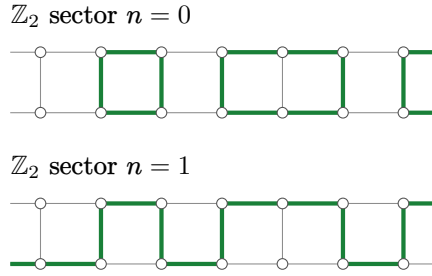
Figure 3.12. Example of two physical configurations (in the electric basis) in a $\mathbb{Z}_2$ theory in the two different super-selection sectors. This shows that states belonging to two different sectors can be quite different.

phase diagram. The latter is the object of discussion of the second part of this chapter, but before doing so we need to introduce the notion of *dualities* and, in particular, *the bond-algebraic approach to dualities*.

3.4 Dualities in physics

Duality is a simple yet powerful idea in physics. They can be intended as specific mathematical transformations connecting seemingly unrelated physical phenomena. They have been know for a long time, indeed a first example would be the duality of the electromagnetic field in the absence of sources, noticed by Heaviside in 1884. Generally in physics, the concept of duality is connected to ideas, like symmetries, mappings between different coupling regimes, perturbative expansions for strongly correlated systems, and the wave-particle duality of quantum mechanics [10, 11].

They play a major role in statistical physics and condensed matter. In statistical mechanics, dualities were introduced for the first time by Kramers and Wannier [12], who found a relation between the high temperature and low temperature regimes of the two-dimensional Ising mode. In this way, they were able to find the critical temperature years before Onsager solution [13]. In this case we speak of self-dualities, where the same model is mapped onto itself but in a different coupling regime. The essential legacy of Kramers and Wannier is the fact that self-dualities can put constraints on the phase boundaries and the exact location of critical points.

Not all dualities are self-dualities. In fact, it also possible to relate two apparently different physical models with a duality transformation. A known example is the Jordan-Wigner transformation [14, 15], where spin degrees of freedom (which are bosonic in nature) are mapped onto fermionic degrees of freedom in one-dimension [elaborare]. This duality shows that, in fact, there is not much difference between bosonic and fermionic degrees of freedom.

[forse aggiungere qualcosa in più]

3.4.1 The bond-algebraic approach

In the following section we will quickly review the bond-algebraic approach to dualities [11], because it offers a powerful and convenient way for dealing with duality transformations, in particular when gauge symmetries are involved. The concept of *bond-algebra* was first introduced in [16] and it exploits the fact that most *Hamiltonian are a sum of simple and (quasi)local terms*:

$$H = \sum_{\Gamma} \lambda_{\Gamma} h_{\Gamma}, \tag{3.58}$$

where Γ is a set of indices (e.g. the lattice sites but can be completely general) and λ_{Γ} are numbers (usually the couplings). Roughly speaking, by quasi-local we mean that a operator h_{Γ} involves a small number of degrees of freedom that are spatially near each other (for example nearest neighbour). The terms h_{Γ} are called *bond operators* (or simply *bonds*). From the bonds h_{Γ} we obtain a *bond algebra* $\mathcal{A}\{h_{\Gamma}\}$, which is the algebra of all the operators generated by all the possible products and sums of the bonds h_{Γ} and their Hermitian conjugates. In practical terms, given a set of bonds $\{h_{\Gamma}\}$, the bond-algebra $\mathcal{A}\{h_{\Gamma}\}$ is the algebra spanned by

$$\{\mathbb{1}, h_{\Gamma}, h_{\Gamma}^{\dagger}, h_{\Gamma}h_{\Gamma'}, h_{\Gamma}^{\dagger}h_{\Gamma'}, h_{\Gamma}h_{\Gamma'}^{\dagger}, h_{\Gamma}^{\dagger}h_{\Gamma'}^{\dagger}, h_{\Gamma}h_{\Gamma'}h_{\Gamma''}, \dots\}$$

By construction, $\mathcal{A}\{h_{\Gamma}\}$ is closed under the operation Hermitian conjugation, but since an Hamiltonian H is Hermitian then $h_{\Gamma}^{\dagger} = h_{\Gamma'}$ for some Γ'. Therefore, $\mathcal{A}\{h_{\Gamma}\}$ is simply spanned by

$$\{\mathbb{1}, h_{\Gamma}, h_{\Gamma}h_{\Gamma'}, h_{\Gamma}h_{\Gamma'}h_{\Gamma''}, \dots\}$$

Notice that the bonds h_{Γ} that generate $\mathcal{A}\{h_{\Gamma}\}$ do not need to be independent.

To make an example, consider the quantum Ising model with a transverse field, which is a chain of spin-$\frac{1}{2}$ with the Hamiltonian

$$H^{\text{Ising}}(h) = \sum_{i} \left(\sigma_i^z \sigma_{i+1}^z + h\sigma_i^x \right), \tag{3.59}$$

where the sums runs over the sites of the chain and h is the transverse field strength. Notice that the Hamiltonian is indeed a sum of quasi-local terms. In particular we have two types of terms: the interaction term $\sigma_i^z \sigma_{i+1}^z$ and the transverse field σ_i^x. They are local or quasi-local because they involve at most two neighbouring sites. These two set of terms are the bonds of the Hamiltonian H^{Ising} and our bond-algebra $\mathcal{A}\{\sigma_i^z \sigma_{i+1}^z, \sigma_i^x\}$ is spanned by

$$\{\mathbb{1}, \sigma_i^z \sigma_{i+1}^z, \sigma_i^z \sigma_{i+1}^z \sigma_j^z \sigma_{j+1}^z, \dots, \sigma_i^x, \sigma_i^x \sigma_j^x, \dots, \sigma_i^z \sigma_{i+1}^z \sigma_i^x, \dots\}.$$

It is important to point out that a single Hamiltonian H can have different bond algebras associated to it. In fact, a bond algebra is determined by the partitioning of the bonds in H. In principle, given any two decomposition of the same Hamiltonian,

$$H = \sum_{\Gamma} \lambda_{\Gamma} h_{\Gamma} = \sum_{\Sigma} \lambda'_{\Sigma} h'_{\Sigma},$$

one should expect $\mathcal{A}\{h_{\Gamma}\} \neq \mathcal{A}\{h'_{\Sigma}\}$ in general (see [11]). To make an example, consider the Hamiltonian

$$H = \sum_{i} (h_x \sigma_i^x + h_y \sigma_i^z).$$

We can either partition the bonds by taking σ_i^x and σ_i^z as generators separately or by taking $h_x \sigma_i^x + h_z \sigma_i^z$ as a single bond. In the former case we would obtain $\mathcal{A}\{\sigma^x, \sigma^z\}$, while in the latter we would have $\mathcal{A}\{h_x \sigma_i^x + h_z \sigma_i^z\}$. These two algebras are clearly different,

$$\mathcal{A}\{\sigma^x, \sigma^z\} \neq \mathcal{A}\{h_x \sigma_i^x + h_z \sigma_i^z\},$$

because $\mathcal{A}\{h_x \sigma_i^x + h_z \sigma_i^z\}$ is commutative, while $\mathcal{A}\{\sigma^x, \sigma^z\}$ is not.

In the framework of bond-algebra, quantum dualities can be formulated as *homomorphisms of bonds-algebras*. By homomorphism we intend a map Φ between two algebras $\mathcal{A}_1$ and $\mathcal{A}_2$ that preserves the linear and multiplicative structure of the algebras. In mathematical terms, given any $u, v \in \mathcal{A}_1$ and any complex number λ we have

$$\Phi(u + \lambda v) = \Phi(u) + \lambda \Phi(v) \quad \text{and} \quad \Phi(uv) = \Phi(u)\Phi(v).$$

To be more precise with our definition of quantum duality, consider two Hamiltonians H_1 and H_2 that act on Hilbert spaces of the same dimensions. They are said to be *dual* if there is some bond-algebra $\mathcal{A}_{H_1}$ of H_1 that is homomorphic to some bond-algebra $\mathcal{A}_{H_2}$ of H_2 and if the homomorphism $\Phi : \mathcal{A}_{H_1} \rightarrow \mathcal{A}_{H_2}$ maps H_1 onto H_2, $\Phi(H_1) = H_2$. These mappings do not need to be isomorphisms, especially when gauge symmetries are involved, and we will explain why later.

In a traditional approach to quantum dualities, one tries to map each degree of freedom of H_1 onto a degree of freedom of H_2. This can be rather cumbersome, because in this way most duality transformations appear to be non-local. In other words, one degree of freedom on one side may correspond to a large number of degrees of freedom on the other side. This is apparent, for example, with the Jordan-Wigner transformation, where a single spin is dual to a whole chain of fermions.

Quantum dualities in the bond-algebraic approach are instead *local*, meaning that each single *bond* h_{Γ_1} of H_1 is mapped onto a single bond h_{Γ_2} of H_2. This may translates in non-locality when treating elementary degrees of freedom and is due to the fact that the generators of a bond algebra are usually two- (or more) body operators and expressing the elementary degrees of freedom with these operators may require large (if not infinite) products.

An isomorphism like Φ is physically sound if it is *unitarily implementable* [11], which means that there is a unitary matrix $\mathcal{U}$ such that the duality isomorphism reads

$$\Phi(\mathcal{O}) = \mathcal{U} \mathcal{O} \mathcal{U}^\dagger, \quad \forall \mathcal{O} \in \mathcal{A}, \tag{3.60}$$

where $\mathcal{A}$ is the operator algebra of the model under investigation. [elaborate]

To make the bond-algebraic approach more clear we will consider two examples: the *quantum Ising model* and the *XY model*. In the first model we will see an examples of self-duality through the use of disorder variables, while in the latter an example of duality that relates two very different models using the Jordan-Wigner transformation. Our intent is not to shine new physics but to show how the use of bond-algebras offers a clear *formalism* for treating dualities of different kinds.

Quantum Ising model The Hamiltonian of the quantum Ising model with transverse field is already written in (3.59). We consider an infinite chain in order to avoid subtleties with the boundaries conditions, which can have major effects on a duality transformation. We recognize as bonds the operators $\{\sigma_i^x\}$ and $\{\sigma_i^z \sigma_{i+1}^z\}$, which generates $\mathcal{A}\{\sigma_i^z \sigma_{i+1}^z, \sigma_i^x\} \equiv \mathcal{A}^{\text{Ising}}$. The relations that defines the generators of $\mathcal{A}^{\text{Ising}}$ can be summarized as follows:

1. each bonds square to the identity operator

$$(\sigma_i^z \sigma_{i+1}^z)^2 = (\sigma_i^x)^2 = \mathbb{1}.$$

2. the bonds σ_i^x anticommutes only with $\sigma_i^z \sigma_{i+1}^z$ and $\sigma_{i-1}^z \sigma_i^z$

$$\{\sigma_i^x, \sigma_i^z \sigma_{i+1}^z\} = \{\sigma_i^x, \sigma_{i-1}^z \sigma_i^z\} = 0.$$

3. the bonds $\sigma_i^z \sigma_{i+1}^z$ anticommutes only with σ_i^x and σ_{i+1}^x

$$\{\sigma_i^z \sigma_{i+1}^z, \sigma_i^x\} = \{\sigma_i^z \sigma_{i+1}^z, \sigma_{i+1}^x\} = 0.$$

Given the symmetric roles that the basic bonds σ_i^x and $\sigma_i^z \sigma_{i+1}^z$ play with each other, we can set up a mapping Φ^{Ising} that exchange their roles:

$$\Phi^{\text{Ising}}(\sigma_i^z \sigma_{i+1}^z) = \sigma_i^x, \qquad \Phi^{\text{Ising}}(\sigma_i^x) = \sigma_{i-1}^z \sigma_i^z. \tag{3.61} \quad \text{\{eq:duality\_ising\}}$$
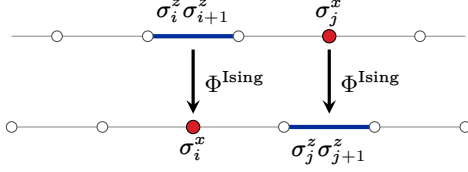
Figure 3.13. Pictorial representation of the duality map Φ^{Ising}, that maps the quantum Ising model on the same model on the dual lattice

This transformation can be extended to the whole $\mathcal{A}^{\text{Ising}}$ through the homomorphic property of Φ^{Ising}. It preserves all the important algebraic relationship and is one-to-one, hence it is an *isomorphism* of $\mathcal{A}^{\text{Ising}}$ onto itself. The Hamiltonian H^{Ising} is just an element of $\mathcal{A}^{\text{Ising}}$. We can apply Φ^{Ising} to H^{Ising} and use its homomorphic property, which yields

$$
\begin{aligned}
\Phi^{\text{Ising}}(H^{\text{Ising}}(h)) &= \sum_i \left(\Phi^{\text{Ising}}(\sigma_i^z \sigma_{i+1}^z) + h \Phi^{\text{Ising}}(\sigma_i^x) \right) \\
&= \sum_i \left(\sigma_i^x + h \sigma_{i-1}^z \sigma_i^z \right) \\
&= h \sum_i \left(\sigma_i^z \sigma_{i+1}^z + h^{-1} \sigma_i^x \right).
\end{aligned}
\tag{3.62}
$$

Notice that the indices in the sum can be freely shifted because we are working with an infinite number of sites. We have obtained

$$
\Phi^{\text{Ising}}(H^{\text{Ising}}(h)) = h H^{\text{Ising}}(h^{-1}),
\tag{3.63}
$$

henceforth Φ^{Ising} is a *self-duality* of (3.59). Notice that $H^{\text{Ising}}(h)$ is mapped onto itself but with the inverted coupling, $h \mapsto h^{-1}$. This means we can map the strongly coupled phase $h \gg 1$ into the weakly coupled phase $h \ll 1$ one and vice versa. What we have obtained is the quantum version Kramers-Wannier duality [12, 17].

If we think the term σ_i^x as living on the site i and of $\sigma_i^z \sigma_{i+1}^z$ as of living on the *link* between the site i and $i+1$, then the map Φ^{Ising} maps (3.59) onto the same model but on the *dual lattice*. In fact, the dual lattice of a chain is still a chain and the site term σ_i^x is mapped onto a link term $\sigma_i^z \sigma_{i+1}^z$ and vice versa.

We want to have a clearer physical picture of the duality map Φ^{Ising} and build a bridge with the traditional approach to dualities for the quantum Ising model. For this reason we want to find the elementary degrees of freedom of the dual model. The degrees of freedom of the dual model lives on the sites of the dual lattice, which corresponds to the links of the original lattice. On these new sites we again have spin-$\frac{1}{2}$ degrees of freedom and, for more clarity, we use μ^x and μ^z for referring to the Pauli matrices acting on these new spins. The dual site i corresponds to the link $(i, i+1)$, while the dual link $(i-1, i)$ corresponds to the site i.
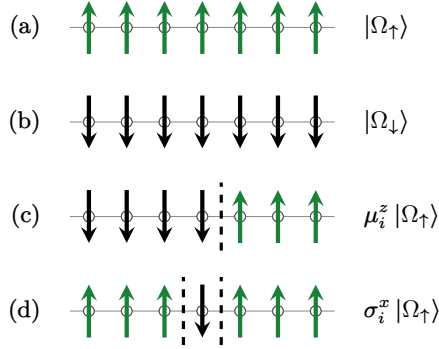
Figure 3.14. *(a)* and *(b)* ferromagnetic ground states $|\Omega_\uparrow\rangle$ and $||\Omega_\downarrow\rangle\rangle$. *(c)* kink created on the link between site i and $i+1$ by the operator μ_i^z. *(d)* kink-antikink pairs created around the site i by the spin flip σ_i^x.

From (3.61), we already know that

$$\sigma_i^z \sigma_{i+1}^z = \mu_i^x \quad \text{and} \quad \sigma_i^x = \mu_{i-1}^z \mu_i^z. \tag{3.64}$$

The role of μ_i^x is evident, it measure the alignment of two neighbouring spins on the sites i and $i+1$, while the meaning of μ_i^z is still opaque. We can arrive at the definition of μ_i^z by exploiting the map Φ^{Ising}. The bond $\mu_{i-1}^z \mu_i^z$ corresponds to the image of σ_i^x through Φ^{Ising}, so we know how they are mapped. Then, if we isolate μ_i^z with an infinite product, we then obtain

$$\mu_i^z = \prod_{j=-\infty}^{i} \mu_{j-1}^z \mu_j^z = \prod_{j=-\infty}^{i} \sigma_j^x. \tag{3.65} \quad \text{\{eq:def\_mu\_z\}}$$

We see that μ_i^z flips all the spins before the i-th site. From (3.65), we can see the non-local origin of the dual degrees of freedom in traditional dualities. When working with two, or more, body terms, in order to isolate a single body term the use of large, or infinite, product is necessary.

To understand the role of μ_i^x and μ_i^z consider now the ferromagnetic ground states $|\Omega_\rho\rangle$ of (3.59), where $\rho = \uparrow, \downarrow$. Say we start from $|\Omega_\uparrow\rangle$. The action of μ_i^z on $|\Omega_\rho\rangle$ is creates a *kink*, which is a domain wall between two ordered regions. From this point of view, a single spin-flip $\sigma_i^x |\Omega_\uparrow\rangle$ creates a *kink-antikink pair*.

3.4.2 Gauge-reducing dualities

In this section we will review the notion of *gauge-reducing dualities*. Gauge symmetries are *local symmetries* of the model that signal the presence of *redundant degrees of freedom*, in fact gauge invariance can be thought as a set of *local constraints* on the elementary degrees of freedom of the model. This means that the state space of the model is larger than set of physical states and these are exactly the states that are invariant under the action of the gauge symmetries, which would mean that they satisfies the local constraints of the model. The same can be applied to the Hermitian operators and the

observables of the model. An Hermitian operator represent a physical observable only if it commutes with the gauge symmetries, which makes them gauge invariant.

When dealing with a gauge model, it would be natural to assume that, in order to establish a duality with any gauge symmetries, these have to be eliminated from the former model. In other terms, that it would be necessary to project out the operator content on the subspace of physical states first or proceed with gauge-fixing. Although this is a common and traditional approach to dualities, with bond algebras this is not strictly necessary. As stated in [11], with the bond-algebraic approach one can find mappings to models without any gauge symmetry that preserve all the important algebraic properties.

The procedure goes as follows: consider a gauge model and let H_{G} be its Hamiltonian and G_Γ its gauge symmetries. Naturally, an operator is said to be gauge-invariant only if it commutes with all the G_Γ and clearly the Hamiltonian has to be gauge-invariant, hence $[H, G_\Gamma] = 0$. Now let H_{GR} be the dual Hamiltonian of a non-gauge model. A *gauge-reducing duality* Φ_{GR} maps H_{G} onto H_{GR} while making all the gauge symmetries of the former model trivial, which means:

$$\Phi_{GR}(H_{\mathrm{G}}) = H_{\mathrm{GR}}, \qquad \Phi_{GR}(G_\Gamma) = \mathbb{1}, \quad \forall \Gamma. \tag{3.66}$$

Unlike the dualities in Sec. 3.4.1, a gauge-reducing duality like Φ_{GR} has to be implementable as a *projective unitary operator* $\mathcal{U}$. Formally, this can be written as

$$\Phi_{\mathrm{GR}}(\mathcal{O}) = \mathcal{U}\mathcal{O}\mathcal{U}^\dagger, \quad \mathcal{U}\mathcal{U}^\dagger = \mathbb{1}, \quad \mathcal{U}^\dagger\mathcal{U} = P_{\mathrm{GI}} \tag{3.67}$$

where P_{GI} is the projector of the subspace of gauge-invariant states, i.e. $G_\Gamma |\psi\rangle = |\psi\rangle$ for all Γ. Roughly speaking, this projective unitary operator can be represented as rectangular matrix that preserves the norm of gauge-invariant states while projecting out all the other states.

A clear example of a gauge-reducing duality is provided by the $\mathbb{Z}_N$, $d = 2$ gauge model

$$H_{\mathrm{G}} = \sum_r \left(V_{(r,\hat{1})} + V_{(r,\hat{2})} + \lambda U_r \right). \tag{3.68}$$

Its group of gauge symmetries is generated by (3.36). In the simplest case where $N = 2$, the V's can be represented by the Pauli operators σ^z and the U's by σ^x. In so doing, the Gauss operator becomes

$$G_r = \sigma^z_{(r,\hat{1})} \sigma^z_{(r,\hat{2})} \sigma^z_{(r,-\hat{1})} \sigma^z_{(r,-\hat{2})}, \tag{3.69} \quad \text{\{eq:gauss\_operator\_Z2\}}$$

and commutes with H_{G} and with the bonds $\left\{\sigma^z_{(r,\hat{1})}, \ \sigma^z_{(r,\hat{2})}, \ U_r\right\}$. In other words, the bond algebra they generate is gauge-invariant, and satisfy three simple relations: (i) all the bonds square to the identity, (ii) each spin σ^z anti-commutes with two adjacent plaquettes operators U, and (iii) each plaquette operator U anti-commutes with four spins σ^z. This set of relations are identical to those satisfied by the bonds of the $d = 2$ quantum Ising model, and the mapping is the following:

$$
\begin{aligned}
\Phi\left(\sigma^z_{(r,\hat{1})}\right) &= \sigma^x_{(r-\hat{2})}\sigma^x_r, \\
\Phi\left(\sigma^z_{(r,\hat{2})}\right) &= \sigma^x_{(r-\hat{1})}\sigma^x_r, \\
\Phi(U_r) &= \sigma^z_r.
\end{aligned}
\tag{3.70}
$$
{eq:duality_2d}

Thus, Φ maps H_{G} to H_{Ising}, if we identify the constants $\lambda \leftrightarrow h$ and $1 \leftrightarrow J$. Moreover, Φ is a gauge-reducing duality homomorphism, since $\Phi(G_r) = \mathbb{1}$. Therefore, H_{Ising} represents all the physics contained in H_{gauge}, but without all the gauge redundancies. In the general case, i.e. for a generic $\mathbb{Z}_N$ symmetry, the duality leads to an N-clock model [18].

3.5   Dualities in two dimensions

[da scrivere]

3.6   Dualities of the ladder

3.6.1   Clock models

In this section we will deal with a class of generalizations of the quantum Ising model known as *clock models* [19, 20], which shows a resemblance to the $\mathbb{Z}_N$ LGT models we introduced previously. This similarity will later be exploited in order to obtain a complete description of the LGT models without any redundant gauge-symmetry.

For a discussion about clock models we start from the Hamiltonian of the quantum Ising model with a transverse field, which can simply be written as

$$
H = -\sum_i \sigma^z_i \sigma^z_{i+1} - h\sum_i \sigma^x_i,
\tag{3.71}
$$
{eq:ising_hamiltonian_duality}

where $\sigma^{x,z}_i$ are the usual 2×2 Pauli matrices for each site i:

$$
\sigma^x_i = \begin{pmatrix} 0 & 1 \\ 1 & 0 \end{pmatrix}, \quad \sigma^z_i = \begin{pmatrix} 1 & 0 \\ 0 & -1 \end{pmatrix}.
\tag{3.72}
$$

43

They are a set of unitary matrices that commute on different sites, while on the same site they anticommute $\sigma^x \sigma^z = -\sigma^z \sigma^x$. Another way to put it is to say that the exchange of σ_x and σ_z on the same site produces a phase $e^{i\pi} = -1$.

Clock models can be thought as generalizations of the quantum Ising model, but not to higher spins. A p-state clock model (or simply a p-clock model) utilizes a set of unitary operators that generalize the algebra of Pauli matrices in the following sense: the operators σ_x and σ_z get promoted to the *clock operators* X and Z, respectively, which are $p \times p$ unitary matrices whose exchange produces a phase $\omega = e^{i2\pi/p}$, instead of -1. The algebraic properties of these clock operators X and Z can be summarized as follows:

$$XZ = \omega ZX, \qquad X^p = Z^p = \mathbb{1}_p,$$
$$X^\dagger = X^{-1} = X^{p-1}, \quad Z^\dagger = Z^{-1} = Z^{p-1}$$

(3.73) {eq:clock_operator_algebra}

We see that the Schwinger-Weyl algebra in (3.31) and the clock operator algebra in (3.73) are basically the same, but there are some key differences to point out betweens a $\mathbb{Z}_N$ LGT and a p-clock model.

The degrees of freedom of a $\mathbb{Z}_N$ LGT live on the links of the lattice while in a p-clock model they live on the sites. But the most important aspect is that we don't have any gauge symmetry in a p-clock model, hence we do not have to impose any local constraints or physical conditions. These models can be derived as the quantum Hamiltonians of the classical 2D vector Potts model, which is a discretization of the 2D planar XY model [21].

A typical p-clock model Hamiltonian with transverse field has the form

$$H^{\text{clock}}(\lambda) = -\sum_i Z_i Z_{i+1} - \lambda \sum_i X_i + \text{h.c.}$$

(3.74) {eq:clock_hamiltonian}

which is, as expected, very similar to the quantum Ising Hamiltonian in (3.71). Furthermore, just like the latter, p-clock models with only transverse field are *self-dual*: the clocks can be mapped into the kinks (or domain walls) and one would obtain the same exact Hamiltonian description but with inverted transverse field [21]. For $p < 5$, the clock models presents a self dual point in $\lambda = 1$, that separates an ordered phase from a disordered one. On the other hand, for $p \geq 5$ we have an intermediate continuous critical phase between the ordered and disordered phase with two BKT transition points, which are related to each other through the self-duality [22].

These models have been thoroughly studied, even with the addition of a longitudinal field $\propto Z_i$ [23] or chiral interactions. In particular, in the case of chiral interactions, it was shown [24] that the Hamiltonian (3.74) can be mapped to a parafermionic chain through a Fradkin-Kadanoff transformation,
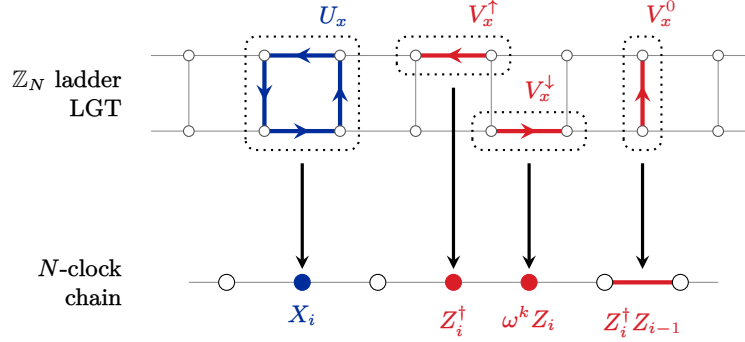
Figure 3.15. Visual representation of the duality transformation from the $\mathbb{Z}_N$ ladder LGT to the N-clock model. The plaquette operator U_x and the electric operators $V^\uparrow$ and $V^\downarrow$ map to one-site operators in the clock model, while the remaining electric operator V^0 maps to a hopping term between nearest neighbouring sites.

and in presence of a $\mathbb{Z}_3$ symmetry, it shows three different phases [25], if open boundaries are implemented: a trivial, a topological and an incommensurate (IC) phase. The case which presents a real longitudinal field term was considered in [26], where some of the critical exponents have been estimated. The general case, where chiral interactions are included in a $\mathbb{Z}_N$ model, has been studied in [24]. Here, the author considered the model as an extension of the Ising/Majorana chain and found the edge modes of the theory. He also calculated the points, in the parameter space, where the model is integrable or 'superintegrable'. All these studies are motivated by theoretical interest and recent experiments, which can be analysed by the above models [27].

3.6.2 Duality onto clock models

In this section we will show how to construct a mapping of the $\mathbb{Z}_N$ ladder LGT onto a N-clock model on a chain with a transversal field and a longitudinal field, the latter depending on the topological sector of the ladder LGT.

The first step is the decomposition of the set of bonds in (3.40). Obviously, the magnetic terms $U_\square$ have to be separated from the electric terms V_ℓ, but the latter cannot be all treated the same. It is clear from the geometry of the ladder, that the links ℓ^0 have a different role when compared with the links $\ell^\uparrow$ and $\ell^\downarrow$, because the former are *domain walls* while the latter are not. Therefore, the duality transformation has to distinguish between the vertical links and horizontal links. Furthermore, also the top links $\ell^\uparrow$ and bottom links $\ell^\downarrow$ have to be treated separately because the electric operator on them have different commutation relations with the plaquette operators. In fact, using

the notation introduced in Sec. 3.3, we have

$$U_x V_x^\downarrow = \omega V_x^\downarrow U_x, \qquad U_x V_x^\uparrow = \omega^{-1} V_x^\uparrow U_x. \tag{3.75}$$

and indeed they acquire different phases.

The plan is to associate to each plaquette a clock degree of freedom, hence we identify a plaquette $\square_x$ with a site i of a clock chain and the magnetic flux of a plaquette becomes the "fundamental gauge invariant degree of freedom" of the LGT ladder model. Given the fact that we are working in the electric basis, we chose for convenience to map the $\mathbb{Z}_N$ magnetic operator U_x to the "momentum" operator X_i of the N-clock chain. The electric field on a vertical link ℓ^0 is the result of the flux difference between the two plaquettes that it separates, which suggests that the operator V_{ℓ^0} have to be mapped to a kinetic-type term like $Z_i^\dagger Z_{i-1}$. This can be readily verified. From (3.51) we get

$$V_x^0 U_x = \omega^{-1} U_x V_x^0, \qquad V_x^0 U_{x-1} = \omega U_{x-1} V_x^0,$$

therefore the maps

$$U_x \mapsto X_i, \qquad V_x^0 \mapsto Z_i^\dagger Z_{i-1},$$

clearly conserves the commutation relations of U_x and V_x^0.

For now we are left with task of finding a suitable mapping of $V^\uparrow$ and $V^\downarrow$. With respect to the other bonds of the theory, both of them commute with V^0 while for (3.75) holds for U_x. Hence, a suitable and general mapping of $V^\uparrow$ and $V^\downarrow$ can be:

$$V_x^\downarrow \mapsto c_i^\downarrow Z_i, \qquad V_x^\uparrow \mapsto c_i^\uparrow Z_i^\dagger, \tag{3.76}$$

where $c_i^\downarrow$ and $c_i^\uparrow$ are complex numbers. Although, they cannot be any complex number. Both $V_x^\downarrow$ and $V_x^\uparrow$ have to be mapped onto unitary operators, which limits the numbers $c_i^\downarrow$ and $c_i^\uparrow$ to be *complex phases*.

To further constraint the value of these coefficients, we can use the Gauss law. In particular, given the fact that we are looking for a gauge-reducing duality, the aim is to make the Gauss law trivial. Using the mappings (3.6.2) and (3.76) in (3.52) yields

$$\begin{aligned}
G_x^\uparrow &\mapsto (c_i^\uparrow Z_i^\dagger)(c_{i-1}^\uparrow Z_{i-1}^\dagger)(Z_i^\dagger Z_{i-1})^\dagger = c_i^\uparrow (c_{i-1}^\uparrow)^*, \\
G_x^\downarrow &\mapsto (c_i^\downarrow Z_i^\dagger)(Z_i^\dagger Z_{i-1})(c_{i-1}^\downarrow Z_{i-1}^\dagger) = c_i^\downarrow (c_{i-1}^\downarrow)^*
\end{aligned} \tag{3.77}$$

Gauss law have to be satisfied in a pure gauge theory, which mean that we have to impose $G_x^\uparrow = \mathbb{1}$ and $G_x^\downarrow = \mathbb{1}$ for all x. This is only possible if

$$c_i^\downarrow = c^\downarrow, \qquad c_i^\uparrow = c^\uparrow, \qquad \forall i. \tag{3.78}$$

Furthermore, thanks to (3.77) we also know how to introduce static matter into this duality, because it can be thought as a violation of the Gauss law. We just have to change the phases $c_i^\uparrow$ and $c_i^\downarrow$.

The last factor to consider is how the $c^\uparrow$ and $c^\downarrow$ are related on the same site i. In this regard, the topological sectors of the theory come to the rescue. As established in Sec. 3.3, the topological sectors are identified by the eigenvalue of S_2 in (3.39), which in the ladder geometry becomes

$$S_2 = V_x^\uparrow V_x^\downarrow \tag{3.79}$$ {eq:top_string_op_ladder}

for any fixed x. Its eigenvalue are simply ω^k, for $k = 0, \ldots, N-1$.

Given a topological sector ω^k, using the mapping (3.76) on (3.79) yields

$$S_2 \longmapsto (c^\uparrow Z_i^\dagger)(c^\downarrow Z_i) = c^\uparrow c^\downarrow = \omega^k. \tag{3.80}$$

From here, in order to solve for the coefficients $c^\uparrow$ and $c^\downarrow$, one needs only to fix one of the to 1 and the other to ω^k. We choose to fix these coefficients as follows:

$$c^\uparrow = 1, \qquad c^\downarrow = \omega^k. \tag{3.81}$$

In conclusion, we summarize the duality mapping for the topological sector ω^k of the $\mathbb{Z}_N$ LGT on a ladder:

$$\begin{aligned} U_x &\longmapsto X_i, & V_x^0 &\longmapsto Z_i^\dagger Z_{i-1}, \\ V_x^\uparrow &\longmapsto Z_i^\dagger, & V_x^\downarrow &\longmapsto \omega^k Z_i. \end{aligned} \tag{3.82}$$ {eq:ladder_duality}

With the duality (3.82), from (3.53) in the sector $(\omega^k, 1)$ we obtain

$$H_{\text{ladder}}(\lambda) \longmapsto \lambda H_{\text{clock}}(\lambda^{-1}) \tag{3.83}$$

where

$$H_{\text{clock}}(\lambda^{-1}) = -\sum_i Z_i^\dagger Z_{i-1} - \lambda^{-1} \sum_i X_i - (1 + \omega^k) \sum_i Z_i + \text{h.c.} \tag{3.84}$$ {eq:dual_ladder_hamiltonian}

We see that (3.84) is a clock model with both *transversal* and *longitudinal* fields. In particular, the longitudinal field carries the information of the topological sector of the ladder model.

Interestingly, for N even the sector $k = N/2$ has a special role. Within this sector $\omega^k = -1$, for which the *longitudinal field disappears* and H_{clock} reduces to self-dual quantum clock models with a known quantum phase transition. This phase transitions for $k = N/2$ can be put in correspondence with a *confined-deconfined* transition, which will be discussed in much more detail in the next section.

Let us remark that the complex coupling $(1 + \omega^n)$ does not make the Hamiltonian (3.84) necessarily chiral [24, 28]. In fact, one can get the real Hamiltonian

$$H_N = H_p(1/\lambda) - 2\cos\left(\frac{\pi n}{N}\right) \sum_i \left(Z_i + Z_i^\dagger\right). \tag{3.85}$$

by absorbing the complex phase in the Z_i-operators, with the transformation $Z_i \mapsto w^{-n/2} Z_i$. This transformation globally rotates the eigenvalues of the Z_i-operators, while preserving the algebra relations. For n even, this is just a permutation of the eigenvalues, meaning that it does not affect the Hamiltonian spectrum. Instead, for n odd, up to a reorder, the eigenvalues are shifted by an angle π/N, i.e. half the phase of ω. The energy contribution of the extra term in (3.85) depends on the real part of these eigenvalues and for n odd we obtain that the lowest energy state is no longer unique, in fact it is doubly degenerate. This means that for $\lambda \to \infty$, where the extra term becomes dominant, we expect an ordered phase with a doubly degenerate ground state. Finally, one can easily prove that the sectors n and $N - n$ are equivalent [1].

3.7   A case study: $N = 2, 3$ and 4

3.7.1   Investigating the phase diagram

We wish to study the phase diagram of the $\mathbb{Z}_N$ LGT phase diagram, in particular we are interested in any *confined* or *deconfined* phase. In a pure gauge theory, these phases are investigated non-local order parameters like the *Wilson loop* (not be confused with the non-contractible Wilson loops in (3.39)) or *string tension*. This is because we expect the deconfined phase to be a topological phase, which can be investigated only with non-local order parameters.

Given a closed region $\mathcal{R}$, a Wilson loop operator $W_\mathcal{R}$ is defined as

$$W_\mathcal{R} = \prod_{\square \in \mathcal{R}} U_\square. \tag{3.86}$$

Alternatively, considering the oriented boundary $\partial\mathcal{R}$ one can write

$$W_\mathcal{R} = \prod_{\ell \in \partial\mathcal{R}} U_\ell, \tag{3.87}$$

where the Hermitian conjugate is implied everytime we move in the negative directions. It is also implied that the curve $\partial\mathcal{R}$ is a contractible loop. Wilson

---

[1]For the sector $N - n$ we have that the overall factor $\cos(\pi(N-n)/N)$ is just $-\cos(\pi n/N)$. The minus sign can then be again absorbed into the Z's operators. This overall operation is equivalent to the mapping $Z \mapsto \omega^{-n/2} Z$ for the sector $N - n$.

showed in [1] that quark confinement is related to the expectation value $\langle W_{\mathcal{R}} \rangle$ of a Wilson loop, which can be thought as a gauge field average on a region. In particular, in the presence of quark confinement the gauge field average follows an *area law*, where it decays exponentially with the area enclosed by $\mathcal{R}$. On the other hand, in the deconfined phase we have a *perimeter law*, where the gauge field average decays exponentially with the perimeter of $\mathcal{R}$.

Unfortunately on a ladder geometry there is not much difference between the area and the perimeter of a Wilson loop. In fact, in units of the lattice spacing, the area of a Wilson loop over n plaquettes is n while its perimeter is just $2n + 2$. They both grow linearly. Nonetheless, we can still look at the behaviour of the Wilson loop, for a fixed length, at different couplings λ.

When the coupling λ in (3.40) is equal to zero, the Toric Code is recovered and in any of its topological sector the ground state is the equal superposition of all the states with any number of closed electrical loops, in a similar fashion to coherent states. This makes the Toric Code a *quantum loop gas*, which is a *deconfined phase*. Furthermore, the operator $W_{\mathcal{R}}$ in (3.86) creates an electrical loop around the region $\mathcal{R}$. From the constraints it can easily be proved that $W_{\mathcal{R}}$ leaves the Toric Code ground states unchanged, showing in fact that they behaves as coherent states, which leads to $\langle W_{\mathcal{R}} \rangle = 1$.

Therefore, $\langle W_{\mathcal{R}} \rangle \approx 1$ signals a deconfined phase and on the other hand a vanishing $\langle W_{\mathcal{R}} \rangle \approx 0$ corresponds to confined phase. For this reason, even tough we lack an area/perimeter law on the ladder geometry it is still sensible to look at the behaviour of the Wilson loop.

Another possible approach for investigating the phase diagram is to use the *string tension*. In two dimensions, given an *open* curve $\tilde{\mathcal{C}}$ on the dual lattice $\tilde{\mathbb{L}}$ we can construct an open 't Hooft string operator $S_{\tilde{\mathcal{C}}}$ as

$$S_{\tilde{\mathcal{C}}} = \prod_{\ell \in \tilde{\mathcal{C}}} V_{\ell} \tag{3.88}$$

with the usual caveat: we have to take the Hermitian conjugate everytime the path goes in the negative direction. Then the string tension is just the expectation value $\langle S_{\tilde{\mathcal{C}}} \rangle$ it is called in this way because it related to the potential energy (tension) between two magnetic fluxes created at the ends of the curve $\tilde{\mathcal{C}}$. Henceforth, in a deconfined phase $\langle S_{\tilde{\mathcal{C}}} \rangle \approx 0$, which means that the magnetic fluxes can be moved freely with no cost in energy, like in the Toric Code.

3.7.2 Implementing the Gauss law

In order to proceed with ED one has to provide two things: (i) the basic operators of the theory (U_{ℓ} and V) and (ii) the physical (gauge-invariant) Hilbert space, given a lattice with specified size and boundary conditions.
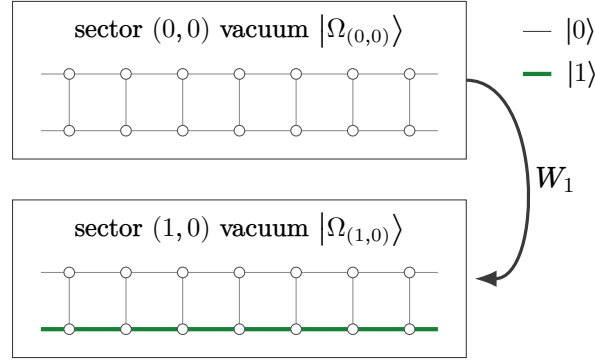
Figure 3.16. The different "Fock vacua" $\big|\Omega_{(0,0)}\big\rangle$ and $\big|\Omega_{(1,0)}\big\rangle$ of the $\mathbb{Z}_2$ ladder LGT. The latter can be obtained from the former by applying the Wilson loop operator W_1. The states $|0\rangle$ and $|1\rangle$ refers to the eigenstates of the electric field operator V, which is just σ_z in the $\mathbb{Z}_2$ model.
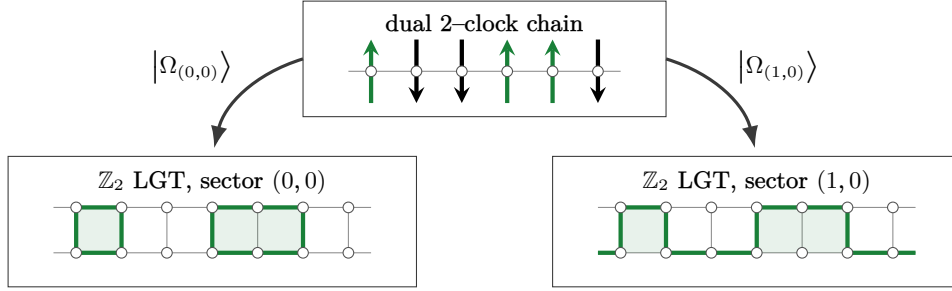
Figure 3.17. Duality between the states of a 2–chain and the states of a $\mathbb{Z}_2$ ladder LGT in the different sectors $(0,0)$ (no non-contractible electric loop) and $(1,0)$ (one non-contractible loop around the ladder). In the sector $(0,0)$ it is evident that all the physical states contains closed electric loops. On the other hand, in the sector $(1,0)$ the physical states are all the possible deformation of the electric string that goes around the ladder.

The former was fairly standard while the latter was the most challenging and interesting part to implement.

If one has to work with only physical states, then one has to check the Gauss law for every site. With the brute-force method one has to generate all the possible states and then filter out all the states that violate Gauss law. This method, like any brute-force method, is not very efficient. To better exemplify this, consider a $\mathbb{Z}_2$ theory on a $L \times L$ periodic lattice, which have L^2 sites and $2L^2$ links. There are therefore 2^{2L^2} possible states and for each one up to L^2 checks (one per site) has to be performed. Moreover, it can be showed that there are only 2^{L^2} *physical* states. As a result, the construction of the physical Hilbert space involves $O(L^2 2^{2L^2})$ operations in a search space of 2^{2L^2} objects for finding only 2^{L^2} elements. All of this makes the inefficiency of this brute-force method very clear, even for moderately small lattices.

The approach adopted in this work exploits the duality in Sec. 3.6 and represents an *exponential speedup* with respect to the brute-force method. It is not a search or pattern-matching algorithm, each physical configuration is procedurally generated from the states of the dual clock model.

Given a $\mathbb{Z}_N$ LGT on a lattice of size $L \times L$, we consider the dual N-clock model on a similar lattice with $A = L^2$ sites, In its Hilbert space $\mathcal{H}_{N\text{-clock}}$ there is no gauge constraint or physical condition to apply, hence the basis is the set of states $|\{s_i\}\rangle \equiv |s_0 s_1 \cdots s_{A-1}\rangle$ with each $s_i = 0, \ldots, N-1$. From a state $|\{s_i\}\rangle$ we can obtain the dual state for the LGT model in the (m, n) sector:

$$|\{s_i\}\rangle \longmapsto \prod_{i=0}^{A-1} U_i^{s_i} \left| \Omega_{(n,m)} \right\rangle, \tag{3.89}$$

where U_i is the plaquette operator on the i-th plaquette and $\left| \Omega_{(m,n)} \right\rangle$ is the "Fock vacuum" of the (m, n) sector. As one can deduce, the information about the topological sector of the LGT model is carried in the Hamiltonian $H_{N\text{-clock}}$ of the dual clock model and not in the structure of $\mathcal{H}_{N\text{-clock}}$. This means that is possible to build each sector $\mathcal{H}_{\text{phys}}^{(n,m)}$ in (3.45) from $\mathcal{H}_{N\text{-clock}}$, with the appropriate $\left| \Omega_{(n,m)} \right\rangle$.

Moreover, also the "Fock vacuums" $\left| \Omega_{(n,m)} \right\rangle$ can be obtained easily, thanks to (3.49):

$$\left| \Omega_{(n,m)} \right\rangle = (W_1)^n (W_2)^m \left| \Omega_{(0,0)} \right\rangle, \tag{3.90}$$

where $\left| \Omega_{(0,0)} \right\rangle$ is just the state $|000 \cdots 0\rangle$ (in the electric basis) for all the links.

If we want to quantify the obtained speedup with this method, in the case of a $\mathbb{Z}_2$ theory on a square lattice $L \times L$ there are 2^{L^2} possible clock configurations. For each configuration, there are at most L^2 magnetic fluxes to apply. This translates into $O(L^2 2^{L^2})$ operations, which is an exponential speedup with respect to the brute-force (notice the lack of a factor 2 in the exponent) and is easily generalizable for any $\mathbb{Z}_N$. Although, it remains an open question whether a similar method can be applied for gauge theories with non-Abelian finite groups.

3.7.3 Non-local order parameters

In Sec. 3.7.1 we talked about how a Wilson loop $W_{\mathcal{R}}$ or an 't Hooft string $S_{\tilde{\mathcal{C}}}$ work as a non-local order parameters and can be used to investigated the phase diagram of a $\mathbb{Z}_N$ LGT model. In fact, we analyzed these exact observables on the ladder geometry for $N = 2, 3$ and 4. Given a ladder of length L, the Wilson loop W have been calculated over a region that covers the first $L/2$

plaquettes, while the 't Hooft string cuts through the first $L/2$ plaquettes (see Fig. 3.18).
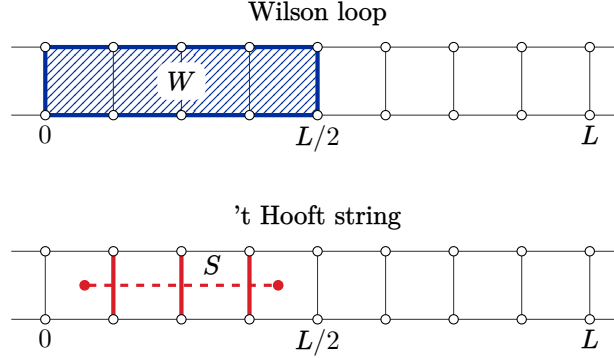
Figure 3.18. The non-local order parameters that have been used for investigating the phase diagram of $\mathbb{Z}_N$ ladder LGT. *Top*: half-ladder Wilson loop. *Bottom*: half-ladder 't Hooft string operator.

We wish to investigate the presence of a *deconfined-confined phase transition* (DCPT) for a given $\mathbb{Z}_N$ ladder LGT. In a pure gauge theory, these phases can be detected with the perimeter/area law for Wilson loops [1], which can be expressed as the products of magnetic operators over a given region. Unfortunately, in a ladder geometry there is not much difference between the area and the perimeter of a loop, since they both grow linearly in the size system L.

Nonetheless, we expect a phase transition by varying λ [7–9] that can still be captured by an operator like $W_{\mathcal{R}} = \prod_{i \in \mathcal{R}} U_i$, the product of magnetic operators U's over a (connected) region $\mathcal{R}$. Indeed, when $\lambda = 0$, the Hamiltonian (3.53) is analogous to a Toric Code [29] which is known to be in a deconfined phase, where the (topologically distinct) ground states are obtained as uniform superpositions of the gauge-invariant states, i.e. closed electric loops. On these ground states $\langle W_{\mathcal{R}} \rangle = 1$, hence a value $\langle W_{\mathcal{R}} \rangle \approx 1$ signals a deconfined phase. On the other hand, when $\lambda \to \infty$, the electric loops are suppressed, hence $\langle W_{\mathcal{R}} \rangle \approx 0$, signalling a confined phase.

In the dual clock model picture, the Wilson loop translates to a disorder operator [17], which means that a deconfined phase can be thought of as a paramagnetic (or disordered) phase, while the confined phase is like a ferromagnetic (or ordered) phase. Moreover, the longitudinal field breaks the N-fold symmetry of the ferromagnetic phase into a one-fold or two-fold degeneracy, depending on the parity (n even/odd) of the super-selection sector.

We study the $\mathbb{Z}_N$ LGT on a ladder numerically through *exact diagonal-*

ization, by evaluating the half-ladder Wilson loop, i.e.

$$W = U_1 U_2 \cdots U_{L/2}, \qquad (3.91)$$

and working in the restricted physical Hilbert space $\mathcal{H}_{\text{phys}}^{(n)}$ ($n = 0, \ldots, N-1$), which has dimension N^L, much smaller than N^{3L} (the dimension of the total Hilbert space).

The naive and brute-force method for building $\mathcal{H}_{\text{phys}}$ would require checking the Gauss law at every site (which are $O(3L)$ operations) for all the possible N^{3L} candidate states. On the other hand, the gauge-reducing duality to clock models provides a faithful and efficient method for building the N^{L+1} basis states of $\mathcal{H}_{\text{phys}}$, yielding a major speedup with respect to the naive method. The procedure is quite simple and it consists in treating a clock state as a plaquette flux state in the following way. Let $|\Omega_0\rangle$ be the vacuum state where all the links are in the $|0\rangle$ state. For each sector n we can build a "vacuum" state $|\Omega_n\rangle$ by applying $\overline{W}$ in (3.39) n times on the true vacuum, i.e. $|\Omega_n\rangle = \overline{W}^n |\Omega_0\rangle$. Then, let $|s_1 s_2 \cdots\rangle$ be a configuration of the dual N-clock model, where $s_i = 0, \ldots, N-1$. Now, the equivalent ladder state in the n-th sector can be obtained with $\prod_i U_i^{s_i} |\Omega_n\rangle$.

In the following, we present the results with $N = 2, 3$ and 4, for different lengths.

Results for $N = 2$ As a warm up, we consider the $\mathbb{Z}_2$ ladder LGT, with lengths $L = 10, 12, \ldots, 18$. This model is equivalent to a $p = 2$ clock model, which is just the quantum Ising chain, with only two super-selection sectors for $n = 0$ and $n = 1$. When $n = 1$, the Hamiltonian contains only the transverse filed and is integrable [23]. Thus, we expect a critical point for $\lambda \simeq 1$, which will be a DCPT in the gauge model language. This is clearly seen in the behaviour of the half-ladder Wilson loop, as shown in the lower panel of Fig. 3.19. For $n = 0$, both the transverse and longitudinal fields are present, the model is no longer integrable [30–32] and we expect to always see a confined phase, except for $\lambda = 0$. This is indeed confirmed by the behaviour of the half-ladder Wilson loop shown in the upper panel of Fig. 3.19.

We can further characterize the phases of the two sectors by looking at the structure of the ground state, for $\lambda < 1$ and $\lambda > 1$, which is possible thanks to the exact diagonalization. In particular, in the deconfined phase of the sector $n = 1$, the ground state is a superposition of the deformations of the non-contractible electric string that makes the $n = 1$ vacuum $|\Omega_1\rangle$. For this reason, this phase can be thought as a *kink condensate* [17] (which is equivalent to a paramagnetic phase), where each kink corresponds to a deformation of
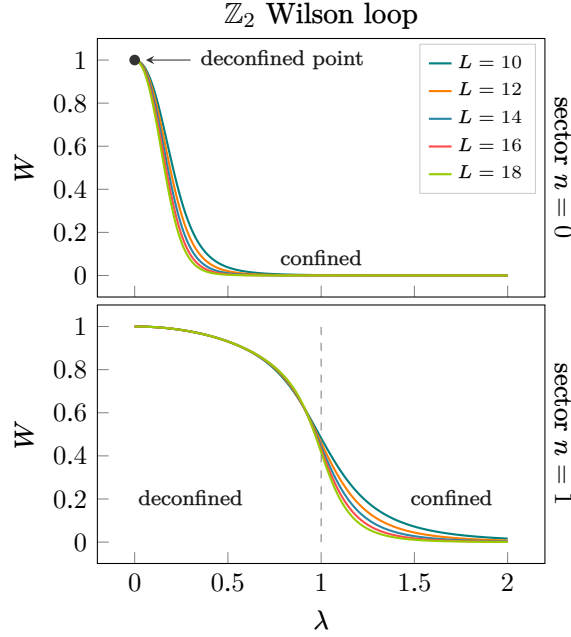
Figure 3.19. $\mathbb{Z}_2$ Wilson loop in the sectors $n = 0$ (*top*) and $n = 1$ (*bottom*), for sizes $L = 10, 12, \ldots, 18$. The sector $n = 0$ presents only a deconfined point at $\lambda = 0$ and then decays rapidly into a confined phase, while the sector $n = 1$ has a phase transition for $\lambda \simeq 1$.

the string. Instead, for $\lambda > 1$, where we have confinement (as in the $n = 0$ sector), the ground state is essentially a product state, akin to a ferromagnetic state.

Results for $N = 3$ The $\mathbb{Z}_3$ LGT is studied for lengths $L = 7, 9, 11$ and 13. This model can be mapped to a 3-clock model, which is equivalent to a 3-state quantum Potts model with a longitudinal field, which is present in all sectors, as one can see from (3.85). This field is expected to disrupt any ordered state and thus it is not possible to observe a phase transition, as it is confirmed by the behaviour of the half-ladder Wilson loops shown in Fig. 3.20. In addition, all the sectors present a deconfined point at $\lambda = 0$. In the case $n = 0$, for $\lambda > 0$ we recognize a quick transition to a confined phase, similar to what happens in [33]. While for $n = 1$ and 2 (which are equivalent), the model exhibits a smoother *crossover* to an ordered phase characterized by a doubly-degenerate ground state, for $\lambda > 1$. Notice that, as discussed above, the presence of the "skew" longitudinal field breaks the three-fold degeneracy expected in the ordered phase of the 3-clock model into a two-fold degeneracy only.
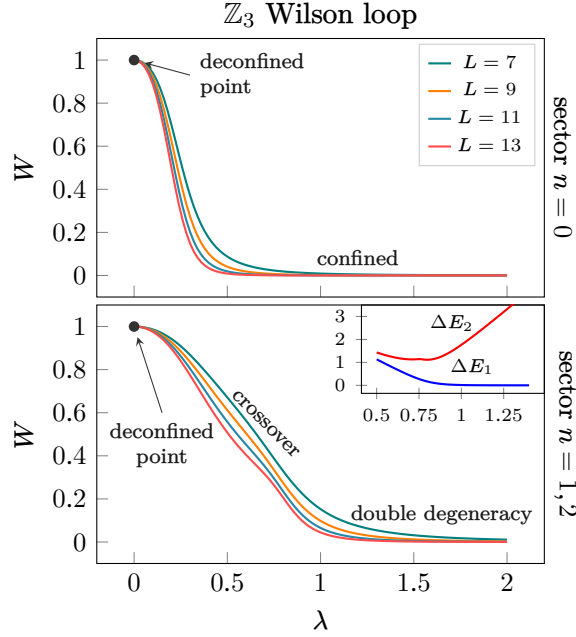
Figure 3.20. $\mathbb{Z}_3$ Wilson loop for the sectors $n = 0$ (*top*) and $n = 1, 2$ (*bottom*, which are equivalent), for sizes $L = 7, 9, 11$ and 13. Inset: energy differences $\Delta E_i = E_i - E_0$ for $i = 1, 2$, as a function of the coupling λ, in the sectors $n = 1, 2$, showing the emergence of a double-degenerate ground state for $\lambda > 1$.

Results for $N = 4$ The $\mathbb{Z}_4$ ladder LGT have four super-selection sectors. The behaviour of half-ladder Wilson loops as function of λ is shown in Fig. 3.21. As in the previous models, for $n = 0$ we see a deconfined point at $\lambda = 0$, followed by a sharp transition to a confined phase. The sector $n = 2$, which has no longitudinal field, is the only one to present a clear DCPT for $\lambda \approx 1$, as it is expected from the fact that the 4-clock model is equivalent to two decoupled Ising chains [21]. In the two equivalent sectors $n = 1$ and 3, where the longitudinal field is complex, the Wilson loop shows a peculiar behaviour, at least for the largest size ($L = 10$) of the chain: it decreases fast as soon $\lambda > 0$, to stabilize to a finite value in the region $0.5 \lesssim \lambda \lesssim 1$, before tending to zero. The characteristics of this phase would deserve a deeper analysis, that we plan to do in a future work. For $\lambda \gtrsim 1$, the system enters a deconfined phase with a double degenerate ground state, as for the $\mathbb{Z}_3$ model.
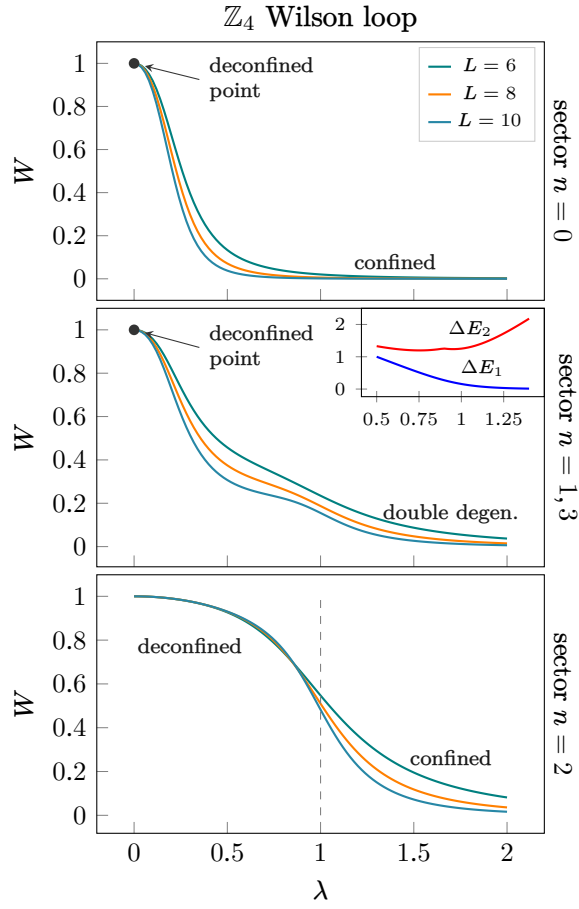
Figure 3.21. $\mathbb{Z}_4$ Wilson loop for sectors $n = 0, \ldots, 3$ and sizes $L = 6, \ldots, 10$. Only the sector $n = 2$ has a clear deconfined-confined phase transition, as expected from the duality with the 4-clock model.

chapter four

Finite Group Gauge Theories

4.1 Kogut-Susskind Hamiltonian formulation

The classical formulation of Hamiltonian LTG is due to Kogut and Susskind, in [citation?]. It can be regarded as the Hamiltonian corresponding to the Wilson action [inserire eqref]. The former can be obtained from the latter by the transfer matrix technique[citation?], where two different lattice spacing are assigned to time and spatial dimensions and then the continuum limit for the time direction is taken. Another derivation can be done by means of Legendre transform, but in this text we will adopt a more modern approach, based on [citare Milsted, Osborne 2018].

As one can expect, the Kogut-Susskind Hamiltonian H_{KS} is made of two terms, the electric part and the magnetic part:

$$H_{\mathrm{KS}} = H_E + H_B. \tag{4.1}$$

These will be constructed separately and for a simple reason. The magnetic term involves only the spatial component of the field strength tensor, i.e., $\boldsymbol{B}^2 \sim F^{ij}F_{ij}$, while the electric term involves also the temporal components, i.e., $\boldsymbol{E}^2 \sim F^{0i}F_{0i}$. Given that in the Hamiltonian formalism time is continuous while space is discrete, the two terms cannot be treated on the same footing. This differs from the Wilson action approach, where the magnetic and electric are treated equally because it has to be Lorentz-invariant.

Another point of divergence with the path-integral approach is that now both the electric field and magnetic term are operators, not simple variables. In order to have well-defined, or defined at all, operators we have to define the appropriate Hilbert space on which these operators act.

4.1.1 Single link Hilbert space and operators

We start by considering a single link ℓ and define the gauge degrees of freedom. In the construction in Sec. 1.2.1, given a gauge group G we have associated an element $g \in G$ to the link ℓ. Hence, the configuration space for each link

ℓ is exactly G. When quantizing, the configuration space G is elevated to a Hilbert space $\mathcal{H}^G$ which is spanned by the elements $g \in G$:

$$\mathcal{H}^G \equiv \operatorname{span}\{|g\rangle : g \in G\}, \tag{4.2}$$

{eq:single_link_Hilbert_space

where the set $\{|g\rangle\}$ is an orthonormal basis. Therefore, an element $|\psi\rangle$ of $\mathcal{H}^G$ can be written as

$$|\psi\rangle = \int \mathrm{d}g \, \psi(g) \, |g\rangle \,, \tag{4.3}$$

where $\int \mathrm{d}g$ is a proper measure in the case of continuous groups (usually the Haar measure) or a simple sum in case of finite groups. In the former case $\mathcal{H}^G$ is equivalent to the space $L^2(G)$ of square-integrable functions of G, i.e., each element $|\psi\rangle$ can be identified with the functions $\psi(g)$. While in the latter case, the space $\mathcal{H}^G$ is equivalent to the so-called group algebra $\mathbb{C}[G]$. The total Hilbert space of the model is simply given by the tensor product

$$\mathcal{H}_{\text{tot}} = \bigotimes_{\ell} \mathcal{H}_{\ell}^G \tag{4.4}$$

Focusing now on the case of continuous groups like $\mathrm{SU}(N)$, given a single link Hilbert space $\mathcal{H}_{\ell}^G$, the first set of operators we can define on it are the *position observables* $\hat{u}_{mn}$, via

$$\hat{u}_{mn} |g\rangle = U(g)_{mn} |g\rangle \,, \tag{4.5}$$

where $U(g)_{mn}$ is the matrix element (m, n) of $U(g)$, the image of g in the fundamental representation U of G. One can then define a matrix of operators $\hat{u}$, whose elements are precisely the operators $\hat{u}_{mn}$. Note that $\hat{u}$ is unitary as long as the chosen representation is unitary, but this not guarantee that each operator $\hat{u}_{mn}$ is unitary. Indeed, it can be shown that $(\hat{u}_{mn})^\dagger = (\hat{u}^\dagger)_{mn}$.

A second set of operators can be defined on $\mathcal{H}^G$, which makes use of the group structure of G. For each element $h \in G$, we define L_h and R_h such that for any $|g\rangle \in G$

$$L_h |g\rangle = |hg\rangle \quad \text{and} \quad R_h |g\rangle = |gh^{-1}\rangle \,, \tag{4.6}$$

which are the *left* and *right* multiplication operators, respectively. If the basis $\{|g\rangle\}$ is considered as the "position basis" then the operators L_h and R_h can be regarded as "translation operators". The left multiplications commutes with the rights one and both L_h and R_h respects the group structure of G, i.e.,

$$L_g L_h = L_{gh} \quad \text{and} \quad R_g R_h = R_{gh}, \tag{4.7}$$

indeed the maps $\hat{L} : h \mapsto L_h$ and $\hat{R} : h \mapsto R_h$ are basically *regular representations* of the group G. It can also be shown that L_h and R_h are unitary operators and satisfy

$$(L_h)^\dagger = (L_h)^{-1} = L_{h^{-1}} \quad \text{and} \quad (R_h)^\dagger = (R_h)^{-1} = R_{h^{-1}}. \tag{4.8}$$

4.1.2 Magnetic Hamiltonian

As already mentioned, it is relatively easy to obtain the magnetic term if we already know the Wilson approach but it order to make the presentation clear we repeat the step for major clarity.

Fixing the lattice orientation, on a link ℓ we define

$$\hat{u}_{mn}(\ell) = \begin{cases} \hat{u}_{mn} & \text{if } \ell \text{ traversed in the positive direction,} \\ \hat{u}_{mn}^{\dagger} & \text{if } \ell \text{ traversed in the negative direction.} \end{cases} \tag{4.9}$$

Then, let γ be a oriented path, which we write as $\gamma = \langle \ell_1 \ell_2 \ldots \ell_q \rangle$. Next, on γ we can define the *Wilson line* W_γ whose matrix elements are

$$(W_\gamma)_{mn} = \sum_{m_1 \ldots m_{q-1}} \hat{u}_{mm_1}(\ell_1)\hat{u}_{m_1 m_2}(\ell_2)\cdots\hat{u}_{m_{q-1}n}(\ell_q), \tag{4.10}$$

which can be written in a more compact way as

$$W_\gamma = \hat{u}(\ell_1)\hat{u}(\ell_2)\cdots\hat{u}(\ell_n), \tag{4.11}$$

where the matrix multiplication is implied. When considering closed path, we can take the trace of W_γ in order to have no free matrix indices:

$$\text{tr} W_\gamma = \sum_m (W_\gamma)_{mm} \tag{4.12}$$

Since $\boldsymbol{B}^2 = \frac{1}{2} F_{ij} F^{ij}$, we can copy the spatial part of the Wilson formulation and consider single plaquette Wilson loops:

$$\text{tr} \hat{W}_\square = \text{tr}\left(\hat{u}(\ell_1)\hat{u}(\ell_2)\hat{u}(\ell_3)^{\dagger}\hat{u}(\ell_4)^{\dagger} \right), \tag{4.13}$$

where $\ell_1, \ldots, \ell_4$ are the links around a purely spatial plaquette. Thus, the magnetic Hamiltonian is

$$H_B = -\frac{1}{g^2 a^{4-d}} \sum_\square \left(\text{tr} W_\square + \text{tr} W_\square^{\dagger} \right), \tag{4.14}$$

where the sum is over the plaquettes of lattice and the coupling is chosen in order to have the correct limit.

4.1.3 Electric Hamiltonian

The construction of the electric term of the Hamiltonian is less trivial, since we cannot use Wilson loops in the time direction. Recall that in the continuum theory the electric field is the infinitesimal generators of translations of the gauge fields. Hence, we have to find the infinitesimal generators corresponding

to the "translations" L_h and R_h. From these then we can build the electric Hamiltonian. In the case of Lie groups there is a recipe we can use for these generators.

So, consider the case of a compact Lie group G and its Lie algebra $\mathfrak{g}$. Given that $\hat{L} : h \mapsto L_h$ and $\hat{R} : h \mapsto R_h$ are regular representations of the Lie group G, we can easily find the regular representations of the Lie algebra. This is a linear map that maps every element $X \in \mathfrak{g}$ into an element $\hat{\ell}(X)$ such that

$$L_{e^{i\epsilon X}} = \exp\left(i\epsilon\hat{\ell}_L(X)\right) \quad \text{and} \quad R_{e^{i\epsilon X}} = \exp\left(i\epsilon\hat{\ell}_R(X)\right). \tag{4.15}$$

The maps $\hat{\ell}_L$ and $\hat{\ell}_R$ are the left and right Lie algebra representations. It does not matter which one we use, so we chose the left representation. Similar calculation can be carried out with the right one as well.

If L_h is unitary, then $\hat{\ell}(X)$ is necessarily Hermitian. Let $\{T^a\}$ be the Hermitian generators of $\mathfrak{g}$ with commutation relations

$$[T^a, T^b] = if^{abc}T^c, \tag{4.16}$$

{eq:Lie_algebra_comm_relati

where f^{abc} are the structure constants. Obviously, $X \mapsto \hat{\ell}_L(X)$ is a ordinary Lie group representation (not to be confused with regular representation). Hence, we can defined the momentum operators as the images of the generators T^a through $\hat{\ell}_L$:

$$\hat{\ell}_L^a \equiv \hat{\ell}_L(T^a), \tag{4.17}$$

and they automatically satisfy (4.16),

$$\left[\hat{\ell}_L^a, \hat{\ell}_L^b\right] = if^{abc}\hat{\ell}_L^c. \tag{4.18}$$

Alternatively, the operators $\hat{\ell}_L^a$ can also be obtained by differentiating L_h:

$$\hat{\ell}_L^a = -i\frac{\mathrm{d}}{\mathrm{d}\epsilon}L_{e^{i\epsilon T^a}}\bigg|_{\epsilon=0} \tag{4.19}$$

The operators $\hat{\ell}_L^a$ will act as "conjugate variables" to the operators $\hat{u}$, with commutation relations

$$[\hat{\ell}_L^a, \hat{u}] = -T^a\hat{u}. \tag{4.20}$$

Bearing in mind that the continuum Hamiltonian contains the square of the electric field, we may then form the group Laplacian on a link ℓ as the square of the generators $\hat{\ell}_L^a$:

$$\Delta_\ell = \sum_a \left(\hat{\ell}_L^a\right)^2. \tag{4.21}$$

This is a Laplacian on the space $L^2(\mathrm{SU}(N))$, in an entirely analogous way to the Laplacian operator of ordinary quantum mechanics, which is given by the sum of squares of the infinitesimal generators of translations in each space direction. With the continuum limit in mind, then the correct form the electric Hamiltonian is

$$H_E = \frac{g^2}{2a^{d-2}} \sum_\ell \Delta_\ell = \sum_\ell \sum_a \left(\hat{\ell}_L^a\right)^2 \tag{4.22}$$

where the sum is taken over the links of the lattice. Therefore, the overall Kogut-Susskind Hamiltonian is given by

$$H = \frac{g^2}{2a^{d-2}} \sum_\ell \Delta_\ell - \frac{1}{g^2 a^{4-d}} \sum_\square \left(\mathrm{tr} W_\square + \mathrm{tr} W_\square^\dagger\right) \tag{4.23}$$

4.1.4 Gauge transformations

4.2 From Lie groups to finite groups

4.2.1 The Hilbert space

Basic construction

In the Hamiltonian formulation of lattice gauge theories [34–36], time is continuous while the d spatial dimensions are discretized into a hypercubic lattice. Classically, we assign a group element $g \in G$ to each spatial lattice link, where G is the gauge group. In the Lie group case, one would typically write $U_\mu(x) = \exp(iA_\mu(x)) \in G$ for the gauge field variable assigned to the lattice link between points x and $x + \hat{\mu}$, where $A_\mu(x)$ is the vector potential. Links are oriented, and if a link is traversed in the opposite orientation, then g is replace with g^{-1}. Note that finite groups have no Lie algebras, so we work with group-valued quantities as far as possible. In what follows, we write $g \in G$ for a group element indifferently for both finite and Lie groups G. Since classically we have a group element g on each lattice link, in the quantum theory the states in the Hilbert space of each link are given by [35]

$$|\psi\rangle = \int dg\, \psi(g) |g\rangle \ , \tag{4.24}$$

where $\{|g\rangle\}$ is the group element orthonormal basis, consisting of one state $|g\rangle$ per group element g; it can be though of as a "position basis" on the group. The wavefunction $\psi(g)$ is square-integrable with respect to the Haar measure. For a finite group, the Haar measure is simply a sum over group elements, $\int dg = \sum_g$. The Hilbert space on each link can then be identified with $L^2(G)$, i.e. the space of square-integrable functions on G [35], while for a finite group

it is simply the *group algebra* $\mathbb{C}[G]$, which is the complex vector space spanned by the group element basis. The overall Hilbert space is then given by the tensor product $\mathcal{H} = \bigotimes_{\text{links}} L^2(G)$, or $\mathcal{H} = \bigotimes_{\text{links}} \mathbb{C}[G]$. Note that for a finite group, $\mathbb{C}[G]$ has finite dimension, because it is spanned by the finitely-many group element states $\{|g\rangle\}$. Therefore the Hilbert space on each link is finite-dimensional and $\mathcal{H}$ is finite-dimensional on a finite lattice; its dimension is in fact given by $|G|^L$ where L is the number of lattice links. For a Lie group, on the other hand, we have infinitely many basis states $\{|g\rangle\}$ and therefore the Hilbert space is infinite-dimensional *on each link*.

In the Hamiltonian formulation of gauge theories, the statement that the theory is invariant under gauge transformations translates at the level of the Hilbert space by restricting the allowed states only to those which are gauge-invariant. In particular, on the single-link Hilbert space one can define left and right "translation" operators, in the analogy where $\{|g\rangle\}$ is a position basis in group space [36],

$$L_g |h\rangle = |gh\rangle \ , \qquad R_g |h\rangle = \left|gh^{-1}\right\rangle \ . \tag{4.25}$$

A local gauge transformation is given by a choice of group element $g_x \in G$ at every site x of the lattice [35]. This acts on the overall Hilbert space $\mathcal{H} = \bigotimes_{\text{links}} L^2(G)$ or $\mathcal{H} = \bigotimes_{\text{links}} \mathbb{C}[G]$ via the operator

$$\mathcal{G}(\{g_x\}) = \bigotimes_{l = \langle xy \rangle \in \text{links}} L_{g_x} R_{g_y} \ , \tag{4.26}$$

where $\{g_x\}$ is an arbitrary choice of group elements g_x at each lattice site x and the link l connects the points x and y. In other words, on each link the gauge transformation is given on basis elements by the familiar $|g_l\rangle \to \left|g_x g_l g_y^{-1}\right\rangle$. The only physical states are those which satisfy the so-called "Gauss' law" constraint [34, 35, 37]

$$\mathcal{G}(\{g_x\}) |\psi\rangle = |\psi\rangle \ , \tag{4.27}$$

for any possible choice of local assignments $\{g_x\}$ of group variables to lattice sites. The states which satisfy eq. (4.27) form the physical, gauge-invariant Hilbert space $\mathcal{H}_{\text{phys}}$. Note that the condition eq. (4.27) only involves group-valued quantities and is thus valid for both Lie groups and finite groups. In the case of finite groups, the condition simplifies because it is sufficient to impose invariance against a set of generators of the finite group.

One can also straightforwardly include matter fields such as fermion fields which live on each lattice site. Under a gauge transformation, they transform as $\Psi(x) \to g_x \Psi(x)$. Since these always have a finite Hilbert space, they do not additional issues for quantum simulation and we focus instead on the pure gauge theory.

The representation basis and the Peter-Weyl theorem

It turns out to be fruitful to introduce a different basis of the overall Hilbert space $\mathcal{H}$, "dual" to the group element basis. The operators L_g and R_g introduced in eq. (4.25) are unitary representations of G, known as the *left* and *right regular* representations [38, 39]. This is because $L_g L_h = L_{gh}$ and $(L_g)^{-1} = L_{g^{-1}} = (L_g)^\dagger$, as can be explicitly checked by acting on the group element basis, and the same holds for R. Their representation theory leads to the Peter-Weyl theorem [35, 39, 40], which states that for a finite or compact Lie group G,

$$L^2(G) = \bigoplus_{j \in \Sigma} V_j^* \otimes V_j \ , \qquad (4.28)$$

{eq:peterweyl}

where j is a label for the irreducible representations (irreps) of G, and Σ is the set of all irreps of G. For finite groups $L^2(G)$ is replaced, as usual, with $\mathbb{C}[G]$. Here V_j is the representation vector space corresponding to representation j and V_j^* its dual vector space. For both compact Lie groups and finite groups the irreps are finite-dimensional and can be chosen to be unitary. For a finite group, Σ is a finite set, while it is countably infinite for a compact Lie group [38, 39]. In terms of the Peter-Weyl decomposition, the left and right regular representations take a particularly simple form [40],

$$L_g R_h = \bigoplus_j \rho_j(g)^* \otimes \rho_j(h) \ , \qquad (4.29)$$

{eq:translations peter weyl}

where ρ_j is the matrix of the jth irrep of G. The individual action of either L_g or R_h may be obtained by setting either g or h to the identity. Eq. (4.29) is especially useful because, as we will see in Section 4.3, it simplifies the action of the Gauss' law constraint eq. (4.27).

The Peter-Weyl theorem provides an alternative basis for the single-link Hilbert space. For each irrep j one chooses appropriate bases for V_j^* and V_j, which we denote $\{|jm\rangle\}$ and $\{|jn\rangle\}$ respectively, where $1 \leq m, n \leq \dim j$. Here $\dim j \equiv \dim V_j$ is the dimension of the representation. On each representation subspace, we use the shorthand notation $|jmn\rangle \equiv |jm\rangle \otimes |jn\rangle$. Then the "representation basis" for $L^2(G)$ or $\mathbb{C}[G]$ is given by the set $\{|jmn\rangle\}$ for all $j \in \Sigma$ and $1 \leq m, n \leq \dim j$. In terms of the group element basis, one has [36]

$$\langle g|jmn\rangle = \sqrt{\frac{\dim(j)}{|G|}} \, [\rho_j(g)]_{mn} \ , \qquad (4.30)$$

{eq:change of basis}

where the bases $\{|jm\rangle\}$, $\{|jn\rangle\}$ are chosen so that ρ_j is unitary. It should be emphasized that eq.(4.30) is valid for both finite and compact Lie groups; $|G|$ is either the order of the finite group or the volume $|G| \equiv \int dU \, 1$ given

by the possibly unnormalized Haar measure [35, 40]. It is a basic result of the representation theory of finite groups that $\sum_j (\dim j)^2 = |G|$, which ensures that the group element basis and the representation basis have the same number of states [38].

Since every group admits a trivial, one-dimensional irrep with $\rho(g) \equiv 1$, we always have a singlet representation state $|0\rangle$, which may be extended to the whole lattice to form the "electric ground state" $|0_E\rangle$,

$$|0_E\rangle = \bigotimes_{l \in \text{links}} |0\rangle_l \ , \qquad |0\rangle = \frac{1}{\sqrt{|G|}} \sum_g |g\rangle \ , \qquad (4.31)$$

where we used eq.(4.30) to express $|0\rangle$ in the group element basis. We have summarized the representation theory of some groups of interest in Appendix B. In the specific case of the group $\mathbb{Z}_N$, the representations are all one-dimensional because $\mathbb{Z}_N$ is Abelian and therefore $m = n = 1$ and can be omitted. The group elements are $\{1, g, g^2, \ldots, g^{N-1}\}$ and the irreps are simply $\rho_j(g^k) = \omega_N^{kj}$ for $j = 0, 1, \ldots, N-1$, with $\omega_N = e^{2\pi i/N}$. The bases $\{|g^k\rangle\}$ and $\{|j\rangle\}$ are related by

$$|j\rangle = \sum_{k=0}^{N-1} |g^k\rangle \langle g^k|j\rangle = \frac{1}{\sqrt{N}} \sum_{k=0}^{N-1} \omega_N^{kj} |g^k\rangle \ , \qquad (4.32)$$

which is just the discrete Fourier transform. In the case of the dihedral groups D_4 with 8 elements, we have four one-dimensional representations, each of which spans a one-dimensional subspace of $\mathbb{C}[G]$. We then have a two-dimensional representation which spans a $2^2 = 4$ dimensional subspace of $\mathbb{C}[G]$ through the four basis elements $|jmn\rangle$ for $1 \leq m, n \leq 2$.

4.2.2 The Hamiltonian

Basic construction

The Hamiltonian for a Yang-Mills gauge theory on the lattice takes the form [34, 36]

$$H = \lambda_E \sum_{l \in \text{links}} h_E(g_l) + \lambda_B \sum_{\square} h_B(g_\square) \ , \qquad (4.33)$$

where h_E depends only on each lattice link, while h_B depends on the lattice plaquettes $\square$ and $g_\square = g_1 g_2 g_3^{-1} g_4^{-1}$ is the product of the four link variables in a lattice plaquette with the appropriate orientation. It is also possible to add matter fields such as fermions, but since this does not pose any further difficulty than in the usual Lie group case, we focus here on the pure gauge theory.

In the Lie group case, the electric and magnetic Hamiltonians form the so-called Kogut-Susskind Hamiltonian where [34, 35]

$$h_E = \sum_a \left(\hat{\ell}_L^a \right)^2 \, , \qquad h_B = \dim \rho - \operatorname{Re} \operatorname{tr} \rho(g_\square) \, , \qquad (4.34)$$

where ρ is the fundamental representation of $\mathrm{SU}(N)$, a is a color index and $\hat{\ell}_L^a$ is the infinitesimal generator of left-translations, i.e. the Lie algebra representation corresponding to L_g. As such, it satisfies $L_{e^{iX}} = \exp\left(i\hat{\ell}_L(X) \right)$ [35]. As the group element basis may be thought of as a "position basis" in group space, the infinitesimal generator of translations $\hat{\ell}_L^a$ may be thought of as a "momentum" operator in group space. Then the electric Hamiltonian h_E, which is the sum of the squares of the "momenta" in all directions, is a Laplacian in group space. Applying the Peter-Weyl decomposition eq. (4.29) to $\hat{\ell}_L^a$, one finds that [35, 40]

$$h_E = \sum_a \left(\hat{\ell}_L^a \right)^2 = \sum_{jmn} C(j) \, |jmn\rangle \langle jmn| \, , \qquad (4.35)$$

where $C(j)$ is the quadratic Casimir operator, which depends only on the representation $C(j)$. For $\mathrm{U}(1)$, for example $C(j) = j^2$, while for $\mathrm{SU}(2)$ one finds $C(j) = j(j+1)$. We note that the magnetic Hamiltonian depends only on group-valued quantities and is therefore well-defined for both Lie groups and finite groups. On the other hand, the electric Hamiltonian depends on the infinitesimal Lie algebra through $\hat{\ell}_L^a$ and therefore the definition does not extend to finite groups. The decomposition eq. (4.35) is well-defined also for finite groups, but one must leave the coefficients $C(j)$ unsatisfactorily unspecified because finite groups do not have a Casimir operator [36].

If one thinks of a finite group as a natural discretization of some parent Lie group, the natural choice of electric Hamiltonian is a discrete Laplacian on the finite group. The geometric structure of a finite group is that of a graph, with group elements as vertices and the group operation defining the edges. This is called a *Cayley graph*. The discrete Laplacian on the finite group is then naturally given by the graph Laplacian of the Cayley graph. This choice also preserves the interpretation of the electric Hamiltonian as a quantum-mechanical rotor in group space [34]. We explain the construction of the finite group Laplacian in detail in Section 4.2.2, and the resulting Hamiltonian takes the form of eq. (4.33) with

$$h_E = \sum_{g \in \Gamma} (1 - L_g) \, , \qquad h_B = h_B(g_\square) \, , \qquad (4.36)$$

where $\Gamma \subset G$ is a subset of the group (*not* a subgroup) such that

1. $1 \notin \Gamma$, i.e. Γ doesn't contain the identity element.

2. $\Gamma^{-1} = \Gamma$, i.e. it is invariant under inversion of group elements. In other words, if $g \in \Gamma$, then $g^{-1} \in \Gamma$ also.

3. $g\Gamma g^{-1} = \Gamma$, i.e. it is invariant under conjugation. In other words, Γ is a union of conjugacy classes of G.

These conditions on Γ ensure that the electric Hamiltonian is gauge-invariant. On the other hand, as usual, the magnetic term is gauge-invariant as long as h_B is any real function such that $h_B(g_1 g_\square g_1^{-1}) = h_B(g_\square)$ for any $g_1 \in G$. As explained in Section 4.2.2, the Hamiltonian eq. (4.36) includes as a special case the transfer-matrix Hamiltonian obtained in [41] which consists in a certain specific choice of subset Γ. The choice of Γ is in fact not unique, a fact which we will also discuss in later sections.

While the magnetic Hamiltonian h_B is diagonal in the group element basis, the electric Hamiltonian h_E is diagonal in the representation basis, and in fact

$$h_E = \sum_{jmn} h_E(j) \,|jmn\rangle \langle jmn| \;, \qquad h_E(j) = |\Gamma| - \frac{1}{\dim j} \sum_{g \in \Gamma} \chi_j(g) \;, \quad (4.37)$$

where $|\Gamma|$ is the number of elements in Γ and χ_j is the character of the irrep labelled j. The electric Hamiltonian may be interpreted as an "on-link" hopping term withing group space; in fact, up to a constant, it may be written as $h_E = \sum_{g \in \Gamma} \sum_{h \in G} |gh\rangle \langle h|$ and it favours each link to sit in the electric ground state eq. (4.31), which is fully delocalized in group space. On the other hand, the magnetic term is a plaquette-based potential which pushes plaquettes close to the identity. The competition between the two non-commuting terms gives rise to non-trivial dynamics.

We would like to emphasize that the description of the electric Hamiltonian h_E in eq. (4.36) as the graph Laplacian of the Cayley graph associated with the group is not simply an interesting analogy, but also a tool which may be used to extract information on the Hamiltonian itself. As an example, we note the well-known fact that the smallest eigenvalue of a graph Laplacian is always zero (given by the trivial representation state eq. (4.31)) and its degeneracy equals the number of connected components of the graph [42]. Moreover, it is not hard to show that the if Γ does not generate the group G, but rather only a subset $\langle \Gamma \rangle < G$, then the Cayley graph splits into connected components which are identified with the cosets of $\langle \Gamma \rangle$ in G. The number of such components, and therefore the degeneracy of the electric ground state, is given by $|G|/|\langle \Gamma \rangle|$. If, instead, Γ generates the whole group, then the electric Hamiltonian is not degenerate. For more details, see Appendix 4.4.1. The degeneracy of the
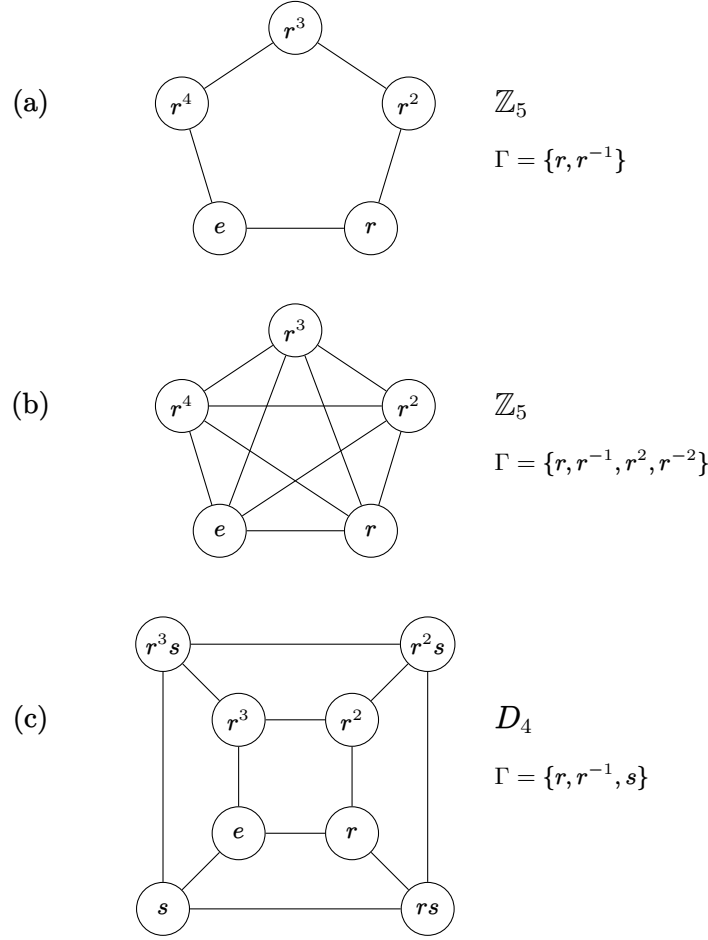
Figure 4.1. Examples of Cayley graphs. (a) and (b) show $\mathbb{Z}_5$ with $\Gamma = \{g, g^{-1}\}$ and $\Gamma = \{g, g^2, g^{-1}, g^{-2}\}$ respectively. (c) shows D_4 with $\Gamma = \{r, r^{-1}, s\}$

electric ground state is not only an important feature of the theory, but also technically important for ground state preparation and adiabatic quantum simulation. As we will already at the end of Section 4.2.2, this can happen already for the dihedral group D_4. In general, this can also occur with the choice of Γ arising from the transfer-matrix formulation of Wilson action, as described in Section 4.2.2. For example, in the permutation group $G = S_5$, starting from the Wilson action in the six-dimensional representation of S_5, one finds Γ to be the conjugacy class of the 5-cycles; then $\langle \Gamma \rangle$ generates the subgroup A_5 and since $|S_5|/|A_5| = 2$, the electric Hamiltonian ground state is two-fold degenerate, with the ground states spanned by the two representation states corresponding to the one-dimensional representations.

The finite group Laplacian

In this section we explain in detail the construction of the finite group Laplacian, which we take as the electric Hamiltonian, as the graph Laplacian of the Cayley graph of the finite group. Given a finite group G, we choose a set of generators $\Gamma \subset G$, which we require to be invariant under inversion, that is $\Gamma^{-1} = \Gamma$, and moreover that it is the union of conjugacy classes, so that it is invariant under conjugation, $g\Gamma g^{-1} = \Gamma$ for any g in G [42]. We choose Γ not to include the identity element and we note that the choice of Γ is not unique. The Cayley graph has the group elements as vertices, and we place an edge between $g \in G$ and $h \in G$ if $hg^{-1} \in \Gamma$. The result is a simple undirected graph. Examples of Cayley graphs for the groups D_4 and $\mathbb{Z}_5$ are shown in Fig. 4.1. Given any graph, its Laplacian is defined as [42]

$$L = D - A \ , \tag{4.38}$$

where A is the adjacency matrix and D is the degree matrix. Each of these matrices acts on the vector space of graph vertices, which in the case of a Cayley graph can be identified with the group algebra $\mathbb{C}[G]$. The degree matrix is always diagonal, and in this case $D = |\Gamma|\mathbb{1}$. The adjacency matrix A is given by

$$A_{gh} = \begin{cases} 1 & gh^{-1} \in \Gamma \\ 0 & \text{otherwise} \end{cases} \tag{4.39}$$

for group elements g, h. On a basis element, one has

$$A \ket{g} \equiv \sum_h A_{hg} \ket{h} = \sum_{k \in \Gamma} \ket{gk} = \sum_{k \in \Gamma} \ket{gk^{-1}} = \sum_{k \in \Gamma} R_k \ket{g} \ , \tag{4.40}$$

where R_k is the right regular representation, and we used the closure of Γ under inversion. Therefore as an operator on $\mathbb{C}[G]$,

$$A = \sum_{k \in \Gamma} R_k = \bigoplus_j \mathbb{1}_j \otimes \left(\sum_{k \in \Gamma} \rho_j(k) \right) \ , \tag{4.41}$$

where we used the Peter-Weyl decomposition of R_k, eq.(4.29). Then we see that

$$\left(\sum_{k \in \Gamma} \rho_j(k) \right) \rho_j(g) = \sum_{k \in \Gamma} \rho_j(kg) = \sum_{k \in \Gamma} \rho_j((gkg^{-1}g)) = \rho_j(g) \left(\sum_{k \in \Gamma} \rho_j(k) \right) \ , \tag{4.42}$$

where we used the closure of Γ under conjugation. Hence the operator $\left(\sum_{k \in \Gamma} \rho_j(k) \right)$ commutes with the irreducible representation ρ_j and as such is proportional

to the identity by Schur's lemma [38]. The constant of proportionality can be readily computed by taking a trace. This therefore implies

$$A = \sum_j \lambda_j P_j \;, \qquad \lambda_j = \frac{1}{\dim j} \sum_{k \in \Gamma} \chi_j(k) \;, \tag{4.43}$$

where $P_j = \sum_{mn} |jmn\rangle \langle jmn|$ is the projector onto the jth representation subspace, and χ_j is the character of the irrep labelled j. Therefore the Laplacian of the Cayley graph is given by

$$L = \sum_j f(j) P_j \;, \qquad f(j) = |\Gamma| - \frac{1}{\dim(j)} \sum_{k \in \Gamma} \chi_j(k) \;, \tag{4.44}$$ {eq:laplacian finite group}

which is the same form as the electric Hamiltonian in the representation basis, eq. (4.37).

We give some examples of this construction. For the group $\mathbb{Z}_N$ it is natural to construct the electric eigenvalues $f(j)$ with the generating set $\Gamma = \{g, g^{-1}\}$, which results in

$$f(j) = f(N - j) = 4 \sin^2\left(\frac{\pi j}{N}\right) \;, \tag{4.45}$$ {eq:fj ZN}

which is the same as in [43]. Moreover for large N,

$$f(j) \to \frac{4\pi^2}{N^2} j^2 \qquad N \, \text{large} \;, \tag{4.46}$$

which is proportional to the Casimir eigenvalues of the $U(1)$ gauge theory [44]. Thus both a truncation of $U(1)$ theory and proper Z_N gauge theory naively approach $U(1)$ theory for large N, albeit in different ways. One can however choose a different generating set, such as $\Gamma = \{g, g^{-1}, g^2, g^{-2}\}$ and the corresponding eigenvalues would be

$$f(j) = f(N - j) = 4 \sin^2\left(\frac{\pi j}{N}\right) + 4 \sin^2\left(\frac{2\pi j}{N}\right) \;. \tag{4.47}$$

For the dihedral group D_4 we can choose for example $\Gamma = \Gamma_1 = \{r, r^3, s, r^2 s\}$, which gives rise to the eigenvalues $f(j)$ shown in table 4.1, where the representations are ordered like in the character table in Table B.1 in Appendix B.2. Note that Γ_1 generates the whole group.

By looking at its character table, we may in fact classify all possible choices of Γ for D_4. In fact, D_4 has five conjugacy classes, $C_0 = \{e\}$, $C_1 = \{r, r^3\}$, $C_2 = \{r^2\}$, $C_3 = \{s, r^2 s\}$, $C_4 = \{rs, r^3 s\}$. One can check that, as is generally true, $\sum_i |C_i| = 8 = |G|$. In this case, all conjugacy classes are invariant under inversion, i.e. $C_i^{-1} = C_i$. Hence any union of the C_is, $i \neq 0$ is a valid choice for Γ. There are 2^4 such possibilities. Note that this is not

		$f(j)$				
Γ	j	0	1	2	3	4
$\{r, r^3, s, r^2 s\}$		0	4	4	8	4
$\{r, r^2, r^3\}$		0	4	0	4	5
$\{r, r^3, s, rs, r^2 s, r^3 s\}$		0	8	8	8	6

Table 4.1. Eigenvalues of the single-link electric Hamiltonian $f(j)$ for the finite group D_4, with three choices of generating sets Γ.

true in general, in which case one must choose conjugacy classes to ensure that $\Gamma^{-1} = \Gamma$. We consider in more detail two specific cases, in particular $\Gamma_2 = C_1 \cup C_2 = \{r, r^2, r^3\}$. Unlike Γ_1, Γ_2 does not generate the whole group D_4; this is reflected in the electric eigenvalues in Table 4.1, with the ground state being two-fold degenerate. Finally, we consider the choice $\Gamma_3 = C_1 \cup C_3 \cup C_4 = \{r, r^3, s, rs, r^2 s, r^3 s\}$. As explained in Section 4.2.2 if we pick h_B as the real part of the trace of the two-dimensional representation of D_4, the choice of Γ_3 corresponds to the Lorentz-invariant Hamiltonian.

Action formulation and Lorentz invariance

The Kogut-Susskind Hamiltonian eq. (4.34) may be obtained via the transfer-matrix formulation from the Euclidean Wilson action [45, 46]

$$S = -\frac{1}{g^2 a^{4-d}} \sum_{\square} \mathrm{Re} \, \mathrm{tr} \rho(g_\square) \, , \tag{4.48}$$

where a is the lattice spacing and g the coupling. The couplings in eq. (4.34) also take the specific form $\lambda_E = \frac{g^2}{2a^{d-2}}$ and $\lambda_B = \frac{2}{g^2 a^{4-d}}$. In the path-integral formulation, the lattice is fully discretized and thus plaquettes extend also in the time direction. The action eq. (4.48) is also perfectly valid for finite groups, as one simply replaces the partition function integration measure over the Lie group with sum over the elements of a finite group. One may then repeat the transfer-matrix formulation for an arbitrary finite group [41]. The resulting finite group Hamiltonian takes the form eq. (4.36), with specific choices of Γ and h_B. In particular, h_B is chosen as usual like in eq. (4.34), while $\Gamma = \{g \in G, \, g \neq e, \max[\mathrm{Re} \, \mathrm{tr} \rho(g)]\}$ is the set of non-identity elements which maximize $\mathrm{Re} \, \mathrm{tr} \rho(g)$. More generally, one may start from a Euclidean action of the form

$$S = -\sum_{\square_t} f_t(g_{\square_t}) - \sum_{\square_s} f_s(g_{\square_s}) \, , \tag{4.49}$$

where $\square_t$ and $\square_s$ are plaquettes in the time and space directions respectively, and f_t, f_s are real functions such that $f(g_1 g_\square g_1^{-1}) = f(g_\square)$ for any $g_1 \in G$. Then via the transfer matrix procedure one obtains a generalized Hamiltonian of the form of eq. (4.36) with $h_B = f_s$ and $\Gamma = \{g \in G, \ g \neq e, \max[f_t(g)]\}$. Even though we do not consider this case here, in order to improve the approach to the continuum it might also be interesting to consider other Euclidean actions [47, 48].

In particle physics applications, one typically requires Lorentz invariance in the continuum. While the lattice breaks the Lorentz symmetry to the subgroup of Euclidean cubic rotations, as long as this subgroup is preserved one expects to recover Lorentz invariance in the continuum limit. Since the action eq. (4.49) is anisotropic in the space and time directions, it breaks the Euclidean cubic symmetry explicitly and it is unclear whether the corresponding Hamiltonian describes a Lorentz-invariant theory in the continuum (unless of course $f_s = f_t$). This includes in particular setting $h_E(j) = j^2$ for subgroups of U(1) and $h_E(j) = j(j+1)$ for subgroups of SU(2) in eq. (4.37), while keeping h_B unchanged. Such choices explicitly break the remnant Lorentz symmetry. In condensed matter applications, however, Lorentz invariant is not necessarily required and one may thus independently choose Γ and h_B, as well as the couplings λ_E and λ_B.

Classification of the possible theories, and other models

The construction of finite group Yang-Mills gauge theories with Hamiltonian eq. (4.36) involves a few arbitrary choices which can be classified. Since the Hilbert space is fixed to the physical, gauge-invariant Hilbert space $\mathcal{H}_{\text{phys}}$, the only possible choices involve the various terms in the Hamiltonian. Given a gauge group G in d spatial dimensions, one may arbitrarily choose:

1. A set Γ of group elements which does not contain the identity, and is invariant under both inversion and conjugation $\Gamma^{-1} = \Gamma$ and $g\Gamma g^{-1}$.

2. A choice for the magnetic Hamiltonian $h_B = h_B(g_\square)$. Since it must be real and satisfy $h_B(g_1 g_\square g_1^{-1}) = h_B(g_\square)$, i.e. it is a *class function*, by a well-known result [38] it may be expanded in a sum of characters of irreducible representations, $h_B(g) = \sum_j c_j \chi_j(g)$ for coefficients c_j which may be chosen arbitrarily, while ensuring that $h_B(g)$ is real.

3. If present, possible choices of representations and Hamiltonians in the matter sector. For example in D_4 gauge theory, one can include *staggered fermions* in the two-dimensional representation.

4. One can also add a Chern-Simons term as in [49]. This is especially interesting for quantum simulation, because such theories have a sign problem.

Further considerations involve the Lorentz symmetry, as explained in Section 4.2.2. Moreover, one may want to choose representations which are non-trivial when restricted to the center of the gauge group [50, 51].

We note that the above construction allows further generalizations. In particular, the discretized d-dimensional space does not have to take the form of a hypercubic lattice, but more generally can be a Bravais or non-Bravais lattice. No difference arises for the electric term, which is link-based, and the plaquette variable in the magnetic term is replaced by an an elementary closed loop in the lattice.

4.3 The physical Hilbert space

As we remarked in Section 4.2.1, while the overall Hilbert space of the pure gauge theory is $\mathcal{H} = \bigotimes_{\text{links}} \mathbb{C}[G]$, only those states that satisfy the so-called "Gauss' law" constraint eq. (4.27) are to be considered physical [34, 35, 37]. For gauge theories based on most compact Lie groups, the Wilson loops (despite being overcomplete) span the space of gauge-invariant states [52, 53]. This, however, is not necessarily true for finite groups [52, 54]; this means that in some cases, it is possible to construct different gauge-invariant states, which nevertheless have the identical Wilson loops. We mention that this difficulty cannot arise for Abelian finite groups such as $\mathbb{Z}_N$, in which case the Wilson loops *do* span the physical Hilbert space $\mathcal{H}_{\text{phys}}$. In the following section we give a description of the gauge-invariant Hilbert space in terms of *spin network states* and explain how this basis of states is particularly suitable to describe the physical Hilbert space of finite group gauge theories. We first consider the pure gauge physical Hilbert space in Section 4.3.1 and compute its dimension in Section 4.3.2. In Section 4.3.3 we extend this construction to matter fields.

4.3.1 Spin networks

The physical Hilbert space of pure gauge theories with either Lie or finite gauge group can be explicitly described in terms of *spin network states* [55, 56]. Spin-network states can be defined indifferently when the d-dimensional space is discretized as an arbitrary graph, and are thus valid in arbitrary dimension with arbitrary lattices and boundary conditions. The first key observation is that the action of the Gauss' law operator eq. (4.27) is block-diagonal in the

representation basis, as can be seen from eq. (4.29). Then starting from the Hilbert space in the representation basis eq. (4.28), we can, as usual, permute the summation and product, obtaining

$$\mathcal{H} = \bigotimes_{\text{links } j \in \Sigma} \bigoplus V_j^* \otimes V_j = \bigoplus_{\{j\} \in \{\Sigma\}} \bigotimes_{l \in \text{links}} V_{j_l}^* \otimes V_{j_l} \ , \tag{4.50}$$

where now $\{j\}$ is an assignment of an irrep j_l to each lattice link l, and $\{\Sigma\}$ is the set of the possible such assignments. The second key observation is that the gauge transformations eq. (4.27) are given by an independent group-valued variable g_x at each site x of the lattice. Moreover, due to eq. (4.29) the gauge transformation associated to one site x acts at most on one of V_j or V_j^* but it cannot act on both. One can then split the two vector spaces V_j and V_j^* associated with each link and reorder the Vs in the tensor product over links so that V_js are now grouped together according to the *sites* and not the links,

$$\mathcal{H} = \bigoplus_{\{j\} \in \{\Sigma\}} \bigotimes_{x \in \text{sites}} \left(\bigotimes_{l_- = x} V_{j_l}^* \right) \otimes \left(\bigotimes_{l_+ = x} V_{j_l} \right) \ , \tag{4.51}$$

where by l_+ and l_- we denote respectively the target and source vertex of link of link l. We can repeat the same set of operations for the gauge transformation operator eq. (4.26), which are therefore given by

$$\mathcal{G}(\{g_x\}) = \bigoplus_{\{j\} \in \{\Sigma\}} \bigotimes_{x \in \text{sites}} \left(\bigotimes_{l_- = x} \rho_{j_l}^*(g_x) \right) \otimes \left(\bigotimes_{l_+ = x} \rho_{j_l}(g_x) \right) \ . \tag{4.52}$$

In the above decomposition, the gauge transformations now act independently for each x and the Gauss' law constraint EQ. (4.27) gives the physical Hilbert space

$$\mathcal{H}_{\text{phys}} = \bigoplus_{\{j\} \in \{\Sigma\}} \bigotimes_{x \in \text{sites}} \text{Inv} \left[\left(\bigotimes_{l_- = x} V_{j_l}^* \right) \otimes \left(\bigotimes_{l_+ = x} V_{j_l} \right) \right] \ . \tag{4.53}$$

Given a representation ρ (not necessarily irreducible) with representation space V_ρ, the set of invariant vectors $\text{Inv}(V_\rho)$ is the set of vectors $v \in V_\rho$ such that $\rho(g)v = v$ for all $g \in G$. Note that this is a separate notion from that of an "invariant subspace". A basis of *spin network states* which arise from the description of eq. (4.53) are of the form $|\{j\}, A\rangle$ where $\{j\}$ is an assignment of irreps to links and $A = (a_1, \ldots a_V)$ labels the choice of a gauge-invar

For a hypercubic lattice in d dimensions with periodic boundary conditions, each site is connected to $2d$ links and therefore $2d$ terms appear in the tensor product within each Inv in eq. (4.53). If instead we choose open boundary
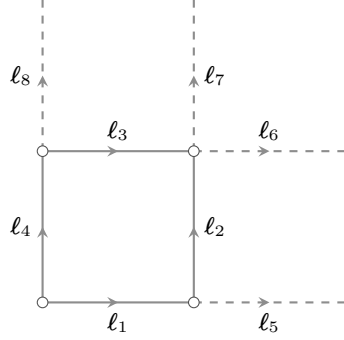
Figure 4.2. A 2×2 square lattice with periodic boundary conditions, showing the labels of the links.

conditions, the sites in the bulk will again be connected to $2d$ links, but the sites on the boundary will be connected to fewer links and thus fewer terms will appear in the tensor product for those sites. In the general case, the number of terms in the tensor product within each Inv may depend on the site. We choose to work directly with the spaces of invariant vectors rather than with spaces of intertwiners more commonly employed in the literature [55, 56].

The calculation of a basis of invariant states (or, equivalently, of the intertwiners) can be difficult in the Lie group case, especially since they admit infinitely many irreps, but can quite easily be performed numerically for finite groups, which only have finitely many irreps. Since the number of links connected to each site is finite and independent of the lattice volume, one needs only compute the invariant states of a finite number of tensor product representations which does not scale with the lattice size.

As an example, we work out explicitly the case of a 2×2 square lattice with periodic boundary conditions. As shown in Fig. 4.2, this system has four vertices and eight links. Expanding explicitly eq. (4.53) we see that in this case

$$\mathcal{H}_{\text{phys}} = \bigoplus_{j_1,\dots j_8} \text{Inv}\Big[V_{j_1}^* \otimes V_{j_4}^* \otimes V_{j_5} \otimes V_{j_8}\Big] \otimes \text{Inv}\Big[V_{j_5}^* \otimes V_{j_2}^* \otimes V_{j_1} \otimes V_{j_7}\Big] \otimes$$

$$(4.54)$$

$$\otimes \text{Inv}\Big[V_{j_6}^* \otimes V_{j_7}^* \otimes V_{j_3} \otimes V_{j_2}\Big] \otimes \text{Inv}\Big[V_{j_3}^* \otimes V_{j_8}^* \otimes V_{j_6} \otimes V_{j_4}\Big] \ .$$

Now consider a single invariant subspace $\text{Inv}\Big[V_{j_1}^* \otimes V_{j_2}^* \otimes V_{j_3} \otimes V_{j_4}\Big]$ with arbitrary assignment of representations. This vector space admits an orthonormal basis $\{|j_1 j_2 j_3 j_4; a\rangle\}$ where $1 \le a \le \text{dimInv}\Big[V_{j_1}^* \otimes V_{j_2}^* \otimes V_{j_3} \otimes V_{j_4}\Big]$ indexes the basis vector. We can expand the basis vectors explicitly in terms of the bases

of the V_j as (see also the discussion around eq. (4.30))

$$|j_1 j_2 j_3 j_4; a\rangle = \sum_{m_1, m_2, n_3, n_4} \psi(j_1 m_1 j_2 m_2 j_3 n_3 j_4 n_4; a) |j_1 m_1\rangle \otimes |j_2 m_2\rangle \otimes |j_3 n_3\rangle \otimes |j_4 n_4\rangle \ .$$

(4.55)

The basis vectors can be chosen orthonormal. By virtue of spanning the space $\mathrm{Inv}\left[V_{j_1}^* \otimes V_{j_2}^* \otimes V_{j_3} \otimes V_{j_4}\right]$, they are invariant vectors of the tensor product representation $\rho \equiv \rho_{j_1}^* \otimes \rho_{j_2}^* \otimes \rho_{j_3} \otimes \rho_{j_4}$; as such, they satisfy $\rho(g) |j_1 j_2 j_3 j_4; a\rangle = |j_1 j_2 j_3 j_4; a\rangle$ for all $g \in G$. The coefficients of the expansion $\psi(j_1 m_1 j_2 m_2 j_3 n_3 j_4 n_4; a)$ may be easily computed, for example by writing the tensor product representation matrices $\rho(g)$ explicitly and then solving the simultaneous equations $\rho(g)v = v$ for all $g \in G$ (it is actually sufficient to do so on a set of generators of G). The dimension of the space of invariant vectors depends on the four representations assigned to the relevant site. Now let $A = (a_1, a_2, a_3, a_4)$, which implicitly depends on $\{j\}$ (because the range of each a_i depends on the irreps assigned to site i). Given any assignment of irreps $\{j\}$, A is a choice of a basis vector of invariant states at the four sites. Therefore an orthonormal basis for the gauge invariant Hilbert space is given by

$$|\{j\}; A\rangle = |j_1 j_4 j_5 j_8; a_1\rangle \otimes |j_5 j_2 j_1 j_7; a_2\rangle \otimes |j_6 j_7 j_3 j_2; a_3\rangle \otimes |j_3 j_8 j_6 j_4; a_4\rangle \ , \quad (4.56)$$

for any possible assignment $\{j\}$ of irreps to links, and then all possible choices A of an invariant vector at each of the four sites.

The spin-network states $|\{j\}; A\rangle$ then form a basis of the gauge-invariant Hilbert space. Expanding the tensor product, we find an explicit expression for these states in terms of the representation basis,

$$|\{j\}; A\rangle = \sum_{n_1, \dots n_8} \sum_{m_1, \dots m_8} \psi(j_1 m_1 j_4 m_4 j_5 n_5 j_8 n_8 | a_1) \psi(j_5 m_5 j_2 m_2 j_1 n_1 j_7 n_7 | a_2) \times$$

(4.57)

$$\times \psi(j_6 m_6 j_7 m_7 j_3 n_3 j_2 n_2 | a_3) \psi(j_3 m_3 j_8 m_8 j_6 n_6 j_4 n_4 | a_4) \times \quad (4.58)$$

$$\times |j_1 m_1 n_1\rangle \otimes |j_2 m_2 n_2\rangle \otimes \cdots |j_8 m_8 n_8\rangle \ , \quad (4.59)$$

where we have restored the ordering of the vector spaces V_js and used again the shorthand $|jmn\rangle = |jm\rangle \otimes |jn\rangle$. We note in particular that despite having introduced a splitting of the variables at each link, in the final answer this splitting disappears and the spin-network states can be entirely expressed in terms of the representation basis $|jmn\rangle$.

4.3.2 The dimension of the physical Hilbert space

As we have seen in the previous section, spin network states give an explicit description of the physical Hilbert space $\mathcal{H}_{\text{phys}}$ as

$$\mathcal{H}_{\text{phys}} = \bigoplus_{\{\rho\} \in \{\Sigma\}} \bigotimes_{v \in \text{sites}} \text{Inv}\left[\left(\bigotimes_{l_-=v} V_{\rho_l}^*\right) \otimes \left(\bigotimes_{l_+=v} V_{\rho_l}\right)\right], \qquad (4.60)$$

where $\text{Inv}(\rho)$ is the space of invariant vectors of the representation ρ, $\{\rho\}$ is an assignment of irreps to links and $\{\Sigma\}$ is the set of such possible assignments. For a finite group,

$$\text{dimInv}(\rho) = \frac{1}{|G|} \sum_{g \in G} \chi_\rho(g) , \qquad (4.61) \quad \text{\{eq:invariant vectors counting}}$$

where χ_ρ is the character of ρ. We prove this result in Appendix 4.4.2. This fact can be used to obtain a general formula for the dimension of the $\mathcal{H}_{\text{phys}}$, which is valid for any lattice in any dimension with any boundary conditions. On a lattice with L links and V sites, we will show that

$$\text{dim}\mathcal{H}_{\text{phys}} = \sum_C \left(\frac{|G|}{|C|}\right)^{L-V} , \qquad (4.62) \quad \text{\{eq:physical hilbert space dim}}$$

where the sum runs over all conjugacy classes C of the group, and $|C|$ is the size of C. The ratio $|G|/|C|$ is always an integer by the orbit-stabilizer theorem [38]. Using eq.(4.61), together with the fact that the character of a tensor product is given by the product of the characters, we may readily prove eq.(4.62). From the general formula for the gauge-invariant Hilbert space, we have

$$\text{dim}\mathcal{H}_{\text{phys}} = \sum_{j_1 j_2 \cdots j_L} \prod_{v \in \text{sites}} \text{dimInv}\left[\left(\bigotimes_{l_-=v} V_{\rho_l}^*\right) \otimes \left(\bigotimes_{l_+=v} V_{\rho_l}\right)\right] =$$

$$= \frac{1}{|G|^V} \sum_{j_1 j_2 \cdots j_L} \sum_{g_1 g_2 \cdots g_V} \prod_{v \in \text{sites}} \left(\prod_{l_-=v} \chi_{j_l}^*(g_v)\right)\left(\prod_{l_+=v} \chi_{j_l}(g_v)\right) .$$

Within the product over all sites, there are exactly $2L$ factors of characters χ, as each link contributes two representation spaces V and each representation space gives rise to a character. Thus grouping characters by link, we obtain

$$\text{dim}\mathcal{H}_{\text{phys}} = \frac{1}{|G|^V} \sum_{g_1 g_2 \cdots g_V} \prod_{l=\langle xx'\rangle \in \text{links}} \langle g_x, g_{x'}\rangle . \qquad (4.63)$$

where we denoted $\langle g, h\rangle = \sum_j \chi_j(g)^* \chi_j(h)$. It is a well-known result that $\langle g, h\rangle$ is zero unless g and h belong to the same conjugacy class, in which case

$\langle g, h \rangle = |G|/|C|$ where C is the conjugacy class of both g and h [38]. If any two adjacent sites x and x' have g_x and $g_{x'}$ in different conjugacy classes, then $\langle g_x, g_{x'} \rangle = 0$ and the corresponding term in the sum is zero. Assuming that the lattice is connected, this implies that the product over all links is zero unless all the g_x at each site x belong to the same conjugacy class. Then, since $\langle g_x, g_{x'} \rangle$ is constant on conjugacy classes, we can write

$$\dim \mathcal{H}_{\text{phys}} = \frac{1}{|G|^V} \sum_C \sum_{g_1 g_2 \cdots g_V \in C} \frac{|G|^L}{|C|^L} = \sum_C \left(\frac{|G|}{|C|} \right)^{L-V}, \qquad (4.64)$$

which concludes the proof. In the Abelian case the above formula simplifies as all conjugacy classes are singlets and therefore $\dim \mathcal{H}_{\text{phys}} = |G|^{L-V+1}$. Thus finite Abelian groups have the largest physical Hilbert space among all groups of the same order. For periodic boundary conditions in a hypercubic lattice, $L = Vd$ and as such $\dim \mathcal{H} = |G|^{Vd}$, while $\dim \mathcal{H}_{\text{phys}} \approx |G|^{V(d-1)}$, so that $\dim \mathcal{H}_{\text{phys}} \approx (\dim \mathcal{H})^{1-1/d}$ and both spaces grow exponentially with the lattice size. For a finite group, one may compute all possible relevant spaces of invariant vectors with little effort as the number of tensor product spaces is bounded in d spatial dimensions by $(\dim j_{\max})^{2d} \leq |G|^d$, owing to $\sum_j (\dim j)^2 = |G|$, independently from the lattice volume. The exponential scaling arises from considering all possible assignments of irreps to lattice links.

As a further example, we consider the dimension of the Hilbert space for pure D_4 gauge theory. Using eq. (4.62), we find for $G = D_4$ on a lattice with L links and V sites,

$$\dim \mathcal{H}_{\text{phys}} = 8^{L-V} \left(2 + \frac{3}{2^{L-V}} \right). \qquad (4.65)$$

The dimension of the physical Hilbert space for some two-dimensional finite square lattices in $2+1$ dimensions is shown in Table 4.2. We see that its size grows quickly with the lattice size. We point out that even for a 2×2 periodic lattice with a small group such as D_4 it is not even feasible to write down all possible gauge-invariant states. Unless the structure happens to be very sparse, writing down the 8960 physical basis elements in terms of the $|G|^L = 8^8$ basis elements in the representation basis using 4B floating point numbers would require roughly 600GB of memory.

4.3.3 Extension to matter fields

The spin network states may be extended to matter

Size	BCs	L	V	$L-V$	$\dim\mathcal{H}_{\mathrm{phys}}$
2 × 2	open	4	4	0	5
	periodic	8	4	4	8960
2 × 3	open	7	6	1	28
	periodic	12	6	6	536576
3 × 3	open	12	9	3	1216
	periodic	18	9	9	269221888

Table 4.2. Dimension of the physical subspace of D_4 gauge theory on some small lattices in $2+1$ dimensions. L is the number of links and V is the number of vertices.

4.4 Some proofs

4.4.1 Degeneracy of electric Hamiltonian

As discussed in Section 4, the degeneracy of the electric Hamiltonian given by the finite group Laplacian Δ is directly related to the structure of the Cayley graph. In particular, it is a standard result that the graph Laplacian always has a zero mode and its degeneracy equals the number of connected components of the graph [42]. Here we show that the Cayley graph is connected if its generating set Γ generates the whole group. If instead $\langle\Gamma\rangle \neq G$, then the Cayley graph splits into connected components identified with the cosets of $\langle\Gamma\rangle$ in G; thus the degeneracy of the finite-group Laplacian Δ equals $|G|/|\langle\Gamma\rangle|$.

Any subset $\Gamma \in G$ generates a subgroup $\langle\Gamma\rangle < G$. The right cosets of $\langle\Gamma\rangle$ are of the form $\langle\Gamma\rangle\, h$ for h in G. Since cosets partition the group, any two group elements g_1 and g_2 will belong to some coset, say $g_1 \in \langle\Gamma\rangle\, h_1$ and $g_2 \in \langle\Gamma\rangle\, h_2$. We want to show that there is an edge in the Cayley graph between group elements g_1 and g_2 if and only if $\langle\Gamma\rangle\, h_1 = \langle\Gamma\rangle\, h_2$. The fact that $g_i \in \langle\Gamma\rangle\, h_i$ means that $g_i = k_i h_i$ for some $k_i \in \langle\Gamma\rangle$. There is an edge between g_1 and g_2 if and only if $g_1 g_2^{-1} = k_1 h_1 h_2^{-1} k_2 \in \Gamma$. But since $k_i \in \langle\Gamma\rangle$ this is equivalent to saying that $h_1 h_2^{-1} \in \langle\Gamma\rangle$, which is equivalent to $\langle\Gamma\rangle\, h_1 = \langle\Gamma\rangle\, h_2$. This concludes the proof.

4.4.2 Counting of invariant states

In Section 4.62 we used the fact that for a generic representation ρ, the dimension of the space of invariant vectors is given by

$$\mathrm{dimInv}(\rho) = \frac{1}{|G|} \sum_{g\in G} \chi_\rho(g)\,, \qquad (4.66)$$

As is well known, if ρ is irreducible then the corresponding character sums to zero and there are no invariant states. This is to be expected since irreducible representations by definition have no non-trivial invariant subspaces, but any invariant vector would span an invariant subspace.

Here we provide a proof of the above formula. If v is an invariant vector for the representation ρ, by definition it satisfies $\rho(g)v = v$ for all $g \in G$. Now we construct a projector onto the subspace of invariant vectors. We define the averaging map $\mathrm{Av} : V_\rho \to V_\rho$,

$$\mathrm{Av}(v) = \frac{1}{|G|} \sum_{g \in G} \rho(g)v \ . \tag{4.67}$$

The averaging map is the projector onto the subspace of invariant vector. In fact, given an arbitrary vector v, we see that $\mathrm{Av}(v)$ is invariant because

$$\rho(g)\mathrm{Av}(v) = \frac{1}{|G|} \sum_{h \in G} \rho(gh)v = \frac{1}{|G|} \sum_{h \in G} \rho(h)v = \mathrm{Av}(v) \ . \tag{4.68}$$

Therefore, Av maps the representation space to the subspace of invariant vectors $\mathrm{Av} : V_\rho \to \mathrm{Inv}(V_\rho)$. Moreover, if v is invariant, then $\mathrm{Av}(v) = v$, and more generally, $\mathrm{Av}^2 = \mathrm{Av}$ by a similar calculation. This means that Av is a projector onto the subspace of invariant vectors. Then the size of projected subspace is as usual given by the trace of the projector, $\mathrm{dimInv}(\rho) = \mathrm{trAv}$, which reproduces the above formula.

Some results in representation theory

In this appendix we sum up some of the basic results of representation theory of finite and compact Lie groups. All the representation theory here presented is taken over the complex field $\mathbb{C}$.

A.1 Basic results

A finite group only has finitely many representations up to equivalence, and they are all unitary:

Theorem 1. *Let G be a finite group and Σ the set of equivalence classes of irreducible representations (irreps) of G. Then, Σ is finite, and the representative of each class can be chosen to be unitary.*

We can then state the following:

Theorem 2 (Burnside)**.** *Let G be a finite group. Then:*

1. *If $\dim(j)$ is the dimension of the j-th inequivalent irreps of G, and there are M such irreps, then*

$$\sum_{j=1}^{M} \dim(j)^2 = |G|, \tag{A.1}$$ {eq:burnside_th_dim}

where $|G|$ is the order of the group.

2. *The number of inequivalent irreducible representations of G is equal to the number of conjugacy classes of G.*

An immediate consequence follows:

Corollary 1. *If G is a finite Abelian group, then it has precisely $|G|$ inequivalent irreps.*

Similar results apply to compact groups. First of all,

Theorem 3. *The irreps of a compact Lie group are finite-dimensional.*

Moreover,

Theorem 4. *Let G be a compact Lie group and Σ the set of equivalence classes of irreducible representations of G. Then, Σ is countable, and the representative of each class can be chosen to be unitary.*

Given the irreps $\{\pi_j\}$ of a group (compact Lie or finite), these satisfy the so-called *orthogonality theorem*. The statement for compact Lie groups is the following:

Theorem 5 (Orthogonality theorem for compact Lie groups). *Let $\{\pi_j\}$ be unitary irreps of G. Then*

$$\int \mathrm{d}g [\pi_j(g)]^*_{nm}[\pi_{j'}(g)]_{n'm'} = \frac{Vol(G)}{\dim(j)}\delta_{jj'}\delta_{nn'}\delta_{mm'}, \qquad (A.2)$$

where the volume of the group is the volume corresponding to the chosen Haar measure.

While the statement for finite groups needs some little adjustments:

Theorem 6 (Orthogonality theorem for finite groups). *Let $\{\pi_j\}$ be unitary irreps of G. Then*

$$\sum_{g \in G} [\pi_j(g)]^*_{nm}[\pi_{j'}(g)]_{n'm'} = \frac{|G|}{\dim(j)}d_{jj'}\delta_{nn'}\delta_{mm'} \qquad (A.3)$$

A useful corollary is that the sum of all matrices of a non-trivial irrep j is zero:

$$\sum_{g \in G} \pi_j(g) = 0. \qquad (A.4)$$

This follows by taking j' equal to the trivial representation, whose matrice elements are all equal to the identity. Then if j is non-trivial, the right-hand side of the orthogonality theorem is always zero. Taking $m' = n'$ on the left-hand side gives the claim

A.2   Character theory

In this section, we will only be concerned with finite groups. The irreps of a finite group G are the function $\chi : G \to \mathbb{C}$ defined as the traces of irreps of G:

$$\chi_j(g) = \mathrm{tr}\pi_j(g). \qquad (A.5)$$

There are as many irreducible charactes as there airreducible representations. We will use the the following result:

Theorem 7. *The characters* $\{\chi_j\}$ *of a group G form a basis for the space of class functions on G.*

A class function f satisfies

$$f(axa^{-1}) = f(x) \qquad \text{for all } x, a \in G, \tag{A.6}$$

which means that it is constant on conjugacy classes. We will also needthe following

Theorem 8 (Orthogonality theorem for characters). *The irreducible characters of a finite group are orthonormal, in the sense that*

$$\frac{1}{|G|} \sum_{g \ inG} \chi_i^*(g)\chi_j(g) = \delta_{ij}. \tag{A.7}$$

The characters also satisfy a different kind of orthogonality relation, where one sums over characters rather than over group elements:

Theorem 9. *The irreducible characters* $\{\chi_i\}$ *of a finite group satisfy*

$$\sum_i \chi^*(g)\chi_i(h) = \begin{cases} |G|/|C(g)| & g \text{ and } h \text{ are conjugate} \\ 0 & otherwise \end{cases} \tag{A.8}$$

where i indices the irreducible characters and $|C(g)|$ is the sice of the conjugacy class of g.

Finally, we can define the *convolution* of two class functions ϕ and ψ:

$$(\phi * \psi)(g) = \sum_{h \in G} \phi(gh^{-1})\psi(h). \tag{A.9}$$

The convolution is symmetric, $\phi * \psi = \psi * \phi$. We will use the fact that the convolution of two characters is again a character,

$$\chi_i * \chi_j = \frac{|G|}{\dim(j)} \delta_{ij}\chi_j. \tag{A.10}$$

This can be showed with a direct computation.

A.3 Peter-Weyl theorem

The Peter-Weyl theorem is instrumental in the formulation of the Hamiltonian in [inserire sec ref]. See [cit. T. Tao e A. W. Knapp]$^{[citation?]}$for the Lie group case and [cit. J. P. Serre]$^{[citation?]}$for the finite group case. The statement for compact Lie groups is:

Theorem 10 (Peter-Weyl for compact Lie groups). *Let G be a compact Lie group. Then*

(i) *The space of square-integrable functions on G can be decomposed as a sum of representation spaces. More precisely, V_j is the vector space for the irreps π_j, then*

$$L^2(G) = \bigoplus_{j \in \Sigma} V_j^* \otimes V_j. \tag{A.11}$$

(ii) *The matrix elements of all the inequivalent irreps of G form an orthogonal basis for $L^2(G)$.*

(iii) *If $\{|g\rangle\}$ is the orthonormal group element basis for $L^2(G)$, then the orthonormal matrix element basis $|jmn\rangle$ satisfies*

$$\langle g|jmn\rangle = \sqrt{\frac{\dim(j)}{\mathrm{Vol}(G)}}[\pi_j(g)]_{mn}. \tag{A.12}$$

Note that there are multiple ways of writing the Peter-Weyl decomposition, as

$$V^* \otimes V \simeq \mathrm{End}V \simeq V^{\oplus \dim V} \tag{A.13}$$

As we will see later, these correspond to different ways of seeing $L^2(G)$ as a representation space.

Note that part *(i)* can be understood as a generalisation of the Fourier decomposition. In fact, since $U(1)$ is Abelian, all of its irreps are one-dimensional and are given by matrix elements of the form $\{e^{inx}\}$ for $x \in S^1 = [0, 2\pi)$. Then the Peter-Weyl theorem states that any square-integrable function on $U(1) \simeq S^1$ can be written as a Fourier series.

Recall that matrix elements are defined as follows. Consider the examples of $SU(2)$ [citare Milstead Osborne]$^{[citation?]}$, but the generalisation is easy. As we know, the irreps of $SU(2)$ are labeled by a half integer $j \in \frac{1}{2}\mathbb{Z}^+$. Then in this case

$$L^2(G) = \bigoplus_{j\ in\frac{1}{2}\mathbb{Z}^+} V_j^* \otimes V_j, \tag{A.14}$$

where $V_j = \mathbb{C}^{2j+1}$ We have irreps π_j for each j and the matrix elements are literally the elements of the matrices representing a certain $U \in \mathrm{SU}(2)$ as a function of U. More precisely, they are functions

$$[\pi_j(\cdot)]_{mn} = \mathrm{SU}(2) \to \mathbb{C}, \qquad g \mapsto [\pi_j(g)]_{mn}, \tag{A.15}$$

where $-j \leq m, n \leq j$ in integer steps. In the general case, it is more natural to take $1 \leq m, n \leq \dim(j)$.

In part *(iii)* $\mathrm{Vol}(G)$ is the volume of the group given by the chosen Haar measure. The resul of part *(iii)* can be readily derived as a consequence of *(ii)* and the orthogonality theorems for representations. The non-trivial statement is that the matrix elements of representations space $L^2(G)$, while the orthogonality is an algebraic statement. In fact, by *(ii)* the matrix elements $[\pi_j]_{mn}$ for a basis for the space of wave-functions $L^2(G)$. The corresponding states are then given by

$$|jmn\rangle = C_{jmn} \int \mathrm{d}U [\pi_j(U)]_{mn} |U\rangle, \tag{A.16}$$

where the constant C_{jmn} can be chosen to ensure that the $|jmn\rangle$ are normalized. Then we can compute their inner product,

$$\langle j'm'n'|jmn\rangle = C^*_{j'm'n'} C_{jmn} \frac{\mathrm{Vol}(G)}{\dim(j)} \delta_{jj'} \delta_{mm'} \delta_{nn'}.$$

It follows that the representation basis $\{|jmn\rangle\}$ is orthonormal with an appropriate choice of constants,

$$C_{jmn} = \sqrt{\frac{\dim(j)}{\mathrm{Vol}(G)}}$$

for compact Lie groups. Everything we have said here also holds for finite groups, with the replacement $\mathrm{Vol}(G) \to |G|$.

Crucially, the Peter-Weyl theorem also holds for finite groups ([citare J.P. Serre][citation?]):

Theorem 11 (Peter-Weyl for finite groups). *Let G be a finite groups. Then*

(i) *The group algebra on G can be decomposed as a sum of representation spaces. More precisely, if V_j is the vector space for the j-th irrep π_j, then*

$$\mathbb{C}[G] = \bigoplus_{j \in \Sigma} V_j^* \otimes V_j. \tag{A.17}$$

(ii) *The matrix elements of all the inequivalent irreps of G form an orthogonal basis for $\mathbb{C}[G]$.*

(iii) If $\{|g\rangle\}$ is the orthonormal group element basis for $\mathbb{C}[G]$, then the orthonormal matrix element basis $\{|jmn\rangle\}$ can be chosen to satisfy

$$\langle g|jmn\rangle = \sqrt{\frac{\dim(j)}{|G|}}[\pi_j(g)]_{mn}. \qquad (A.18)$$

The result is essentially the same as in the compact case. Note that in the finite group case there is no issue of convergence, and as such we do not need to specify further information on the group algebra. The duality relation can be shown to hold in the same manner as for compact Lie groups.

Some groups of interest

B.1 The cyclic groups $\mathbb{Z}_N$

The cyclic group of order N, which we denote as $\mathbb{Z}_N$, consists of the powers $1, r, \ldots, r^{N-1}$ of an element r such that $r^N = 1$. This can be written formally as

$$\mathbb{Z}_N = \langle r | r^N = 1 \rangle. \tag{B.1}$$

The group $\mathbb{Z}_N$ can be realized as the group fo rotations through angles $2\pi k/N$ around an axis.

It is an Abelian group, therefore all its irreps are of degree 1. Such a representation associates with r a complex number $\chi(r) = \omega$, and with r^k the number $\chi(r^k) = \omega^k$. Since $r^N = 1$, we have $\omega^N = 1$, that is, ω is a root of unity of degree N, which means

$$\omega = e^{i2\pi j/N}, \qquad \text{for } j = 0, 1, \ldots, N-1. \tag{B.2}$$

Thus, all the irreps are labeled by an integer $j = 0, \ldots, N-1$ and are all of degree 1. So we do not need to specify the matrix elements obviously. The characters $\chi_0, \chi_1, \ldots, \chi_{N-1}$ are given by

$$\chi_j(r^k) = e^{i2\pi kj/N}. \tag{B.3}$$

{eq:character_ZN}

It is immediate to see that $\chi_n \chi_{n'} = \chi_{n+n'}$, where $n + n'$ is taken modulo N. Because $\mathbb{Z}_N$ is Abelian, all its conjugacy classes are singlets, i.e. contains only one element, hence we have N conjugacy classes.

Regarding the basis of the group algebra $\mathbb{C}[\mathbb{Z}_N]$, the group basis $\{|r^k\rangle\}$ and the irreps basis $|j\rangle$ are related by the trasformation

$$|j\rangle = \sum_{k=0}^{N-1} |r^k\rangle \langle r^k | j \rangle = \frac{1}{\sqrt{N}} \sum_{k=0}^{N-1} \omega^{kj} |r^k\rangle, \tag{B.4}$$

which is just the *quantum Fourier transform*.

B.2 The dihedral groups D_N

The dihedral group D_N of order N is the group of rotations and reflections of the plane which preserve a regular polygon with n vertices. It contains N rotations, which forma a subgroup isomorphic to $\mathbb{Z}_N$, and N reflections. Its order is $2N$. If we denote by r the rotation through an angle $2\pi/N$ and if s is any of the reflections, we have:

$$r^N = 1, \qquad s^2 = 1, \qquad srs = r^{-1}. \tag{B.5}$$

Each dihedral group D_N can be regarded as a finite subgroup of the Lie group $O(2)$. Each element of D_N can be written uniquely, either in the form r^k (with $k = 0, \ldots, N-1$) if it is just a rotation or in the form $r^k s$ (with $k = 0, \ldots, N-1$). Notice that $srs = r^{-1}$ implies $sr^k s = r^{-k}$, hence $(r^k s)^2 = 1$.

It is useful to note that D_N may be written as the semi-direct product of two cyclic groups,

$$D_N = \mathbb{Z}_2 \ltimes \mathbb{Z}_N \ , \qquad (h_1, g_1)(h_2, g_2) = (h_1 h_2, g_1 \varphi_{h_1}(g_2)) \ . \tag{B.6}$$ {eq:semidirect product}

Here $\mathbb{Z}_N$ is the subgroup of rotations, and the $\mathbb{Z}_2$ factor gives the action of the reflection. Setting $\mathbb{Z}_2 = \{e, h\}$, the twist φ acts as $\phi_e(g) = g$ and $\phi_h(g) = g^{-1}$.

Irreps for N even First, there are 4 irreps of degree 1, obtained by letting ± 1 correspond to r and s in all possible ways. The characters of the one-dimensional irreps will be denoted with $\psi_0, \ldots, \psi_3$ and are given by the following table:

	r	r^k	s	$r^k s$
ψ_0	$+1$	$+1$	$+1$	$+1$
ψ_1	$+1$	$+1$	-1	-1
ψ_2	-1	$(-1)^k$	$+1$	$(-1)^k$
ψ_3	-1	$(-1)^k$	-1	$(-1)^{k+1}$

Next we consider representations of degree 2. Put $\omega = e^{i2\pi/N}$ and let h be an arbitrary integer. We define a representation ρ^h of D_N by setting:

$$\rho^h(r) = \begin{pmatrix} \omega^h & 0 \\ 0 & \omega^{-h} \end{pmatrix} \quad \text{and} \quad \rho^h(s) = \begin{pmatrix} 0 & 1 \\ 1 & 0 \end{pmatrix}. \tag{B.7}$$ {eq:irreps_2d_DN}

A direct calculation shows that this is indeed a representation and for generic elements r^k and $r^k s$ we have:

$$\rho^h(r^k) = \begin{pmatrix} \omega^{hk} & 0 \\ 0 & \omega^{-hk} \end{pmatrix} \quad \text{and} \quad \rho^h(r^k s) = \begin{pmatrix} 0 & \omega^{hk} \\ \omega^{-hk} & 0 \end{pmatrix}. \tag{B.8}$$

Moreover, ρ^h and ρ^{N-h} are isomorphic. Hence we may assume $0 \le h \le N/2$. The extreme cases $h = 0$ and $h = N/2$ are uninteresting: The former corresponds to the one-dimensional irrep with character $\psi_0 + \psi_1$, while the latter to $\psi_2 + \psi_3$. On the other hand, for $0 < h < N/2$, the representation ρ^h are *irreducible*. The corresponding characters χ_h are given by:

$$\chi_h(r^k) = \omega^{hk} + \omega^{-hk} = 2\cos\frac{2\pi hk}{N} \quad \text{and} \quad \chi_h(r^k s) = 0 \qquad \text{(B.9)} \quad \text{\{eq:chars\_2d\_DN\}}$$

The irreducible representations of degree 1 and 2 constructed above are the *only irreducible representations* of D_N, up to isomorphism. In fact, thesum of the squares of their degrees

$$4 \times 1 + \left(\frac{N}{2} - 1\right) \times 4 = 2N$$

equals to the order of D_N (see (A.1)).

Irreps for N odd In the case of odd N we only have *two one-dimensional irreps*, with character table

	r	s
ψ_0	$+1$	$+1$
ψ_1	$+1$	-1

We are missing the irreps ψ_2 and ψ_3 of the previous case because $(-1)^N = +1$ is true only for N even.

The representations ρ^h of degree 2 are defined by the same formulas (B.7) as in the case where N is even. Those corresponding to $0 < h < N/2$ are irreducible and pairwise non-isomorphic. Observe that, since N is odd, the condition $h < n/2$ can also be written as $h \le (n-1)/2$. The formulas of their characters is the same as (B.9).

These representations are the *only* ones. Indeed, it can be readily verified with formula (A.1) of Th. 2. The sum of the squares of their degrees is equal to

$$2 \times 1 + \frac{N-1}{2} \times 4 = 2N,$$

which is in fact the order of D_N.

The case $N = 4$ We describe in more detail the dihedral group D_4 of order 8. Its elements are

$$D_4 = \{1, r, r^2, r^3, s, rs, r^2 s, r^3 s\}$$

	$\{e\}$	$\{r, r^3\}$	$\{r^2\}$	$\{s, r^2s\}$	$\{rs, r^3s\}$
χ_0	$+1$	$+1$	$+1$	$+1$	$+1$
χ_1	$+1$	-1	$+1$	$+1$	-1
χ_2	$+1$	$+1$	$+1$	-1	-1
χ_3	$+1$	-1	$+1$	-1	$+1$
χ_4	$+2$	0	-2	0	0

Table B.1. Character table of D_4

and it has 5 conjugacy classes:

$$\{e\}, \quad \{r, r^3\}, \quad \{r^2\}, \quad \{s, r^2\}, \quad \{rs, r^3s\}.$$

We also have 5 irreps $\{\pi_j\}$, which we number them with $j = 0, \ldots, 4$. For $j = 0, \ldots, 3$ we have the one-dimensional irreps, while for $j = 4$ we have the only two-dimensional irrep:

$$\pi_4(r) = \begin{pmatrix} i & 0 \\ 0 & -i \end{pmatrix} \quad \text{and} \quad \pi_4(s) = \begin{pmatrix} 0 & 1 \\ 1 & 0 \end{pmatrix}. \tag{B.10}$$

Alternatively, we can choose another two-dimensional representation $\overline{\pi}_4$ which uses only real matrices

$$\overline{\pi}_4(r) = \begin{pmatrix} 0 & -1 \\ 1 & 0 \end{pmatrix} \quad \text{and} \quad \overline{\pi}_4(s) = \begin{pmatrix} 1 & 0 \\ 0 & -1 \end{pmatrix} \tag{B.11}$$

and isomorphic to π_4. The character table is shown in Table B.1.

As the $j = 4$ is the only faithful representation, it is a natural choice for the magnetic Hamiltonian. [forse ci sono un po' di notazione inconsistenti]

Bibliography

1. Wilson, K. G. "Confinement of quarks". *Phys. Rev. D* **10,** 2445 (1974).

2. Notarnicola, S. *et al.* "Discrete Abelian gauge theories for quantum simulations of QED". *Journal of Physics A: Mathematical and Theoretical* **48,** 30FT01 (2015).

3. Ercolessi, E., Facchi, P., Magnifico, G., Pascazio, S. & Pepe, F. V. "Phase transitions in Z_n gauge models: Towards quantum simulations of the Schwinger-Weyl QED". *Phys. Rev. D* **98,** 074503 (7 Oct. 2018).

4. Schwinger, J. "Unitary operator bases". *Proceedings of the National Academy of Sciences* **46,** 570–579. ISSN: 0027-8424 (1960).

5. Schwinger, J. & Englert, B. *Symbolism of Atomic Measurements.* 2001.

6. Weyl, H. *The theory of groups and quantum mechanics* (Courier Corporation, 1950).

7. Tagliacozzo, L. & Vidal, G. "Entanglement renormalization and gauge symmetry". *Phys. Rev. B* **83,** 115127 (2011).

8. Hamma, A. & Lidar, D. A. "Adiabatic Preparation of Topological Order". *Phys. Rev. Lett.* **100,** 030502 (3 Jan. 2008).

9. Trebst, S., Werner, P., Troyer, M., Shtengel, K. & Nayak, C. "Breakdown of a Topological Phase: Quantum Phase Transition in a Loop Gas Model with Tension". *Phys. Rev. Lett.* **98,** 070602 (7 Feb. 2007).

10. Savit, R. "Duality in field theory and statistical systems". *Rev. Mod. Phys.* **52,** 453–487 (2 Apr. 1980).

11. Cobanera, E., Ortiz, G. & Nussinov, Z. "The bond-algebraic approach to dualities". *Advances in physics* **60,** 679–798 (2011).

12. Kramers, H. A. & Wannier, G. H. "Statistics of the two-dimensional ferromagnet. Part I". *Phys. Rev.* **60,** 252 (1941).

13. Onsager, L. "Crystal Statistics. I. A Two-Dimensional Model with an Order-Disorder Transition". *Phys. Rev.* **65,** 117–149 (3-4 Feb. 1944).

14. Schultz, T. D., Mattis, D. C. & Lieb, E. H. "Two-Dimensional Ising Model as a Soluble Problem of Many Fermions". *Rev. Mod. Phys.* **36,** 856–871 (3 July 1964).

15. Jordan, P. & Wigner, E. P. "About the Pauli exclusion principle". *Z. Phys* **47,** 14–75 (1928).

16. Nussinov, Z. & Ortiz, G. "Bond algebras and exact solvability of hamiltonians: Spin $S = 1/2$ multilayer systems". *Phys. Rev. B* **79,** 214440 (2009).

17. Fradkin, E. & Susskind, L. "Order and disorder in gauge systems and magnets". *Phys. Rev. D* **17,** 2637 (1978).

18. Radicevic, D. *Spin Structures and Exact Dualities in Low Dimensions.* 2019. arXiv: 1809.07757 [hep-th].

19. Fendley, P. "Free parafermions". *Journal of Physics A: Mathematical and Theoretical* **47,** 075001 (2014).

20. Baxter, R. J. "A simple solvable Z_N Hamiltonian". *Physics Letters A* **140,** 155–157 (1989).

21. Ortiz, G., Cobanera, E. & Nussinov, Z. "Dualities and the phase diagram of the p-clock model". *Nuclear Physics B* **854,** 780–814 (2012).

22. Sun, G., Vekua, T., Cobanera, E. & Ortiz, G. "Phase transitions in the Z_p and $U(1)$ clock models". *Phys. Rev. B* **100,** 094428 (2019).

23. Baxter, R. J. *Exactly solved models in statistical mechanics* (Elsevier, 2016).

24. Fendley, P. "Parafermionic edge zero modes in Z_n-invariant spin chains". *Journal of Statistical Mechanics: Theory and Experiment* **2012,** P11020 (Nov. 2012).

25. Zhuang, Y., Changlani, H. J., Tubman, N. M. & Hughes, T. L. "Phase diagram of the Z_3 parafermionic chain with chiral interactions". *Phys. Rev. B* **92,** 035154 (3 July 2015).

26. Huang, R.-Z. & Yin, S. "Nonequilibrium critical dynamics in the quantum chiral clock model". *Phys. Rev. B* **99,** 184104 (18 May 2019).

27. Bernien, H. *et al.* "Probing many-body dynamics on a 51-atom quantum simulator". *Nature* **551,** 579–584 (2017).

28. Whitsitt, S., Samajdar, R. & Sachdev, S. "Quantum field theory for the chiral clock transition in one spatial dimension". *Phys. Rev. B* **98,** 205118 (20 Nov. 2018).

29. Kitaev, A. Y. "Fault-tolerant quantum computation by anyons". *Annals of Physics* **303,** 2–30 (2003).

30. Bañuls, M. C., Cirac, J. I. & Hastings, M. B. "Strong and Weak Thermalization of Infinite Nonintegrable Quantum Systems". *Phys. Rev. Lett.* **106,** 050405 (5 Feb. 2011).

31. Kormos, M., Collura, M., Takács, G. & Calabrese, P. "Real-time confinement following a quantum quench to a non-integrable model". *Nature Physics* **13,** 246–249 (2017).

32. Pomponio, O., Werner, M. A., Zarand, G. & Takacs, G. "Bloch oscillations and the lack of the decay of the false vacuum in a one-dimensional quantum spin chain". *SciPost Phys.* **12,** 61 (2 2022).

33. Nyhegn, J., Chung, C.-M. & Burrello, M. "$\mathbb{Z}_N$ lattice gauge theory in a ladder geometry". *Phys. Rev. Research* **3,** 013133 (1 Feb. 2021).

34. Kogut, J. & Susskind, L. "Hamiltonian formulation of Wilson's lattice gauge theories". *Phys. Rev. D* **11,** 395–408 (2 Jan. 1975).

35. Milsted, A. & Osborne, T. J. "Quantum Yang-Mills theory: An overview of a program". *Physical Review D* **98.** ISSN: 2470-0029 (July 2018).

36. Zohar, E. & Burrello, M. "Formulation of lattice gauge theories for quantum simulations". *Phys. Rev. D* **91,** 054506 (5 2015).

37. Tong, D. *Gauge Theory.* 2018 (accessed in June 2020).

38. Serre, J.-P. *Linear Representations of Finite Groups.* ISBN: 978-1-4684-9460-0 (Springer, New York, NY, 1967).

39. Knapp, A. W. *Lie Groups: Beyond an Introduction.* ISBN: 978-1-4757-2453-0 (Birkhäuser, Boston, 1996).

40. Mariani, A. *Finite-group Yang-Mills lattice gauge theories in the Hamiltonian formalism.*

41. Harlow, D. & Ooguri, H. *Symmetries in quantum field theory and quantum gravity.* 2018.

42. Chung, F. R. K. *Spectral Graph Theory* (American Mathematical Society, 1997).

43. Notarnicola, S. *et al.* "Discrete Abelian gauge theories for quantum simulations of QED". *Journal of Physics A* **48** (2015).

44. Ercolessi, E., Facchi, P., Magnifico, G., Pascazio, S. & Pepe, F. "Phase Transitions in Z_n Gauge Models: Towards Quantum Simulations of the Schwinger-Weyl QED". *Physical Review D* **98** (2018).

45. Creutz, M. "Gauge fixing, the transfer matrix, and confinement on a lattice". *Phys. Rev. D* **15,** 1128–1136 (4 Feb. 1977).

46. Kogut, J. B. "An introduction to lattice gauge theory and spin systems". *Rev. Mod. Phys.* **51,** 659–713 (4 1979).

47. Hasenfratz, P. & Niedermayer, F. "Unexpected results in asymptotically free quantum field theories". *Nucl. Phys. B* **596,** 481–494. arXiv: hep-lat/0006021 (2001).

48. Alexandru, A. *et al.* "Gluon Field Digitization for Quantum Computers". *Phys. Rev. D* **100,** 114501. arXiv: 1906.11213 [hep-lat] (2019).

49. Caspar, S., Mesterházy, D., Olesen, T., Vlasii, N. & Wiese, U.-J. "Doubled lattice ChernSimonsYangMills theories with discrete gauge group". *Annals of Physics* **374,** 255–290 (Nov. 2016).

50. HOLLAND, K. & WIESE, U.-J. in *At The Frontier of Particle Physics* 1909–1944 (WORLD SCIENTIFIC, Apr. 2001).

51. Cohen, T. D. "Center symmetry and area laws". *Physical Review D* **90** (Aug. 2014).

52. Sengupta, A. "Gauge Invariant Functions of Connections". *Proceedings of the American Mathematical Society* **121,** 897–905. ISSN: 00029939, 10886826 (1994).

53. Durhuus, B. "On the structure of gauge invariant classical observables in lattice gauge theories". *Letters in Mathematical Physics* **4,** 515–522 (Nov. 1980).

54. Cui, S. X. *et al.* "Kitaev's quantum double model as an error correcting code". *Quantum* **4,** 331. ISSN: 2521-327X (Sept. 2020).

55. Baez, J. C. "Spin Networks in Gauge Theory". *Advances in Mathematics* **117,** 253–272 (Feb. 1996).

56. Burgio, G., Pietri, R. D., Morales-Técotl, H., Urrutia, L. & Vergara, J. "The basis of the physical Hilbert space of lattice gauge theories". *Nuclear Physics B* **566,** 547–561 (Feb. 2000).